

ENG 280-(EQC 1999/422)

**Methodology for the assessment of face loaded unreinforced
masonry walls under seismic loading**

E L Blaikie, R A Davey, Opus International Consultants Ltd



Report Prepared for the EQC Research Foundation

Methodology for the Assessment of Face Loaded Unreinforced Masonry Walls under Seismic Loading



*Opus: an accomplished work,
a creation, an achievement*

ENG
280


Report Prepared for the EQC Research Foundation

Methodology for the Assessment of Face Loaded Unreinforced Masonry Walls under Seismic Loading

Prepared By


E L Blaikie
Senior Design Engineer

Reviewed By


R A Davey
Principal Consultant, Structural

Opus International Consultants Limited
Wellington Office
Level 9, Majestic Centre
100 Willis Street, PO Box 12-003
Wellington, New Zealand

Telephone:	+64 4 471 7000
Facsimile:	+64 4 471 1397
Email	ted.blaikie@opus.co.nz
Date:	May 2000
Reference:	C5643.00
Status:	Final

This document is the property of Opus International Consultants Limited.
Any unauthorised employment or reproduction, in full or part is forbidden.

Abstract – NonTechnical

In the early 1980's US researchers (ABK, 1982) subjected full-scale specimens representing a face loaded wall element spanning between two adjacent floor diaphragms, to earthquake motions. They found that a single horizontal crack tended to form near mid-height of the test specimens and another crack formed at the test bed floor, and that the walls were able to sustain large displacements, comparable with the wall thickness. This ability to withstand large displacements without collapse resulted in the walls having a significant post cracking seismic resistance. The term "dynamic stability" was used to distinguish this type of behaviour from the behaviour that might have been expected from static force calculations.

Subsequently this concept was used to develop the current New Zealand National Society of Earthquake Engineering (NZNSEE) Guidelines for the assessment of face loaded walls. These Guidelines are based on the equal energy method and the initial elastic stiffness of the wall (Priestley, 1985). However, in this study the current NZNSEE Guidelines were shown to be an unreliable, and often very unconservative, method of predicting the seismic resistance of URM walls.

In this study a more reliable method of assessing the seismic behaviour of face loaded URM walls, originally proposed in a previous EQC Research Foundation funded project (Blaikie, Spurr, 1992), has been developed to a stage that is suitable for design office use. A computer model was used to test and refine the methodology, and full size walls sample were laboratory tested to calibrate the computer model. The influence of "near fault" earthquake motions on the wall response was included as this may become an important consideration for locations near to active faults such as Wellington.

Abstract –Technical

An assessment methodology that can be used to predict the seismic stability of a cracked face-loaded URM wall was refined and developed in of this study. The methodology makes use of both the acceleration and displacement response spectra for an earthquake motion. The acceleration spectrum is used to predict the earthquake intensity that will just open the joint cracks in the wall. The displacement spectrum is used to predict the earthquake intensity that will generate mid-storey wall displacements equal to the displacement at which the wall becomes unstable. Modification factors are applied to allow for the effect of storey boundary conditions and to allow for amplification of the earthquake motion due to the overall building response and any diaphragm flexibility.

It was found that a relatively simple formula can be used to calculate the period of the motion of a cracked face-loaded URM wall when the peak mid-storey displacement is 60% of the displacement at which the wall becomes unstable. The formula is not dependant on the wall slenderness, overburden load, wall thickness or presense of top flexural fixity. The period calculated using the formula can be used in conjunction with a displacement spectra as part of the methodology used to predict the stability of face-loaded URM walls.

Design charts have been prepared to enable rapid design office assessment of a face-loaded wall in terms of the NZS4203 Loading Standard design EQ spectra. Similar design charts could be prepared for other earthquake records or code design spectral intensities using the proposed methodology.

A three-storey, dynamic inelastic computer model was used to examine the effect of a number of parameters on the seismic stability of a cracked face-loaded URM wall. Parameters examined included interaction between the face-loaded walls segments in adjacent storeys, effect of building flexibility and effect of diaphragm flexibility and/or yielding. The analyses indicated that the earthquake intensity required to collapse a face-loaded wall, as indicated by the computer modelling, is conservatively predicted by the proposed methodology. However, the current New Zealand National Society of Earthquake Engineering (NZNSEE) Guidelines were shown to be an unreliable, and often very unconservative, method of predicting the seismic resistance of URM walls.

The free vibration responses of 2 test specimens were modelled using the computer model. The tests demonstrated that the computer model can be used to model the dynamic displacement response, and hence the seismic stability, of a URM face-loaded wall.

The response of the 3-storey wall model was evaluated using an earthquake motion recorded in the near-fault zone during the Kobe earthquake. The near-fault motion had a quite different frequency content and spectral shape from that used as the basis of traditional code design spectra. The analyses showed that the formulae proposed for calculating the seismic resistance of face-loaded URM walls, when the building and diaphragms are rigid, can be used for a wide range of different earthquake motions including near fault earthquakes. However under the near-fault earthquake motion, amplification factors included in the assessment methodology to allow for building and diaphragm flexibility, must also increase with increasing building and/or diaphragm flexibility. Poor performance of face-loaded URM walls in near-fault earthquake zones is predicted.

Contents

1	Introduction.....	1
2	Behaviour of Cracked Face Loaded URM Walls	2
2.1	Behaviour of Face-Loaded URM walls subjected to Static Loads.....	2
2.2	Computer model	4
2.3	Period of Free Vibration Response	4
2.4	Face Loaded URM Wall Behaviour with Top Fixity.....	6
2.5	Effect of Top Fixity, Slenderness and Overburden Load on Free Vibration Response Period.....	7
3	Laboratory Tests	8
3.1	Introduction	8
3.2	Test Specimens	8
3.3	Loading Procedure	10
3.4	Recorded Measurements.....	10
3.5	Computer Modelling of Test Specimens	11
3.6	Results for Test Specimen 1	12
3.7	Modelling Test Specimen 1 With Reduced Number of Nodal Masses	15
3.8	Results for Test Specimen 2	16
3.9	Modelling Energy Loss and Damping.....	19
3.10	Australian Free Vibration Test Results	22
4	Prediction of Face Loaded Wall Stability Using Response Spectra	23
4.1	Prediction of Wall Stability using a Displacement Spectrum.....	23
4.2	Prediction of Wall Stability using Acceleration Spectrum and first Crack Opening....	25
4.3	Prediction of Wall Stability using Displacement & Acceleration Spectra	26
4.4	Prediction of Wall Stability using NZNSEE Guidelines	27
4.5	Comparison between Proposed Formula and Computer Model	28
5	3 Storey Face-Loaded Wall Model	30
5.1	Model Description	30
5.2	Effect of Storey Boundary Conditions on Face-Loaded Wall Stability	32
5.3	Effect of Storey Elevation and Building Deflected Shape on Wall Stability	34
5.4	Proposed Storey Elevation Amplification Factors for NZS4203 EQ Motion.....	39
5.5	Effect of Diaphragm Flexibility on the Stability of Face-Loaded URM Walls	41
5.6	Effect of Diaphragm Yielding on the Stability of Face-Loaded URM Walls.....	43
6	Response of Face Loaded URM Walls to Near Fault EQ Motions	50
6.1	Characteristic of Near Fault EQ Motions	50
6.2	Kobe Earthquake Near-Fault Ground Motion.....	51
6.3	Effect of Boundary Conditions on Face-Loaded Wall Stability – Near-Fault EQ.....	52

6.4	Storey Elevation Amplification Factors for Near-Fault Earthquake Motions.....	53
6.5	Effect of Diaphragm Flexibility on Storey Elevation Amplification Factors - Near-Fault Earthquake Motions	54
6.6	Effect of Diaphragm Yielding on Storey Elevation Amplification Factors - Near-Fault Earthquake Motions	57
6.7	Capacity of Face-Loaded URM Walls Predicted by Proposed Formula – Kobe Near Fault EQ Motion.....	59
7	Comparison of Predicted Capacities Using NZSEE Guidelines and Proposed Formulae .	63
8	Summary and Conclusions	65
8.1	Laboratory Testing.....	65
8.2	Computer Modelling.....	66
8.3	Assessment Methodology.....	66
8.4	Effect of Near Fault Earthquake Motion.....	67
8.5	Design Charts	67
9	References.....	68

Appendix A: Drain2dx Input File for Modelling Test Specimen 1

Appendix B: Methodology for The Assessment of Face Loaded Walls

Appendix C: Diaphragm Reactions at First Crack opening for Face Loaded URM Walls – UDL Seismic Load

1 Introduction

In the 1980's a consortium of Californian engineers, called the ABK Joint Venture (ABK, 1982), carried out a pioneering investigation into the post-cracking seismic resistance of URM. This investigation included the testing of full-scale specimens representing a face loaded wall element spanning between two adjacent floor diaphragms.

When the test specimens were subjected to earthquake motions imposed at the supporting floor diaphragm levels, ABK found that a single horizontal crack tended to form near mid-height of the test specimens and another crack formed at the test bed floor. These 2 cracks acted as fuses and no further intermediate cracking was observed. During the test, these 2 cracks opened up and allowed the centre of the wall to undergo large displacements, comparable with the wall thickness. This ability to withstand large displacements without collapse resulted in the walls having a significant post cracking seismic resistance. ABK used the term "dynamic stability" to distinguish this type of behaviour from the behaviour that might have been expected from static force calculations where "failure" is assumed to occur when the wall cracks.

Subsequent to the ABK investigations, Priestley developed an equal energy procedure for the assessment of face loaded (Priestley, 1985). This method depends on the initial elastic stiffness of the wall. For example, if the assumed elastic modulus of the masonry is increased by 100%, an increase in seismic resistance of approximately 40% is predicted. It appears that this increase is unlikely as the initial elastic deflection of the wall, prior to cracks opening in the wall, is usually small compared with the wall displacement at which the wall becomes unstable. This Methodology was incorporated in draft guidelines for assessing and strengthening earthquake risk buildings have been published by the New Zealand National Society of Earthquake Engineering (NZNSEE, 1995)

As part of a previous research project, funded the EQC Research Foundation, (Blaikie, Spurr, 1992) an alternative methodology was proposed that can be used to assess the seismic behaviour of face loaded URM walls. This methodology was based on the use of displacement spectra and was not dependent on the initial elastic stiffness of the wall.

This report describes research carried out to further develop and refine the proposed methodology. As part of this research two face-loaded URM wall test specimens were displaced at mid-height to open pre-formed cracks then allowed to respond under free vibration conditions. The test specimen response was then modelled using an inelastic dynamic computer model. This established that the computer model could be used to evaluate the inelastic behaviour of face-loaded URM walls.

The computer model was then used to test the proposed assessment methodology for a range of parameters and establish modification factors to allow for the effect of "top fixity" and to allow for amplification of the earthquake motion that is expected because of the overall building response and diaphragm flexibility.

2 Behaviour of Cracked Face Loaded URM Walls

2.1 Behaviour of Face-Loaded URM walls subjected to Static Loads

The behaviour of cracked face loaded URM walls is described in a previous research report, (Blaikie, Spurr, 1992) and a paper based on that previous research (Blaikie, Davey, 1999). It is summarised here so that the current report can be read without reference to the earlier work.

Face loaded walls in URM buildings normally span vertically between floor framing. They may also be supported by roof framing or by the ground. When subjected to sufficient lateral load, a multi-storey URM wall can be expected to crack at the level of the supports and near the mid-height of the wall elements that span between the supports providing the supports do not fail. Figure 1(a) shows the forces assumed to act on a cracked wall element spanning, H , between supports and subjected to a static lateral load V . The wall has a total weight, W , and effective thickness, t . The overburden load, O , represents the weight of a parapet or the weight of any upper storey walls and is assumed, initially, to act at the wall centre line.

At the base of the wall element the vertical reaction, $O + W$, is assumed to act near the face of the wall at a point that is $t/2$ from the wall centreline. As a small compression zone depth would be required to develop the reaction and as the mortar may not extend to the outside face of the wall, the effective wall thickness t , will be less than the nominal wall thickness.

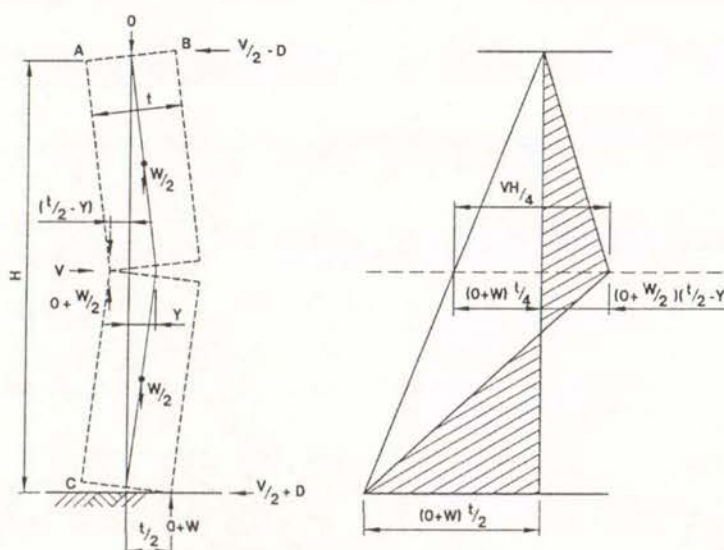


Figure 1: Behaviour of face loaded wall under static loading - a) forces assumed to act on the wall and - b) wall bending moment distribution.

At the mid-height crack, the reaction between the upper and lower halves of the wall is also assumed to be located $t/2$ from the deflected centre line of the wall or $(t/2 - Y)$ relative

to the undeflected wall centre line as indicated. Figure 1(b) shows the bending moments developed in the wall when the wall is subjected to a point load, V , acting laterally at the mid-height crack. The bending moments (shown shaded) are relative to the undeflected wall centre line.

Equating the simply supported bending moment to the wall moments at the mid-height crack:

$$\frac{VH}{4} = (O+W)\frac{t}{4} + (O+\frac{W}{2})(\frac{t}{2}-Y) \quad \text{Eqn 1}$$

$$\therefore V = \frac{2}{H} \left(W(t-Y) + O(\frac{3t}{2}-2Y) \right) \quad \text{Eqn 2}$$

V will have a maximum value, V_{\max} when $Y = 0.0$

$$\therefore V_{\max} = \frac{2t}{H} [W+1.5O] \quad \text{Eqn 3}$$

The wall will become unstable when the applied load, V , reduces to zero and the wall displacement, Y , will then have its maximum static value, Y_{\max} as shown in Figure 2. Therefore rearranging Eqn 2 and substituting $V = 0.0$:

$$Y_{\max} = \left(\frac{W+1.5O}{W+2O} \right) t \quad \text{Eqn 4}$$

Using Eqn 3 and Eqn 4 to replace O and W in Eqn 2 and rearranging Eqn 2 it can also be shown that:

$$V = V_{\max} (1 - Y/Y_{\max}) \quad \text{Eqn 5}$$

This equation is shown graphically below:

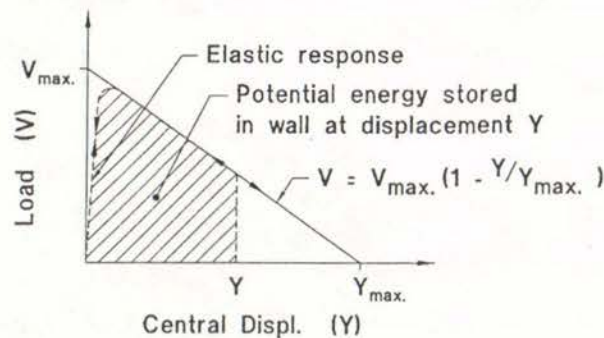


Figure 2 Load Deformation Relationship for Point Load Acting at Mid-Height Crack

The difference in reactions at the top and bottom support levels, D , indicated in Figure 1(a), can be obtained by taking moments about the undeflected wall centre line at the mid-height crack. This results in the expression:

$$D = [O + W] \frac{t}{2H} - \frac{WY}{2H} \quad \text{Eqn 6}$$

If a uniformly distributed load, wH replaces the point load, V , in Figure 1(a), the simply supported bending moment will be $wH^2/8$. Therefore the load, V , in equations Eqn 1 to Eqn 5 would need to be replaced by $wH/2$ if the load applied to the wall was uniformly distributed.

$$\text{i.e., } wH = 2V \quad \text{Eqn 7}$$

Therefore, if the load is uniformly distributed, twice the load is required to produce the same wall displacement.

The equations used to calculate Y_{\max} and D (Eqn 4 and Eqn 6) are not affected by the load distribution and remain the same for a uniformly distributed load.

Equations Eqn 3 and Eqn 7 can also be used to find the seismic lateral load coefficient, C_d , at which the cracks in the wall will start to open:

$$C_d = \frac{wH}{W} = \frac{2V_{\max}}{W} = \frac{4t}{H} (1 + 1.5 \frac{O}{W}) \quad \text{Eqn 8}$$

2.2 Computer model

A computer model was developed that could be used to evaluate the inelastic dynamic behaviour of a face-loaded URM wall.

The model allows the wall to deform as indicated in Figure 1(a). Opening of cracks at mid-height and at the base of the wall is accommodated by the link members that buckle when subjected to any compressive load.

The model was analysed using the inelastic dynamic analysis program Ram Xlinea which incorporates DRAIN-2DX Version 1.1. The program uses time step-by-step numeric integration to perform inelastic dynamic analysis.

2.3 Period of Free Vibration Response

Previous research (Blaikie, Spurr, 1992) showed that if a face loaded wall specimen is displaced as indicated in Figure 1(a), the free damped response of the wall will be similar to that shown in Figure 3.

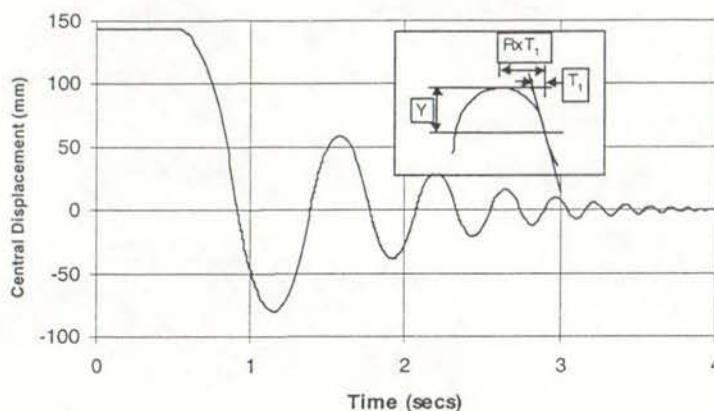


Figure 3: Free Damped Response of Face Loaded Wall Specimen

It can be seen that the free vibration period of the wall decreases with decreasing lateral wall displacement.

The peak potential energy stored in the wall at a displacement Y can be calculated with reference to Figure 2.

$$\begin{aligned}
 E_o &= (V_{\max} + V) \frac{Y}{2} \\
 &= V_{\max} \left(2 - \frac{Y}{Y_{\max}} \right) \frac{Y}{2}
 \end{aligned}
 \tag{Eqn 9}$$

This peak potential energy will be equal to the peak kinetic energy, E_k , stored in the wall at zero displacement (if losses are ignored).

$$\begin{aligned}
 E_k &= \frac{MV_o^2}{2} \quad \text{and therefore} \\
 V_o^2 &= \frac{3YV_{\max}}{M} \left(2 - \frac{Y}{Y_{\max}} \right)
 \end{aligned}
 \tag{Eqn 10}$$

Where V_o is the maximum velocity at the centre of the wall at zero displacement and M is the total mass of the wall.

It was also established as part of the previous research (Blaikie, Spurr, 1992) that the shape of each of the half cycles in the response was practically independent of the peak displacement and the thickness of the wall for walls of a constant height to thickness ratio.

This property of the half cycle response is illustrated in the inset diagram in Figure 3. From the diagram it can be seen that the full cycle period is given by:

$$T = 4RT_1 \tag{Eqn 11}$$

where $T_1 = \frac{V_o}{Y}$ and the Period Shape Factor, R , has a constant value of approximately 2.45.

Substituting for T_1 and then V_o in Eqn 11, the period of the wall free vibration, when the peak displacement is $0.6Y_{max}$, is given by:

$$T = \sqrt{\frac{0.0014 Y_{max} W}{V_{max}}} \quad \text{Eqn 12 (a)}$$

where V_{max} and Y_{max} are given by Eqn 3 and Eqn 4 and the units are kN and mm

Substituting for V_{max} and Y_{max} yields an alternative version of Eqn 12(a):

$$T = \sqrt{\frac{0.7H}{1 + 2\frac{O}{W}}} \quad \text{Eqn 12(b)}$$

Where units for the wall storey height, H is in meters.

This period of the wall response can be used in conjunction with a displacement spectrum to help predict the seismic stability of face loaded URM walls.

2.4 Face Loaded URM Wall Behaviour with Top Fixity

In Figure 1(a) the overburden load is shown acting at the centre line of the wall. If the overburden load is due to a floor slab that extends to the outside face of the wall, or is due to an upper storey wall that does not crack and displace significantly, the overburden load can move to the outer face of the wall. This would provide fixity at the top of the wall similar to that shown at the base of the wall in Figure 1(a). An additional restraining moment of $O/2 \times t/2$ would then need to be included at the top of the bending moment diagram shown in Figure 1(b).

In this case it can be shown simply that the term $(W + 1.5O)$ in equations Eqn 3, Eqn 4, and Eqn 8 (used to calculate V_{max} , Y_{max} and C_d respectively) becomes $(W+2O)$. Therefore, where the wall has top fixity, these parameters increase by a top fixity factor, F_{top} given by:

$$F_{top} = \frac{1 + 2\frac{O}{W}}{1 + 1.5\frac{O}{W}} \quad \text{Eqn 13}$$

It will be shown that the seismic resistance of a face-loaded wall is proportional to Y_{max} and C_d so that the resistance can be expected to increase by F_{top} where the wall has top fixity. However, as the ratio of Y_{max}/V_{max} does not change, Eqn 12(a) can still be used to calculate

the period of the wall motion at 60% of the collapse displacement, Y_{max} , providing it can be shown that the Period Shape Factor, R , is not effected by top fixity.

2.5 Effect of Top Fixity, Slenderness and Overburden Load on Free Vibration Response Period

Previous research (Blaikie, Spurr, 1992) established that the Period Shape Factor, R , is independent of the wall thickness for walls of the same slenderness ratio.

To establish that the Period Shape Factor, R , is also independent of overburden load, slenderness ratio and top fixity, the free vibration response of a number of face-loaded wall models were evaluated. For each of the free vibration responses the Period Shape Factor, R , was evaluated by rearranging Eqn 11. The results are shown in Figure 4.

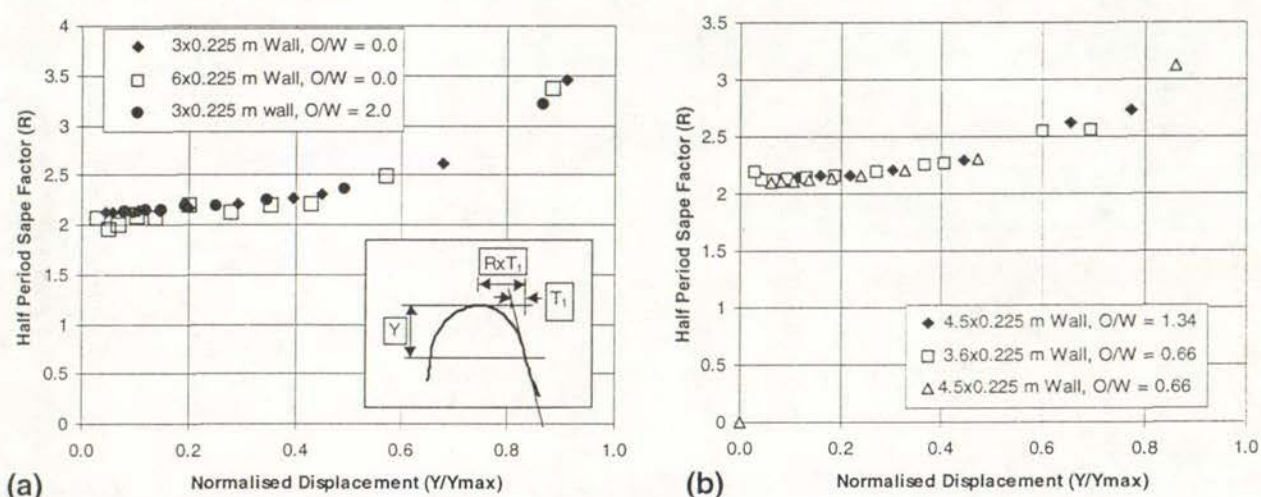


Figure 4: Insensitivity of Period Shape Factor, R , to Wall Slenderness and Overburden Load (a) Without Top Fixity, (b) With Top Fixity

It can be seen that for peak displacements less than 60% of the instability displacement, Y_{max} , R is insensitive to wall slenderness, overburden load and top fixity. It can also be seen that a constant value of R , of approximately 2.45, is applicable when the peak amplitude of the motion is $0.6 Y_{max}$.

This establishes that a relatively simple equation (Eqn 12) can be used to calculate the period of the motion of a face-loaded URM wall when the peak displacement is $0.6 Y_{max}$ and that the formula is independent of wall slenderness, overburden load, top fixity or wall thickness.

3 Laboratory Tests

3.1 Introduction

As part of the previous EQC funded project (Blaikie, Spurr, 1992), inelastic dynamic analysis methods were used to model the seismic behaviour of a face-loaded URM wall. The wall was modelled as uncracked except for cracks at the diaphragm levels and mid-storey height. These cracks were free to open and close as the wall deflected under lateral loads.

This computer model was used to predict the behaviour of a laboratory test specimen that was part of the pioneering USA investigation into the behaviour of URM (ABK, 1981). Agreement between the predicted and observed displacements of the wall specimens was good given the uncertain nature of the input motion used in the ABK test. This demonstrated that the model could be used to predict the behaviour of face-loaded URM walls. However, the detailed response predicted by the computer model was sensitive to both the damping assumed and small changes in the earthquake motion. Therefore, uncertainty in the actual motion used in the ABK tests meant that the appropriate damping to use in the model could not be determined.

The model also indicated that, for rigid floor diaphragms, very high anchorage forces could develop between the wall and supporting floor diaphragms. These high anchorage forces are associated in the model with the impact that occurs when the wall cracks close.

A laboratory test was, therefore, carried out to establish appropriate levels of damping to use in the computer model and to investigate whether the high anchorage forces would be realised in practice. It was also intended that the test would demonstrate that the computer model could be used to predict the dynamic behaviour of a cracked face loaded URM wall and hence increase confidence in the results predicted by the computer modelling.

3.2 Test Specimens

The face loaded wall test specimen was nominally 3.0m high, 230mm thick and 490mm in length. Recycled old bricks were used to construct the wall.

For the first test, horizontal cracks were partially formed at the base of the wall specimen and at mid-height. At the base joint the bricks were coated with a bond breaker (2 coats of Rohm and Haas Primal AC-6501M acrylic emulsion) agent before placing the first course of bricks on the mortar joint that had been spread on the strong-room floor. At the mid-height joint the bricks were coated with the bond breaker before placing the mortar joint. For this test, the mortar in the vertical joints was continuous across the pre-formed joints.

The second test reused the first test specimen but the mortar in the pre-formed horizontal joints was replaced with a weaker mortar intended to duplicate the properties of, say, an

aged weak lime mortar. In this case the pre-formed joints were made continuous across the full wall cross section using computer paper soaked in CRC 556. Properties of the mortar are given in Table 1. The first test mortar was designed to be intermediate between a 1:3 cement mortar and a 1 : 1 : 6 mortar common in New Zealand between 1900 and 1930. The second test mortar was designed to have properties similar to a 1 : 3 lime mortar with a quarter of the lime replaced with cement to mimic the long term strength gain of a lime mortar.

Table 1: Mortar Properties:

Properties Mortar	Test 1	Test2 *
Lime : Cement : Sand	1 : 2 : 9	3 : 1 : 12
Compressive Strength (200x100 cylinder) MPa	14.0, 13.5, 14.0, 14.0	2.0, 2.0, 2.0
Age of Mortar at time of Testing cylinders and specimen	28 days	22 days
Average Modulus of Elasticity - GPa	11.0	2.5
Nail Punch Penetration – top half wall** (mm)	12, 10, 11	Not available
Nail Punch Penetration–bottom half wall** (mm)	18, 16, 11	Not available
<p>* Opening joint mortar courses only.</p> <p>** 6 firm blows on a 3 mm ended nail punch with a builders hammer in vertical mortar joints. A similar test on the lime mortar of a Dannevirke building varied between 11 and 35 with an average of 19.1mm penetration. As a further indicator of mortar quality, with moderate pressure and twisting (10-15 turns) a car key penetrated 2 mm into Test 1 mortar and only 5 mm into the mortar used for Test 2.</p>		

The faces of the brickwork were irregular relative to a vertical plane, particularly on the rear (South) face. The faces were measured, adjacent to the 4 corners, relative to a straight line set 8mm off the top and bottom bricks. The relative position of the top and bottom bricks in each corner was also measured relative to a plumb bob. The 2 sets of corner measurements on each face were averaged to define an average face location for each brick course. These measurements allowed the centroid of each course of bricks to be determined relative to a vertical centre line through the middle of the base joint.

After the test, the upper and lower halves of the wall were weighted and this permitted the mass of each brick course to be computed assuming a uniform course depth, density and wall length for the 2 halves of the wall.

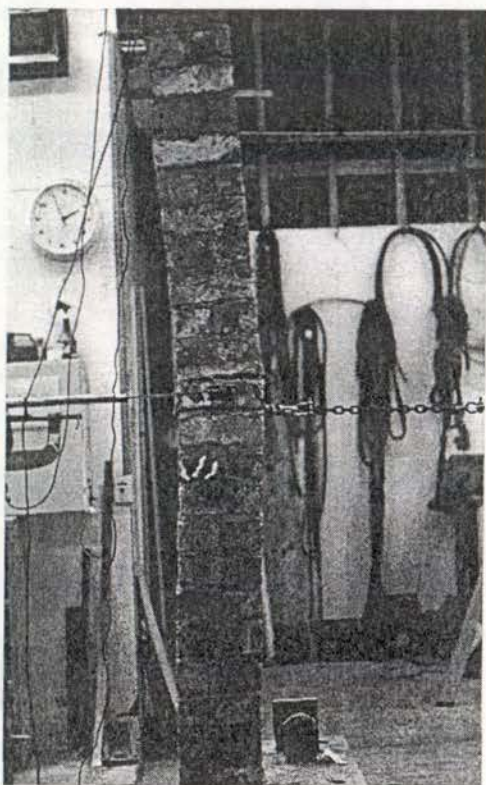


Photo 1: Test Specimen During Static Loading

3.3 Loading Procedure

The test specimen was loaded horizontally via an anchor fixed through the wall just below the mid-height opening joint. The anchor was connected to a hand operated hydraulic jack via a chain incorporating a load cell.

The first test specimen was subjected to 3 load cycles. The first load cycle took the wall up a point where the base and mid-height cracks opened (load of approx. 3.982 kN). The next cycle was up a mid-height wall displacement of approximately 6mm. This cycle was used to evaluate the initial elastic properties of the wall. For the third test cycle the centre of the wall was displaced approximately 143 mm then released so that the wall's free damped response could be recorded. This dynamic part of the test was then repeated. Photo 1 shows the test specimen during the static part of the loading.

The second test specimen (first test specimen with weak mortar in the opening joints) was only subjected to a single load cycle. The wall's static response was recorded during the initial loading up to a central displacement of approximately 160mm. The wall was then released and its dynamic response recorded.

3.4 Recorded Measurements

The wall's horizontal displacements were measured on both sides of the specimen approximately 25 mm below the mid-height opening joint and near the centreline (at mid-thickness) of the wall. For the second test the mid-height displacement was also recorded on the rear face of the specimen for the first 10mm of static displacement.

Horizontal movements of the wall near the top and bottom of the specimen were also recorded on one side of the specimen near the mid-thickness centreline of the wall.

The top of the wall was connected to a heavy reaction frame using a load cell. The load cell was formed from 12.7 OD stainless steel tube with a wall thickness of 0.9mm. It was approx. 450 mm long and connected to the load frame and top of the wall with rod end ball joints to virtually eliminate bending stresses in the load cell.

Vertical accelerations were also recorded at the top of the wall during the dynamic part of the test.

3.5 Computer Modelling of Test Specimens

Figure 5 shows diagrammatically the computer model used to analysis the test walls. The corresponding Drain2dx input file is shown in Appendix A. The input file gives details of the wall geometry and properties of the elements used to model the test 1 wall specimen. The numbers given in the diagram correspond to the node numbers in the input file.

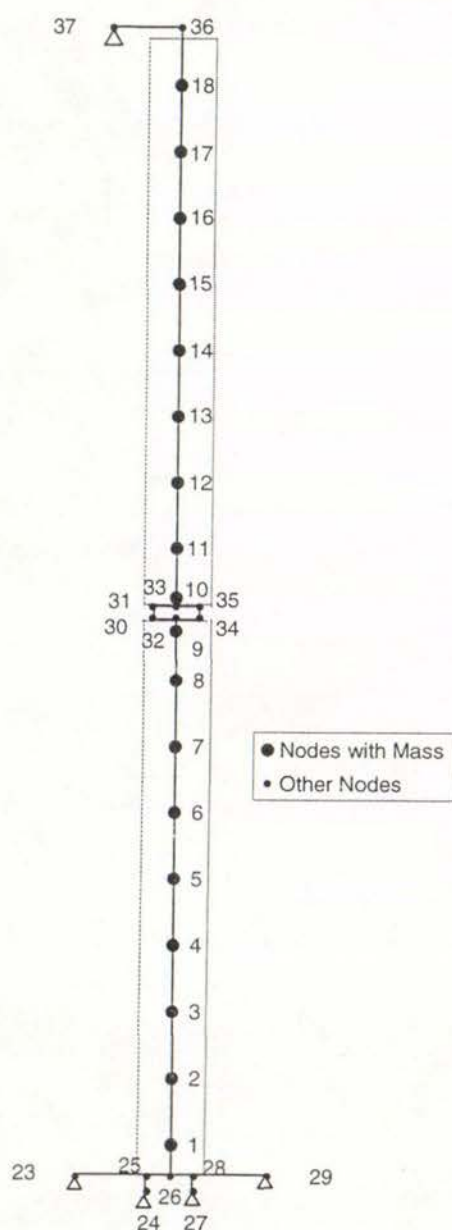


Figure 5: Computer Model used For Test Specimen 1

The model allows the wall to deform as indicated in Figure 1(a). Opening of the cracks at the mid-height and base of the wall is accommodated by link members that can only carry compressive forces. These are shown at an exaggerated vertical scale in the diagram for clarity and were actually modelled as only 2 mm long.

The model is similar to that used in the previous research project (Blaikie, Spurr, 1992) except that the current model includes rotational mass inertia elements at each of the mass nodes. The previous model also used truss members buckling in compression in place of the link members and had fewer mass modes.

The horizontal support conditions at the base of the wall were also modelled using link members that were only able to carry compressive forces.

The horizontal support member at the top of the wall modelled the load cell member located at this position on the test specimen.

A compacted computer model was also used to evaluate the effect of reducing the number of nodal masses used to model the wall mass from 18 to 10. In this model the 8 pairs of nodes between nodes 1 to 8 and 11 to 18 were combined into 8 single nodes at the centroid of each node pair. The masses at nodes 9 and 10 were also relocated at nodes 32 and 33 on the mid-height crack.

The computer model used for the test specimen 2 was similar to that used for test specimen 1.

However, when the 2 mortar joints in specimen 1 were replaced to construct specimen 2, the wall centroid had a slope away from the loaded face of approximately 20 mm at the top of the wall. The wall also had a small additional kink towards the loaded face (i.e. compared with the measurements made for test specimen 1 and relative to a straight line joining the top and bottom of the wall, the upper and lower parts of the wall were offset 1.5 and 4.1 mm respectively towards the loaded face at the mid-height joint). Adjustments to the geometry of the computer model were made to allow for these differences in specimen geometry.

3.6 Results for Test Specimen 1

Figure 6 shows the test results for the static loading of wall specimen 1. The wall behaviour that was predicted by a push over analysis using the computer model is also shown. The first plot, Figure 6(a), shows the behaviour for the second loading cycle up to a central wall displacement of 6 mm. The second plot, Figure 6(b), shows the behaviour for the third loading cycle up to the displacement of 142mm prior to releasing the wall for the dynamic test.

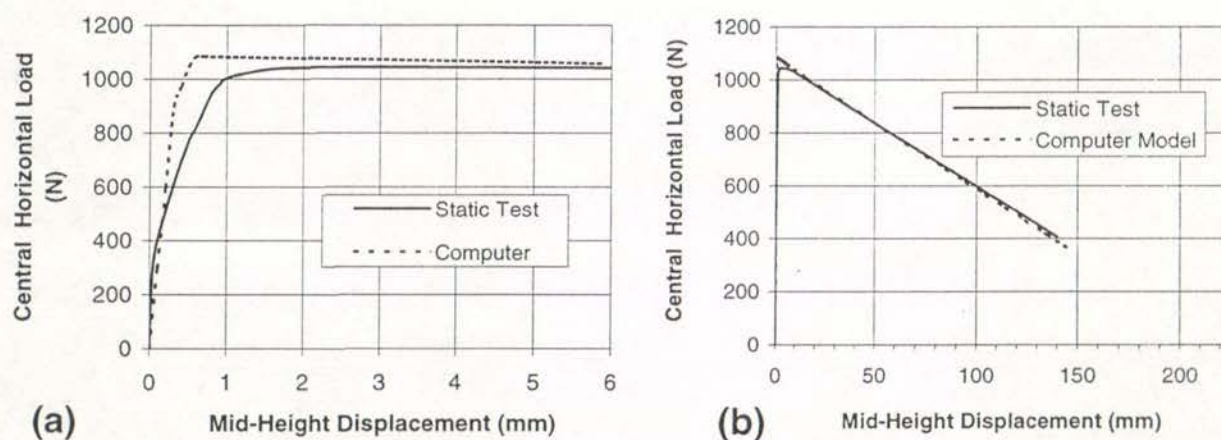


Figure 6: Static Push Over Test Specimen 1 and Behaviour Predicted by Computer Model (a) for first 6 mm of displacement (b) up to maximum test displacement

In the first plot a change of slope can be seen test specimen displacement prior to the maximum load being reached. This corresponds to the mid-height crack opening. The maximum load is reached when the crack at the base of the wall opens. It can be seen that the computer model predicts the mid-height crack will open latter in the loading cycle than actually occurred in the test. This is probably due to the load cell at the top of the wall carrying some load after the first load cycle that was used to initially crack the wall. Some initial tensile load in the load cell would have caused additional bending in the wall at mid-height and resulted in early opening of the crack at this position. Unfortunately the load in the top load cell was only recorded during the dynamic loading cycle so that this could not be confirmed. However, it was observed that after the initial cracking cycle the

wall had a residual deflection of 4 mm (towards the loaded face and away from the load cell support frame) which is consistent with residual tension in the load cell.

In the second plot, Figure 6(b), it can be seen that the initial elastic displacement of the wall was not significant compared with the displacement imposed on the wall before the wall was released for the dynamic test. If the falling branch of the plot is projected to the horizontal axis it can be seen that instability of the wall would occur at a central displacement of approximately 225mm. This was the effective thickness of the wall used in the computer model and is significantly less than the nominal thickness of the opening joints measured in the test specimen. The measured average nominal thickness of the wall at the base joint and mid-height joints were 234mm and 232mm respectively. This indicates that an equivalent rectangular stress block for the opening joints would have had a depth of 5 to 9mm. Assuming an average stress of 85% of the measured crushing strength of the mortar given in Table 1, the calculated stress block depths are only 0.6 and 1.2 mm at the base and mid-height respectively. This suggests that calculated stress block depths are likely to be unrealistic and non-conservative.

Figure 7 presents the response of Test Specimen 1 after it was released from its maximum displaced position. The wall response predicted by the computer model is also shown.

Figure 7(a) shows the horizontal displacement response just below the central opening joint (at the level where the displacement was measured in the test). To impose the initial peak displacement during the computer modelling, an acceleration pulse was applied to the supports for a short period (0.2 seconds). This initial pulse would have had no effect on the response that followed the first peak.

To obtain the excellent agreement between test and predicted displacements shown in Figure 7(a), the magnitude of the initial acceleration pulse and the damping used in the model were adjusted using an iterative process. The final mass and stiffness damping values used for the plot were $\alpha = 0.18$ and $\beta = 0.0006$ respectively.

The agreement shown in Figure 7(a) demonstrates that the computer model can be used to model the dynamic displacement response, and hence the seismic stability, of a URM face-loaded wall.

Figure 7(b) shows the reaction measured at the top of the test specimen. It can be seen that peak reactions occur just after the impact associated with crack closing. Crack closing corresponds to the times in Figure 7(a) when the displacement is zero. Unfortunately the data logger truncated the peak reactions at 975 N although this did not effect the reading for the first impact. A rerun of the dynamic test, with the data logger reset, yielded a peak reaction of 1450 N. It is interesting that this maximum occurred on the fifth impact and not the first impact as would have been expected.

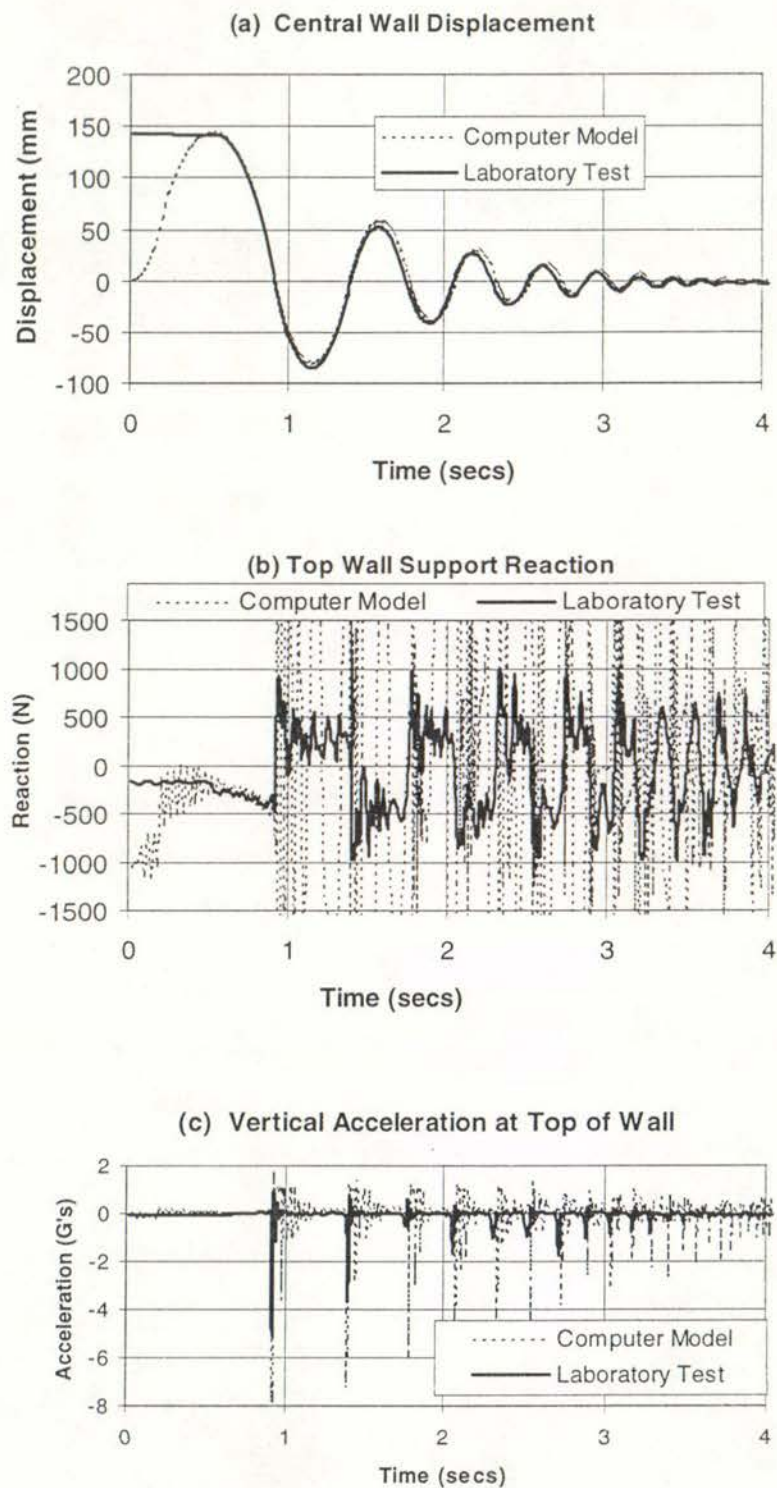


Figure 7: Free Vibration Test Results for Specimen 1 and Comparison With Response Predicted by Computer Model, (a) Displacement Response at Mid-Height of wall (b) Horizontal Reaction at Top of Wall and (c) Vertical Acceleration at top of Wall

The reactions at the top of the wall predicted by the computer model are also shown in Figure 7(b). The plot of the reaction predicted by the computer model is truncated so that the more important reaction measured in the test is shown in more detail. The maximum reaction predicted by the model was 6500 N, which was considerably greater than that measured.

This indicates that the model can not be used to predict the diaphragm reaction forces associated with impact. However, it should be noted that the measured maximum diaphragm reaction force of 1450 N is 560% of that calculated from Eqn 3, the maximum expected under static loading conditions when the joints in the wall just open. *This demonstrates that impact forces can not be ignored when evaluating diaphragm anchorage forces where the diaphragm is rigid and the anchorage load path contain brittle components.*

Figure 7(c) shows the measured and predicted vertical acceleration response at the top of the wall. For the first impact the predicted peak acceleration of 7.8 G is significantly greater than the measured maximum acceleration of 5.25 G.

The high frequency accelerations and forces in the model mainly effect the damping of the system and can be modelling using appropriate damping coefficients. The poor prediction of their magnitude using the computer model does not prevent the model being used to predict the displacement response and hence the seismic stability of URM walls.

Measurements of the horizontal displacement at the top and bottom of the test specimen 1 during the dynamic response, indicated that no significant residual movement occurred at these locations. Also, an inspection of the two opening joints after completion of the testing provided very little evidence that the wall had been subjected to 142 mm of displacement and a number of impact cycles. In fact the cracks were hard to detect!

3.7 Modelling Test Specimen 1 With Reduced Number of Nodal Masses

Figure 8 shows the effect on the predicted free vibration response of test specimen 1 of reducing the number of nodal masses used in the computer model from 18 to 10. The effect of not including rotational inertia component at each of the nodal mass locations is also shown.

To obtain the good agreement between the response predicted by the 18 and 10 nodal mass models the coefficient for the stiffness damping had to be increased from $\beta = 0.0006$ to $\beta = 0.0008$. It can be seen that excluding the rotational inertia from the model is also equivalent to a small reduction in effective damping.

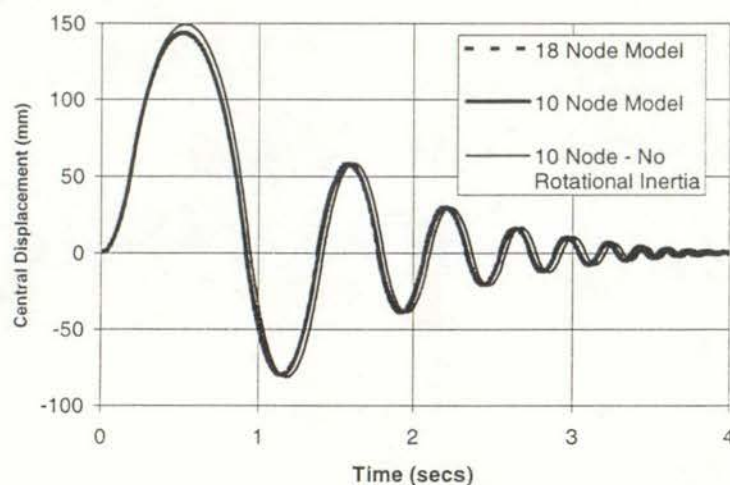


Figure 8: Free Vibration Response of Test Specimen 1 Predicted by Model using Reduced Number of Nodal Masses and Without Inclusion of Rotational Inertia

Given the small difference between the response predicted by the 18 and 10 nodal mass models the 10-node model was adopted as the basic configuration for modelling all other non-test specimen URM walls for this research project.

3.8 Results for Test Specimen 2

Figure 9 shows the test results for the static part of the loading cycle used for test specimen 2. The response of the wall predicted by the computer model is also shown.

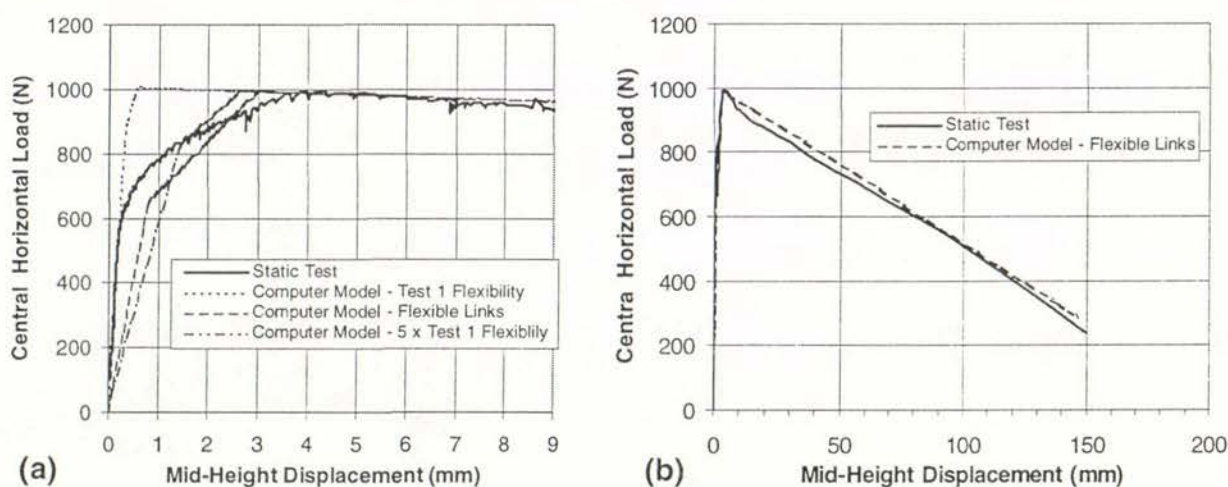


Figure 9: Static Push Over Test Specimen 2 and Behaviour Predicted by Computer Model - (a) for first 9 mm of displacement and (b) up to maximum test displacement

Three plots of the response up to 9mm mid-height displacement as predicted by the computer model are shown in Figure 9(a). The first assumed the same wall and link element flexibility as used to model test specimen 1. The second assumed the links (used to model the opening cracks) had fifteen times the flexibility and the wall elements had 100 times the flexural stiffness. The third plot assumed the wall and link element flexibility were both 5 times that used to model test specimen 1.

The flexible link model gave the better prediction of when the mid-height crack opened (first change of slope). However, the model using 5 times the flexibility that was used to model test specimen 1 was adopted for the model used to predict the dynamic behaviour of test specimen 2 as it gave better control over damping and the numeric stability during the analysis. Trial analyses using either the test 1 flexibility or 5 times this flexibility made very little difference to the earthquake resistance predicted by the model. This is not surprising when the initial elastic displacement at maximum load is compared with the instability displacement in Figure 9(b).

Figure 9(b) indicates that instability would be expected at a displacement of about 200mm, and this was adopted as the effective thickness of the wall used for the computer model. As the wall had a nominal thickness of approximately 230mm this indicates an average equivalent stress block depth of 30mm in this case. This can be compared with computed equivalent stress block depths (making the same assumptions used for test specimen 1 above) of only 4.2 and 8.4 mm at the base and mid-height of the wall respectively.

Figure 10 shows the response of test specimen 2 for the free vibration part of the load cycle. The motion is more heavily damped and the impact forces and vertical accelerations are of lower magnitude than those measured for test specimen 1.

It can be seen from Figure 10(a) that the test specimen motion practically damped out after the third impact (third crossing of the zero displacement line). To obtain the best prediction of the motion up to this point an effective wall thickness of 200mm (as indicated by the static test) and mass and stiffness damping coefficients of $\alpha = 0.6$ and $\beta = 0.04$ respectively were used in the computer model.

In retrospect it may have been better to repeat the static part of the test after the dynamic test to determine the effective wall thickness after dynamic testing and to have used an intermediate effective wall thickness to model the dynamic part of the load cycle.

Inspection of the test specimen at the end of the dynamic test indicated that the base of the wall had moved approximately 10 mm towards the loaded face and 10 mm laterally towards one side. At the mid-height crack, offsets at the corners of the joint of 1 to 2mm, indicated that the top half of the wall had rotated relative to the bottom half of the wall. There was also some evidence of minor spalling and crushing near the faces of the opening joints. This spalling was more evident at the base joint than at the mid-height joint.

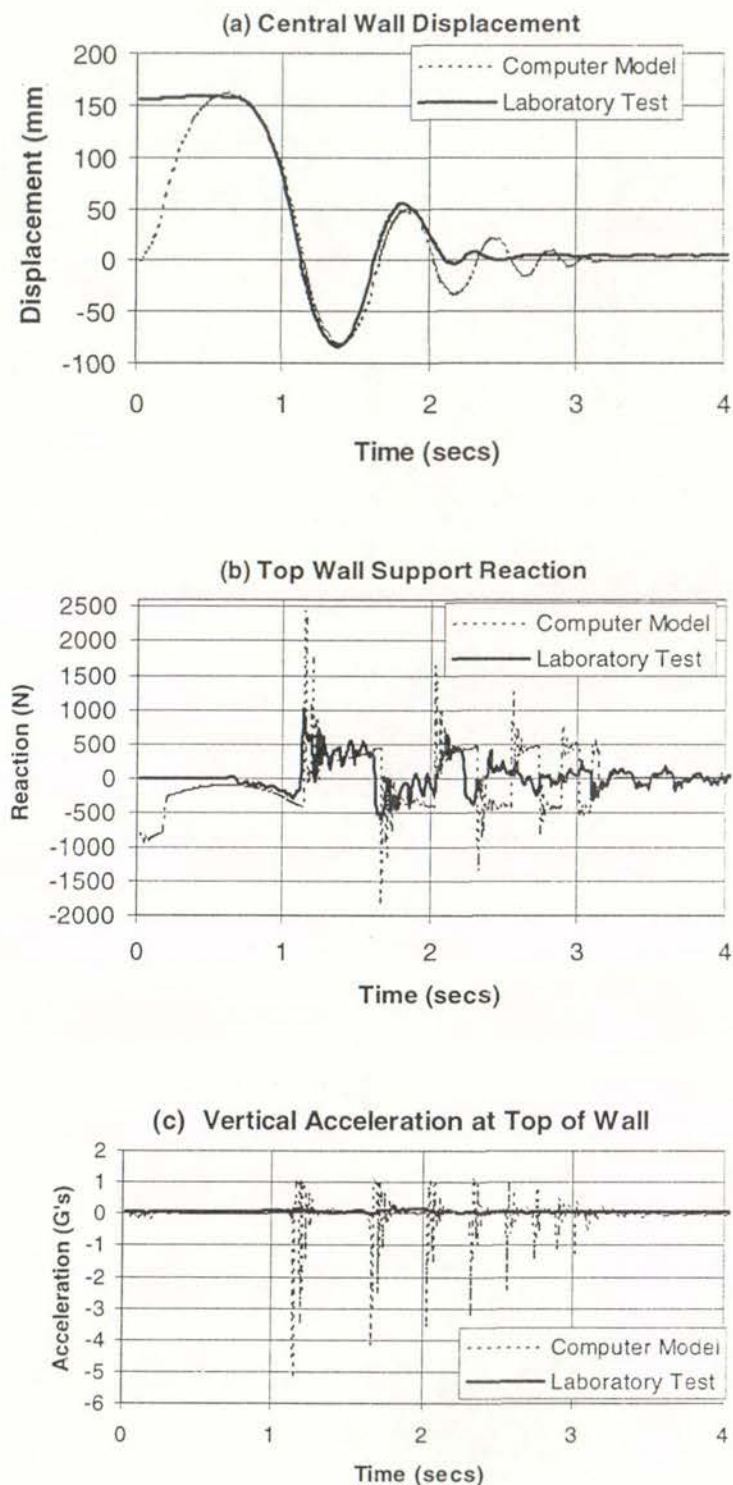


Figure 10: Free Vibration Test Results for Specimen 2 and Comparison With Response Predicted by Computer Model, (a) Displacement Response at Mid-Height of wall (b) Horizontal Reaction at Top of Wall (c) Vertical Acceleration at top of Wall

Some trial analyses to determine the seismic resistance of face-loaded walls indicated that the additional damping due to the movements and spalling at the opening joints may be sufficient to compensate for the smaller effective wall thickness. However, these trial analyses were only carried out for the conditions that apply in a rigid building with rigid diaphragms.

3.9 Modelling Energy Loss and Damping

For a face loaded URM wall the main source of damping will be the energy loss that occurs on impact as the opening joint cracks close. Drain2dx attempts to ensure that no energy loss occurs during each time step during the analysis except for the work done by viscous damping. Therefore the energy losses in Drain 2dx occur through out the response and not just at impact.

Some of the problems associated with modelling the damping of an URM wall have been discussed as part of previous research (Blaikie, Spurr 1992). These included:

- Stiffness damping of the link elements must be set to zero or the opening joints will lock up as stiffness damping in Drain2dx is based on the high initial stiffness of these elements not their secant stiffness.
- Additional damping can occur in the model because Drain2dx bases geometric stiffness on the static loads acting on the wall and does not update this stiffness to allow for the effects of vertical impact forces. Varying the proportion of the vertical inertia modelled can control the amount of this "numeric damping" as the amount of vertical inertia determines the magnitude of the impact forces.
- The logarithmic decrement method of defining the amount of damping in the system is not applicable to inelastic systems especially where strength declines rather than increases with displacement.
- Mass damping is dependent on nodal mass and velocity. It is most effective for larger amplitude cycles when the nodal velocity is higher.
- Inclusion of stiffness damping has more effect on the damping of the model response than would be expected from considering an equivalent elastic system. This seems to be related to the high frequency vibrations generated by impact in the model. The energy associated with these high frequency vibrations is mainly stored in the wall elements and is effected by the flexural stiffness used to model the wall elements. The magnitude of the impact forces is primarily determined by the axial stiffness of the link elements and by the proportion of vertical inertia included in the model. By varying these parameters and evaluating their effect on the free vibration response of the wall the amount of damping in the model can be adjusted to the required amount.

The 10 nodal mass model used to model test specimen 1 was further simplified to have a uniform mass distribution up the wall and a straight vertical mid-thickness centroidal axis. The first row of Table 2 shows the peak amplitudes predicted by this model for successive

half-period cycles of a free vibration response. The second row of the table shows the velocity at the mid-height of the wall just before and after impact, computed using Eqn 10.

By definition the coefficient of restitution, e , is the ratio of the walls angular velocity after impact compared with that before impact. If the small elastic displacements of the wall are ignored (i.e. rigid body rotations are assumed) e will also equal the ratio of mid-height wall velocity after impact compared with that before impact. The resulting values for e computed for each impact is also shown in the table and can be seen to be remarkably constant.

For the first 7 impacts when the peak displacement varied between 90% and 5% of the wall effective thickness, the coefficient of restitution only varied between 0.84 and 0.86 and averaged 0.85. As the energy loss on each impact = $1-e^2$ this indicates that a constant 28% of the energy stored in the wall was lost on each impact.

Table 2: Calculation of Coefficient of Restitution for Test Specimen 1 Modified Model

Item	Impact Sequence from start of Free Vibration Response				
	1	2	3	4	5
Peak amplitude Before/After impact (mm)	205/102	102/66	66/45.4	45/32.4	32/23.5
Mid-height Velocity Before/After impact *	.99/.83	.83/.70	.70/.60	.60/.51	.51/.44
Coefficient of Restitution for impact	0.84	0.85	0.85	0.86	0.86

* Velocity calculated using Eqn 10 (m/sec)

When similar calculations were carried out for the actual test specimen 1 and the unmodified computer model responses shown in Figure 7(a), the average coefficient of restitution for the first 6 impacts was similar. However, the individual impact values varied for the 2 displacement directions about the wall mid-thickness centreline. The difference between the 2 computer models suggests that departure from geometric mass symmetry can effect the individual impact results. The differences between the model and test specimen results suggest that some re-zeroing of the geometry is occurring after each impact. This is discussed further in the next section of the report. When successive impact values for the 2 displacement directions were averaged for the first 6 impacts, the average values were (0.83, 0.86, 0.87) and (0.85, 0.86, 0.86) for the test specimen and unmodified computer model respectively.

For rocking bodies the coefficient of restitution is not only dependent on the properties of the impacting surfaces. It can be easily demonstrated by simple desktop tests that the motion of a squat rocking body damps out more quickly than that of a similar slender body. This characteristic of rocking bodies is a result of only the vertical component of a wall momentum changing at impact. In squat walls this component makes up a larger

proportion of the total momentum (and energy) stored in the wall. Energy losses, and therefore damping, are greater for squat walls.

It has been established (Yim et al, 1980) that, for the idealised conditions of a rigid block rocking on a rigid base with inelastic impact, the coefficient of restitution is given by:

$$e = 1 - \frac{3}{2} \sin^2 \theta \quad \text{Where } \theta = \tan^{-1} \frac{2t}{H} \quad \text{Eqn 14}$$

The slenderness term t/H used in the original formula has been replaced by the term $2t/H$ in Eqn 14 to allow application of the formula to a face loaded wall which is essentially 2 rocking blocks of half the wall slenderness. In the formula the second term represents the proportion of the vertical component of the momentum that is stored in the wall at impact.

When Eqn 14 is used to calculate the value of e for the same wall slenderness to which the values in Table 2 apply, a value of 0.967 is obtained. This is significantly higher (i.e. represents lower damping) than the average value of 0.85 obtained for the test specimen 1 Model in Table 2.

In this project, the damping used to model a wall with a different slenderness to that tested was obtained by adjusting the coefficient of restitution obtained for test specimen 1 (0.85) using the ratio of the coefficients of restitution calculated for the 2 walls using Eqn 14. For more slender walls the full reduction in damping was applied but for more squat walls only half the increase in damping (i.e. adjustment of e) was applied to be conservative.

An iterative procedure was used to adjust the damping in the computer model. The e value expected for the free vibration response of the wall was calculated. Adjustments were then made to the modelled mass and stiffness damping coefficients, the vertical inertia, the wall flexural stiffness and the link axial stiffness until the target e value was approached for the main impacts associated with crack closing. Only impacts where the mid-height displacement of the wall model was greater than 5% of the wall thickness were considered.

It is not clear to the author what effect a higher overburden load would have on damping. It may increase the proportion of vertical momentum in the system and hence increase the amount of damping. However, recent tests in Australia have indicated that "energy losses are only slightly higher for wall with applied overburden" (poster presentation, 12WEEC conference Doherty K et. al., 2000). The influence of overburden load on potential damping was, therefore, not considered further.

For test specimen 2, using weak mortar in the opening joints, the calculated values of e for the first 2 impacts of the computer modeled response were 0.81 and 0.83. These are only a modest reduction on the corresponding values of 0.84 and 0.85 obtained for the stronger mortar used for test specimen 1.

3.10 Australian Free Vibration Test Results

Extensive testing and modelling of thin unreinforced masonry walls has recently been carried out in Australia (Doherty K et. al., 2000). Results of some of the free vibration tests carried out as part of this research were supplied to the author in private correspondence.

Coefficients of restitution values calculated from the test results obtained from the free vibration test of a 1500x110-mm test specimen are shown in Table 3.

Table 3: Coefficient of Restitution Calculated for Australian Test Specimen

Item	Impact Sequence from start of Free Vibration Response					
	1	2	3	4	5	6
Coefficient of Restitution for impact:						
- Without baseline adjustment	0.88	0.83	0.93	0.82	0.80	0.94
- With baseline adjustment	0.87	0.85	0.89	0.87	0.85	0.90

The first row of results are as supplied and indicate that damping varied for the 2 displacement directions about the wall mid-thickness centreline. If a 1.0mm shift is made in the reference point from which the wall displacements were measured, the results are more uniform as indicated in the 2nd row of values in the table. This may indicate that a small amount of impact damage to the mortar in the joints is effectively re-zeroing the initial geometry of the test specimen after each impact.

Applying the baseline adjustment increases the average e value for the 1st six impacts from 0.86 to 0.87. These values are slightly higher than the average e value of 0.85 calculated for test specimen 1 and indicate a slightly lower level of damping. The Australian test specimen was only slightly more slender but was constructed using softer mortar (1:1: 6 mix with effectively $\frac{1}{4}$ the cement replaced with lime). Therefore, a higher level of damping would have been expected. *This indicates that thicker walls of the same slenderness may have marginally higher damping.*

4 Prediction of Face Loaded Wall Stability Using Response Spectra

4.1 Prediction of Wall Stability using a Displacement Spectrum

The stability of a face-loaded wall depends mainly on the displacement at the mid-height of the wall so that it seems logical to use a displacement response spectrum to help predict the earthquake intensity required to cause collapse. This approach assumes that the wall's elastic response is sufficient to open the mid-height crack in the wall by a significant margin.

A pseudo displacement response spectrum can easily be derived from an acceleration design spectrum using the relationship:

$$Y = (T / 2\pi)^2 A \quad \text{Eqn 15}$$

where A is the spectral acceleration (in m/sec^2) for a SDOF elastic oscillator with period T and Y is the pseudo spectral displacement.

The resulting pseudo displacement spectrum for the Basic Seismic Hazard Spectra given in New Zealand's loading code for intermediate soils is shown in Figure 11

A computer program (WAVE) was used to modify the 1st 15 seconds of acceleration time history of the 1940 El Centro NS earthquake motion so that its 5% damped spectra more closely matched the Basic Seismic Hazard Spectra. This modified earthquake record is referred to in this report as the NZS4203 earthquake motion. Spectra for this EQ motion are also shown in Figure 11.

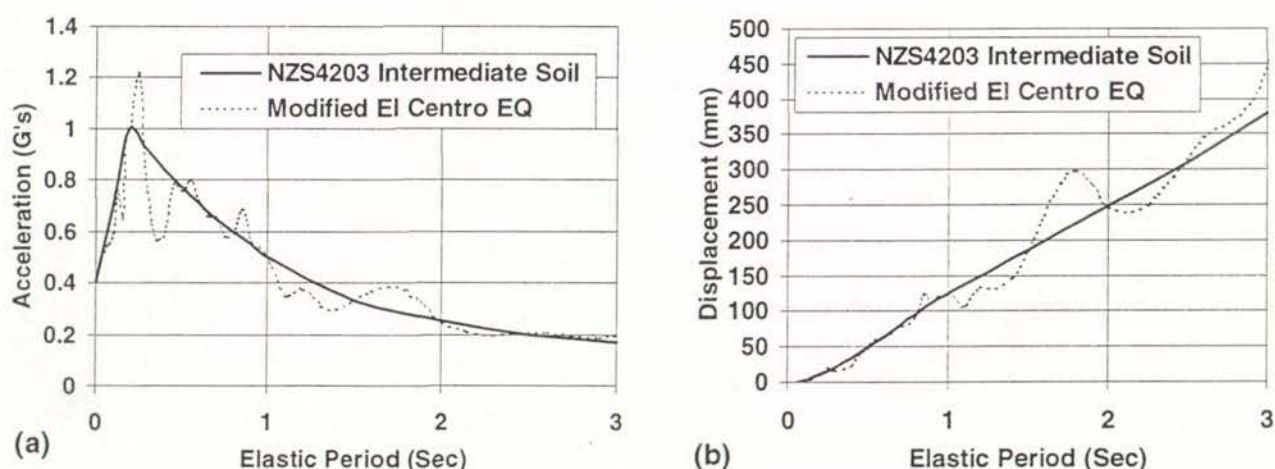


Figure 11: Elastic Displacement Response Spectra for NZS4203 Design Earthquake (Intermediate Soils – 5% damping) and the El Centro EQ Record modified to match NZS4203
(a) Acceleration spectra and (b) Pseudo Displacement spectra

It can be seen from Figure 2 that a smaller increment of energy input is required for an incremental increase in displacement as the central deflection of a cracked face loaded wall increases. When the wall is displaced beyond about $0.6Y_{max}$ only a small additional adverse acceleration pulse is required to make the wall unstable and the stability of the wall becomes somewhat erratic. Therefore, it is proposed that the displacement response spectra be used to predict the earthquake intensity required to generate a peak wall displacement of $0.6Y_{max}$. Collapse is then assumed to occur at about 20% greater earthquake intensity as indicated by the computer analysis results.

If the cracked wall was responding elastically to an earthquake motion, the peak displacement at the centre of the wall would be 1.5 times that predicted using a SDOF displacement response spectrum (i.e. a modal participation factor of 1.5). Therefore a factor of 1.5 is used to scale the 5% damped spectral displacements and predict the displacement expected at mid-height of the wall. Because the response is inelastic and the damping is not 5% this procedure could be expected to give results that are conservative relative to the envelope of results predicted using the computer model. It therefore includes a safety factor.

A summary of the calculations required to estimate the stability of a face loaded wall using the proposed displacement spectra methodology is given in Table 4. The wall evaluated has a 225mm effective thickness and is assessed for the NZS4203 earthquake displacement spectral intensity given in Figure 11(b). The calculations apply to each of the 3 stories of the 3 storey wall described latter in section 5.1. For the lower 2 stories the top fixity factor given in Eqn 13 is included in the calculations. The earthquake scaling factors, I_{sp} , are the scaling factors that must be applied to the NZS4203 motion so that the predicted displacements of the wall will be equal to the instability displacement, Y_{max} .

Table 4: Calculations of NZS4203 Scaling Factor, I_{sp} , for Wall Collapse Predicted Using the Displacement Spectrum

Storey Level	H/t	O/W	t mm	W (kN)	O (kN)	Y_{max} mm	V_{max} (kN)	T (Sec)	1.5 x Spectral Displ for period T (9)	0.60 x Y_{max} $=0.6 \times (6)$ (mm) (10)	EQ Scaling Factor Corresponding to:	
											$0.6Y_{max}$ $= (10)/(9)$ (11)	$I_{sp} =$ Collapse $= (11) \times 1.2$ (12)
3 rd	9.33	0.14	225	9.7	1.35	213	2.5	1.07	199	128	0.64	0.77
2 nd	16	0.66	225	16.6	10.9	225	4.8	1.04	194	135	0.70	0.84
1 st	20	1.33	225	20.7	27.6	225	7.6	0.93	172	135	0.78	0.94
Notes: Col (1) wall height H, to effective thickness, t, ratio Col (2) overburden weight, O, to wall weight, W, ratio. Cols (4) & (5) wall weight and overburden weight / m. Wall 230mm nominal thickness & 20kN/m ³ density Col (6) displacement at which wall becomes statically unstable: - Eqn 4 Col (7) point load at wall mid-height to open cracks: - Eqn 3 and Eqn 13 Col (8) free vibration period of wall when peak displacement = $0.6Y_{max}$: - Eqn 12 Col (9) spectral displacement read from Figure 11(b) for 5% damping and scaled by a factor of 1.5												

In Table 4 the period, T , used to evaluate the expected displacement of the wall from the NZS4203 displacement response spectrum in Figure 11(a), is calculated using Eqn 12 assuming the wall is responding with peak displacements of 60% of the instability displacement ($0.6 Y_{max}$). In some cases the displacement spectrum has an early peak similar to that evident in Figure 11(a) for the modified El Centro motion. At a period of about 1.8 seconds it can be seen that the spectral displacement peaks at about 300mm and then declines for periods up to about 2.4 seconds. In a case like this, if the period calculated for peak displacements of $0.6 Y_{max}$ lay in the range 1.8 to 2.4 seconds, it is proposed that the early peak displacements of 300 mm be used in the calculations. Effectively this means that any "dips" in the displacement response spectra are ignored. This seems reasonable, as the wall will pass through the peak displacement period range prior to reaching 60% of the collapse displacement.

4.2 Prediction of Wall Stability using Acceleration Spectrum and first Crack Opening

By examining Figure 2 it can be seen that relatively high inertia forces are required to initially open the mid-storey cracks in the wall. This initial "force hump" needs to be overcome before the displacement response of the wall can develop. Using the displacement spectrum to predict the stability of a face-loaded wall can result in a predicted collapse earthquake intensity that is not sufficient to open the cracks if the wall is assumed to respond elastically. This is most likely to be the case for squat wall elements with high overburden loads.

Table 5 illustrates the calculations required to evaluate the scaling factor, I_{cr} , that must be applied to the NZS4203 earthquake intensity so that the mid-storey cracks would just open. To enable later comparisons with collapse intensities predicted by the computer model, collapse of the wall using this approach, was initially assumed to occur at 250% of the EQ intensity corresponding to first crack opening.

The initial elastic period of the wall, T_o , was calculated assuming the third storey wall segment behaves as a propped cantilever and the first and second storey wall segments behave as if they are fixed ended. This period, and the acceleration spectrum given in Figure 11(a), was then used to evaluate the peak elastic response of the wall expected for the NZS4203 intensity motion (column (7)).

The seismic coefficient, C_d (column (5), corresponding to the UDL lateral load that would be just sufficient to open the cracks in the wall was then calculated using Eqn 8. By comparing the values in columns (5) and (7), the earthquake scaling factor, I_{cr} , that must be applied to the NZS4203 EQ motion to just open the wall joints was evaluated and is shown in column (8).

Table 5: Calculations of NZS4203 Scaling Factor, $2.5I_{cr}$, for Wall Collapse Predicted Using the Acceleration Spectra

Storey Level	H/t	O/W	t mm	W (kN)	C_d (G's)	T_o (Sec)	NZS4203 Spectral Accel for period T_o (G's) (7)	EQ Scaling Factor Corresponding to:	
								I_{cr} = Crack Opening = (5) / (7) (8)	$2.5 I_{cr}$ = Collapse = 2.5 x (8) (9)
3 rd	9.33	0.14	225	9.7	0.52	0.039	0.52	1.0	2.51
2 nd	16	0.66	225	16.6	0.58	0.094	0.69	0.84	2.11
1 st	20	1.33	225	20.7	0.73	0.147	0.85	0.86	2.16

Notes:

Col (1)	wall storey height H, to effective thickness, t, ratio	Col (5)	Seismic coefficient corresponding to crack opening: - Eqn 8 and Eqn 13
Col (2)	overburden weight, O, to wall weight, W, ratio.	Col (6)	Initial elastic period of wall – propped cantilever 3 rd storey and fixed ended for lower 2 storeys.
Col (4)	wall weight / m. Wall 230mm nominal thickness & 20kN/m ³ density.	Col (7)	spectral acceleration from Figure 11(a) for period T_o .

The initial elastic period, T_o , given in Table 5 was calculated assuming an elastic modulus of 1.0Gpa for the masonry. In practice there is likely to be considerable scatter in the actual values of the elastic modulus of masonry and an increase in value up to 4.0Gpa has been allowed for in when preparing the design charts given in Appendix B. This allowance, for possible variation in the elastic modulus, has been applied conservatively. When the initial elastic period, T_o , indicated that the wall response was on the rising branch of the acceleration spectrum, the lower 1.0Gpa value of modulus was used and when the wall response was on the descending branch (i.e. some slender walls) the 4.0Gpa value was used in the calculations.

4.3 Prediction of Wall Stability using Displacement & Acceleration Spectra

By comparing the right hand columns of Table 4 and Table 5 it can be seen that the earthquake intensity predicted to cause wall collapse is much smaller when the displacement spectrum procedure is used than when the acceleration spectra procedure is used. For example, at the 3rd floor level, the predicted scaling factor that must be applied to the NZS4203 earthquake intensity to cause wall collapse using the displacement spectra procedure, I_{sp} , is only 0.77. This can be compared with the scaling factor ($2.5 I_{cr}$) of 2.51 predicted using the first crack opening and acceleration spectra procedure.

Calculations indicate that, in the case of very slender walls, the collapse intensity predicted using the displacement spectra procedure would be greater than that predicted using the first crack opening procedure. In these cases, crack opening will occur at relatively low shaking intensities compared with that required to cause collapse and the “force hump” would not be expected to have a marked effect on the predicted collapse intensity. Under

these conditions it is proposed that the predicted collapse intensity be based on the displacement spectra procedure only.

For very squat walls the collapse intensity predicted using the first crack opening procedure would be very much greater than that predicted using the displacement spectra procedure. In these cases the earthquake intensity required to cause collapse is not likely to exceed the intensity required to first open the cracks by the 250% margin assumed for the first crack opening procedure.

Therefore, it is proposed that the earthquake intensity scaling factor required to cause collapse, $I_{collapse}$, be based on the following relationships:

$$I_{collapse} = I_{sp} \quad \text{when } I_{sp} \geq 2.5I_{cr}$$

or

$$I_{collapse} = \frac{I_{sp} + 2.5I_{cr}}{2} \quad \text{when } I_{sp} < 2.5I_{cr}$$

Eqn 16

where: I_{sp} is 1.2 times the earthquake scaling factor corresponding to a mid-storey wall displacements of 60% of the collapse displacement, Y_{max} as predicted using the displacement spectra procedure and,

I_{cr} is the earthquake scaling factor corresponding to the earthquake intensity that will just open the joint cracks in the wall.

4.4 Prediction of Wall Stability using NZNSEE Guidelines

Draft guidelines for assessing and strengthening earthquake risk buildings have been published by the New Zealand National Society of Earthquake Engineering (NZNSEE, 1995) and these were discussed briefly in the introduction.

The NZNSEE procedures will not be repeated here as calculations using these procedures were only carried out for comparative purposes. For these calculations a number of adjustments and simplifications were made to the NZNSEE procedures:

- The NZNSEE procedures allow for the effect of the curved part of the displacement response of the wall as indicated in Figure 2. Except for slender walls with high overburden loads the influence of this curved part of the response is small. The NZNSEE procedures also exaggerate the curved part of the response because they incorrectly assume that the cracked stiffness of the wall applies through out the wall height and not just at the opening joint locations. Straight-line load deflection relationships for the initial elastic and degrading strength branches of the load deflection relationship were assumed.
- The NZNSEE procedures include 2 amplification factors, one for the elevation of the wall in the building (storey elevation factor) and the other an amplification factor of 2

to allow for amplification of the earthquake motion due to flexible floor diaphragms. These amplification factors are based on NZS4203 procedures. In this report a single amplification factor is applied to the ground motion to allow for the combined influence of storey elevation in the building and diaphragms flexibility (i.e. the diaphragms are treated as part of the overall building response). To enable comparisons to be made with the assessment procedures proposed in this report, the NZNSEE diaphragm amplification factor of 2 is applied to the ground acceleration and treated as part of the response of the wall "part". This is the same approach used by NZS4203 for general application to other "parts".

- When using the NZS4203 design spectra shown in Figure 11(a) as part of the NZNSEE Guideline procedures the rising branch and peak of 1.0G are ignored giving an effective peak response of the wall equal to 0.8G. This is approximately twice the effective ground acceleration (response for zero period) of approximately 0.4G. Application of the NZNSEE "diaphragm amplification factor" of 2 to the ground acceleration gives 0.8G as the response of the wall as a "part". A response of 0.8G was, therefore, used to assess face-loaded walls using the Guidelines for the analysis cases when the building and diaphragms were rigid. When applying the NZNSEE procedure for other earthquake motions in this report the acceleration spectrum for the motion was smoothed in a similar fashion to obtain the effective ground acceleration and hence response of the wall "part". Amplification of the ground motion due to any building flexibility was then evaluated as given in the NZNSEE procedure (i.e. NZS4203).

4.5 Comparison between Proposed Formula and Computer Model

The Earthquake Intensity Scaling Factors corresponding to wall collapse as predicted by the NZNSEE Guidelines, the proposed formulae (Eqn 16) and as predicted by the inelastic computer model are compared in Table 6 for a range of earthquake motions. The wall identified in the table as having a scale factor of 1 had a height of 4.8m, an effective thickness, t , of 330mm, a nominal thickness of 350mm and had a small overburden to wall weight ratio O/W of 0.14. Half and 2 x scale walls were also evaluated. These walls had the same slenderness ratio, H/t , but had half or double the effective thickness and height respectively.

The scaling factor predicted by the computer model, column (8), corresponds to the lower envelope of the wall responses obtained from analyses carried out as part of previous research and reported elsewhere (Blaike Spurr, 1992 & Blaikie Davey, 1999). The lower level of damping used for the computer model used for these analyses is now considered too low so that the results should be conservative. To compensate for this, to a limited degree in the calculations, a factor of 1.4 was used to scale up the SDOF spectral displacements for the multi-degree of freedom wall instead of the factor of 1.5 now considered appropriate.

Table 6: Comparison Between Earthquake Intensity Scaling Factors for Collapse Predicted by NZSEE Guidelines, Proposed Formulae and Previous Inelastic Computer modelling for Various Earthquake motions – Rigid Structure and Diaphragm conditions.

EQ MOTION	Wall Scale Factor	PERIOD T when $Y=0.6Y_{max}$ (sec's)	Earthquake Intensity Scaling Factors Required for Collapse					
			As Predicted by:					Ratio Predicted: by Formula by Computer Model
			NZNSEE Guidelines	Proposed Formulae			Computer Model	
				I_{sp}	$2.5I_{cr}$	$I_{collapse}$		
(1)	(2)	(3)	(4)	(5)	(6)	(7)	(8)	(9) = (7)/(8)
TABAS (Iran, 16 Sept. 1978 - Transverse component) component)	1/2	1.13	0.46	0.32*	0.46	0.39	0.48	0.81
	1	1.6	0.34	0.52	0.32	0.52	0.58	0.90
	2	2.26	0.24	0.65	0.23	0.65	1.0	0.65
WEBER (NZ, 13 May ,1990 - N67E component)	1/2	1.13	1.74	0.7	1.9	1.3	1.34	0.97
	1	1.6	1.26	1.15*	0.85	1.15	1.7	0.67
	2	2.26	0.89	2.29*	1.03	2.29	2.4	0.95
NZS4203 (intermediate soil spectral intensity)	1/2	1.13	1.73	0.57	1.34	0.95	1.0	0.95
	1	1.6	1.29	0.8	1.0	0.9	1.25	0.72
	2	2.26	0.88	1.13	0.83	1.13	1.4	0.81
ELCENTRO NS x 1.3	1	1.6	1.04	1.09	1.12	1.1	1.12	1.00
DIAPHRAGM (0.5 second period)	1	1.6	0.37	0.6*	0.6	0.6	0.65	0.92
Notes:								
Col (5) to (6): Component Earthquake Scaling factors used in Eqn 16 to calculate $I_{collapse}$								
* Peak spectral displacement occurring at period less than period T used in calculation.								

The 3 scaled models of the wall analysed had the same H/t ratio. However, the computer model predicts that the earthquake intensity required to cause collapse will increase by 40 to 100% as the effective wall thickness is increased from 166 to 660mm. The same trend is evident in Table 6 for earthquake intensity scaling factors corresponding to collapse, $I_{collapse}$, predicted by the proposed formula. *This indicates that wall stability is dependent on wall thickness as well as the height to thickness ratio for the 3 earthquake motions used in these analyses.* However, it should be noted that the trend in the capacities predicted by the formula is not very strong for the NZS4203 EQ motion. By inspection of the design charts given in Appendix C prepared for this EQ motion, it can be seen that the trend only becomes pronounced for slender walls.

It is interesting to observe, in column (4), that the opposite trend is indicated by the NZNSEE procedure, which predicts that the seismic capacity of a wall will decline with increasing wall thickness for a given H/t ratio.

Comparing the values in columns (7) and (8) of the table indicates that the earthquake intensity required to collapse a face-loaded wall, as indicated by the computer modelling, is conservatively predicted with reasonable accuracy by the proposed formula.

5 3 Storey Face-Loaded Wall Model

5.1 Model Description

Figure 12 illustrates diagrammatically the components of a 2D three-storey inelastic computer model that was used to evaluate a number of parameters that effect the stability of face-loaded URM walls. The model of the masonry wall on the right of the diagram is linked through floor diaphragm elements to the model of a shear wall.

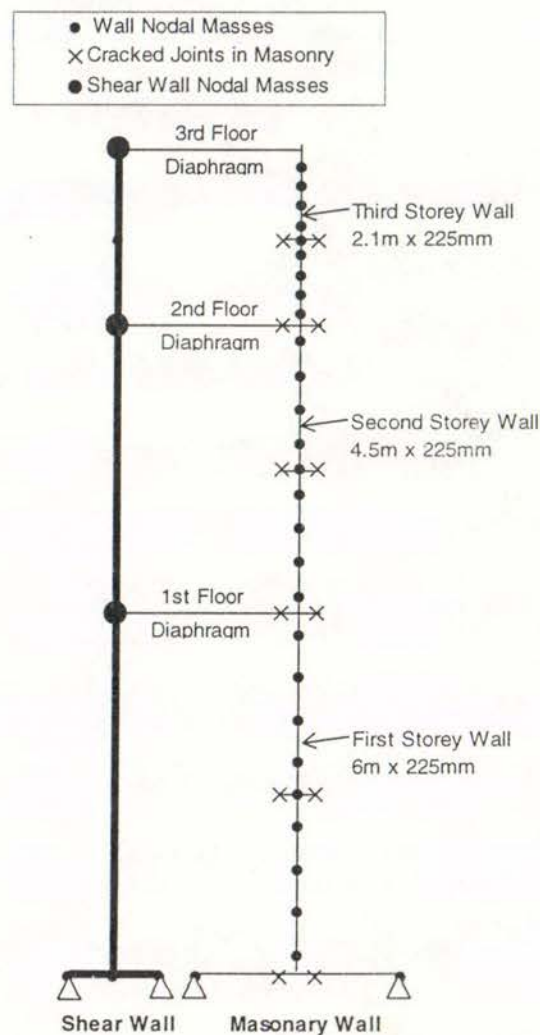


Figure 12: Diagram of 3-storey Inelastic Computer Model for Face-loaded Masonry wall

5.1.1 Masonry wall Modelling

The face-loaded walls for each storey were initially modelled separately. These single storey models were similar to those used to model the test specimens and described previously in section 3.5. However, the number of nodal masses modelling the wall inertia for each storey was reduced from 18 to 10 as described in section 3.7 and the damping for each storey model was adjusted as described in section 3.9.

5.1.2 Shear wall Modelling

Properties of the shear wall model were adjusted so that the wall either deformed in a pure flexural mode (convex deflected shape), only with shear deformations to model the deflected shape expected for a frame building (concave deflected shape), or with only foundation level rotation (intermediate straight line deflected shape).

Additional nodal masses were modelled at each floor level of the shear wall. These had a magnitude equal to approximately twice the tributary mass of the adjacent masonry wall.

The shear wall was modelled as having a fundamental period of either 0.0 (i.e. rigid), 0.5 or 1.0 seconds. Target damping for the wall was 10% of critical. Drain2dx only permits damping of the wall to be fixed for 2 response periods. For the wall modelled with a fundamental period of 0.5 seconds the 10% damping was fixed for response periods of 0.1 and 0.6 seconds and for the wall modelled with a 1.0 second fundamental period the 10% damping was fixed for response periods of 0.2 and 0.9 seconds.

The shear wall periods and damping were selected to make some allowance for soil-structure interaction and to include an allowance for minor hysteric damping.

5.1.3 Floor Diaphragm Modelling

The floor diaphragm members were modelled to have a fundamental period of either 0.0 (i.e. rigid), 0.5 or 1.0 seconds. Damping of the diaphragms was modelled using stiffness damping only and fixed at 5% for the fundamental period.

The fundamental periods were calculated assuming the full tributary mass of the wall could be considered as being concentrated at the masonry wall end of the diaphragm. This would be a reasonably accurate while the face-loaded wall remains elastic. However, previous research by the author (Blaikie Spurr, 1992) has shown that a higher mode response can develop when the masonry wall cracks open and large mid-storey wall displacements occur. This higher mode can be visualised as the ends of the wall, that are fixed to the diaphragms, oscillating while the centre of the masonry wall remains stationary. Under these conditions the effective mass acting with the diaphragm is only approximately $\frac{1}{4}$ of the tributary masonry wall mass so that the period of this mode is half the fundamental period.

As stiffness damping for a mode is proportional to the mode period, damping of the higher mode would be approximately 10%. However, as adjacent storeys tend not to respond in

phase this higher mode may not be as active in the lower 2 diaphragms as at the 3rd floor level.

Stiffness damping, as modelled in Drain2dx, is proportional to initial elastic stiffness. It is also dependent on the magnitude of the diaphragm deformations so that it could become excessive if significant yielding took place. Therefore, when elasto-plastic yielding of the diaphragms was modelled, the viscous damping of the diaphragms was set at 5% of the value used for elastic diaphragms.

5.1.4 Analysis Procedure

Generally, for each set of parameters modelled, the earthquake intensity required to cause collapse was required. Therefore, a scaling factor was applied to the earthquake motion used for the analysis and this was incremented until the analysis indicated collapse had occurred. The increment in the earthquake scaling factor used was between 2 and 3% and the last increment for which the wall was stable was used to determine the collapse earthquake intensity.

5.2 Effect of Storey Boundary Conditions on Face-Loaded Wall Stability

The assessment procedure for face-loaded walls given in the New Zealand National Society of Earthquake Engineering Draft Guidelines (NZNSEE, 1995) assumes that a storey high segment of a multi-storey wall can be considered to be supported at the mid-thickness centreline of the wall at its base. The Guidelines also assume that any surcharge can also be considered as being applied at the centreline of the wall.

Previous research by the author assumed that the base of at least a single storey wall could be considered as being supported near its outer edge as indicated in Figure 1. The resulting base fixity enhances the seismic resistance of the wall.

In section 2.4 it was postulated that "top fixity" may also develop when a storey wall segment has another storey above it. In this case the enhancement of the seismic resistance of the wall was predicted as given by the factor F_{top} (Eqn 13).

The storey heights for the 3 storey wall model shown in Figure 12 were selected so that the predicted seismic resistance of each of the storey height wall segments using Eqn 16 would be similar for the conditions of a rigid shear wall and rigid diaphragms. When the 3 storey height segments have similar seismic resistance there would be a higher probability that when, for example, the 2nd storey wall was collapsing towards the outside of the building the 1st and 3rd storeys could be collapsing towards the building's interior. If this collapse mode developed the 2nd storey wall could not be expected to have effective top and bottom fixity and the boundary conditions assumed by the NZNSEE Guidelines would be most likely to be applicable.

The first row of data in the Table 7 gives the results obtained using the computer models when the 3 storey high wall segments were analysed separately. The scaling factors that

were applied to NZS4203 earthquake motion to cause wall collapse using the first and second storey level models are presented.

The computer models for the first and second storeys were then modified to include top fixity. To achieve top fixity an opening crack, similar to that modelled at the base and mid-storey height in the wall, was also modelled at the top of the wall segment. The member modelling the top surface of the crack was fixed against rotation (held horizontal) and the overburden force applied through this member. However, when modelling the vertical inertia at this level only 20% of the overburden mass was included. This limited the magnitude of the impact forces developed at the top "crack" and kept the level of damping in the system at a similar level to that used for the model without top fixity.

The enhanced seismic resistance of the first and second storey walls with top fixity was 33% and 28% respectively, as shown in column (2) and (5) of the table. The comparable percentage increases predicted by Eqn 13 were 22% and 17% as shown in columns (3) and (6) of the table.

When the 3-storey computer model was used for the analysis, the increase in seismic resistance due to top fixity was 40% and 37% at the first and second storeys respectively as indicated by the last row of values in the table.

Table 7: Effect of Top Fixity on NZS4203 EQ Motion Collapse Intensity as Predicted by Computer Models and Proposed Formula – Rigid Shear Wall and Rigid Diaphragms.

Method of Modelling Single Storey Wall Segment	First Storey			Second Storey		
	Collapse EQ Scaling Factor	Top Fixity Increase		Collapse EQ Scaling Factor	Top Fixity Increase	
		Computer Model	F_{top} (Eqn 13)		Computer Model	F_{top} (Eqn 13)
		(2)	(3)		(5)	(6)
Without Top Fixity- as Single Wall	2.11	NA	NA	1.99	NA	NA
With Top Fixity - as Single Wall	2.82	1.33	1.22	2.55	1.28	1.17
As Part of 3 Storey Wall	2.96	1.40	1.22	2.74	1.37	1.17

When the 3-storey model was used for the analysis, the lowest earthquake intensity corresponding to a wall storey segment collapse was for collapse of the third storey. As the analysis using the computer model automatically stops at "collapse" the earthquake intensity causing collapse at the second floor level could only be determined by enhancing the seismic resistance of the third storey wall segment. This was achieved by increasing the third storey wall width, at the mid-storey crack, from 225mm to 500mm. Similarly, to force collapse to occur in the first storey wall, the wall width was increased to 450mm above mid-height of the second storey.

An alternative method of enhancing the resistance of adjacent wall segments, to force collapse into the storey under investigation, was also evaluated. This method used elastic link members across the mid-storey opening cracks acting in parallel with the buckling link members. This method does not significantly effect the earthquake level at which the cracks first open but restrains the cracks from opening to an extent that "collapse" of the wall storey segment would occur. The advantage of this method is that it has less influence on the maximum forces developed in the floor diaphragms, which are also of interest. Therefore, this method of adjacent storey seismic resistance enhancement was used for all subsequent analyses. A limited number of analyses indicated that the method of enhancing the seismic resistance of adjacent storeys did not significantly effect the predicted collapse earthquake intensity for a particular storey.

It may be concluded from the data in Table 7 that the lower storeys of a multi-storey masonry wall behave as if they have full fixity at their top and bottom boundary joints.

5.3 Effect of Storey Elevation and Building Deflected Shape on Wall Stability

The 3-storey computer model was analysed with the shear wall able to deform with a deflected shape corresponding to either the flexural, shear or foundation rotation deformation mode. The scaling factors that must be applied to the NZS4203 earthquake motion to cause collapse of the face-loaded masonry wall at each of the 3 storey levels are given in Table 8. Results are given for the case where the shear wall is modelled with either a 0.5 or 1.0 second fundamental period. Similar results for the rigid shear wall case given in Table 7 are repeated in Table 8 to enable a comparison to be made.

One analysis series was carried out with the model subjected to both horizontal and vertical components of the earthquake simultaneously. In this case the vertical component of the 1940 El Centro record was used as the vertical earthquake motion and this was scaled by the same factor as used for the (NZS4203) horizontal component of the earthquake record. By comparing the results in columns (2) and (3) in Table 8 it can be seen that *the vertical component of the earthquake does not significantly effect the stability of face-loaded URM walls*. This confirms previous research by the author using single storey computer models (Blaikie, Spurr 1992). The influence of the vertical component of the earthquake motion was not considered further as part of this research project.

Table 8: Effect of Building Deformations on Collapse EQ intensity as predicted by computer model for the NZS 4203 EQ motion. Diaphragms Rigid.

Deflected Shape Shear Wall (& Masonry Wall Storey Level)	NZS 4203 Earthquake Scaling Factors Corresponding to Collapse			
	Rigid Wall (without Vert EQ)**	0.5 sec Wall Period		1.0 sec Wall Period (without Vert EQ)
		without Vert EQ	with Vert EQ	
	(1)	(2)	(3)	(4)
Foundation Rotation:				
3rd Storey	2.34/1.74	0.80	0.78	1.12
2nd Storey	2.74/2.55	1.20	1.20	1.90
1st Storey	2.92/2.82	2.70*	2.50	2.47
Flexural Mode:				
3rd Storey	2.34/1.74	0.78	-	1.02
2nd Storey	2.74/2.55	1.42	-	2.00
1st Storey	2.92/2.98	2.70	-	2.45
Shear Mode:				
3rd Storey	2.34/1.74	0.80	-	1.12
2nd Storey	2.74/2.55	1.20	-	1.48
1st Storey	2.92/2.32	2.50	-	2.40
* 2.65 with relatively rigid links @ mid-storey L3 & L2				
** First value for wall element modelled as part of 3-storey wall / 2nd value obtained when the wall storey segment modelled using a single storey computer model.				

A number of observations can be made regarding the data in Table 8:

- seismic resistance declines strongly as the elevation of a face-loaded wall in the building increases (i.e. storey elevation amplification factor increases with elevation as expected)
- the seismic resistance of the face-loaded walls are not strongly influenced by the deflected shape of the shear wall. The intermediate foundation rotation deflected shape (straight line) was, therefore, assumed for all subsequent analyses
- when the shear wall is modelled with a 1.0 second period, rather than a 0.5 second period, there is an increase in the seismic resistance of the face-loaded walls at the upper 2 levels but a reduction at the 1st floor level.

The walls at all 3 storey levels of the model have a free vibration period of about 1.0 seconds for peak displacements of 60% of the collapse displacement. Therefore, it was anticipated that when the shear walls were modelled with a 1.0 second period, resonance would occur and a reduced seismic resistance would be predicted by the model. As this was not the case, the wall model behaviour was investigated in more detail.

The 3 storey computer model was run for the earthquake intensity just below that required for collapse and the absolute accelerations were output at the mid-storey level of the shear wall adjacent to the face-loaded masonry wall where collapse was eminent for the next increment of EQ intensity. The resulting acceleration time history records were used to produce acceleration and displacement response spectra for the mid-storey motion of the shear wall (i.e average floor response spectra). The resulting spectra for the 3 storey levels of the model are shown in Figure 13.

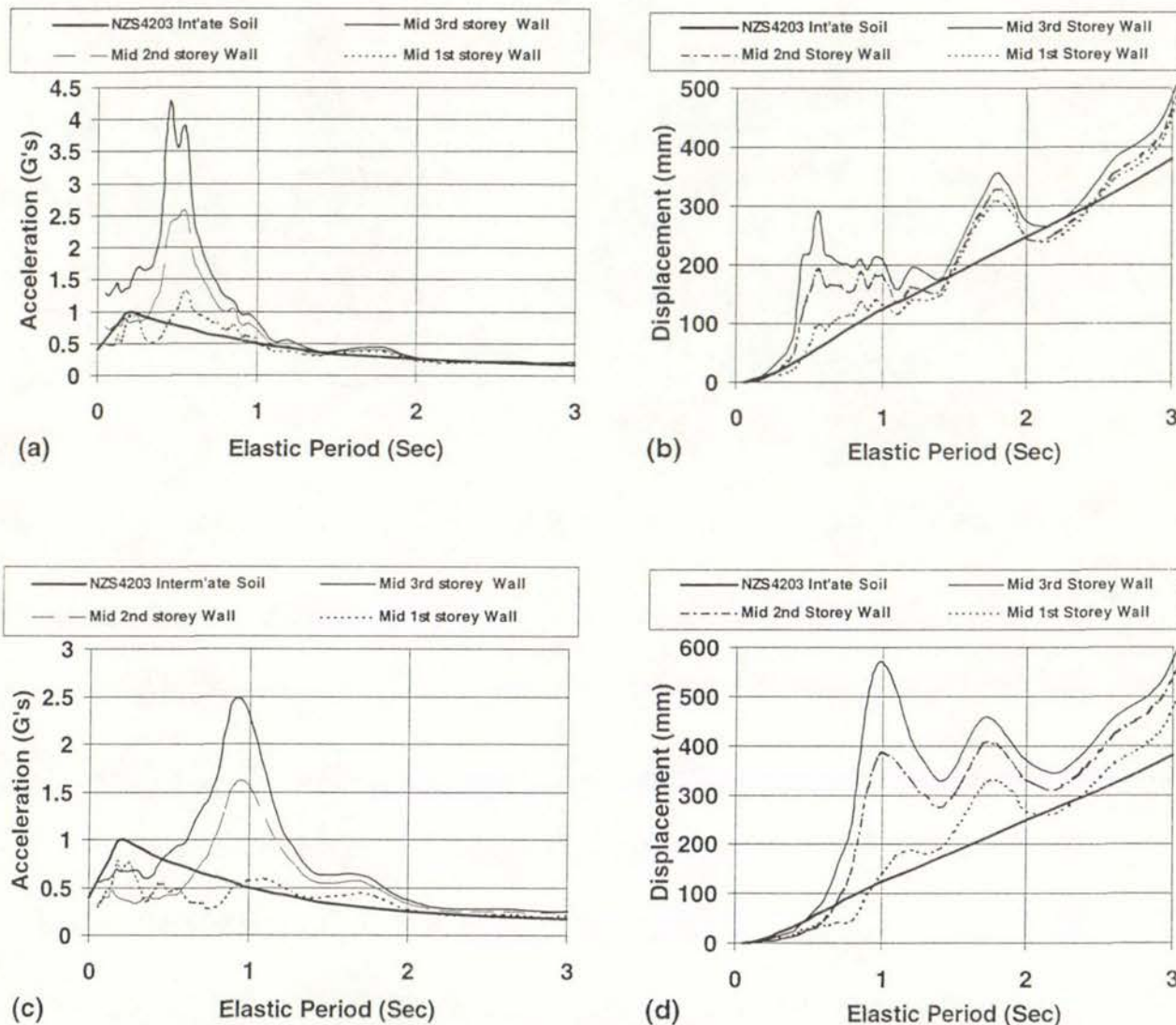


Figure 13: Response Spectra for Motion Occurring at Mid-Storey Level in the Shear Wall just prior to Collapse of Adjacent Face-Loaded Masonry wall (normalised to 1.0 x NZS4203 EQ Intensity). (a) & (b) Acceleration and Displacement Response spectra when Shear Wall Modelled with 0.5 second period

and
(c) & (d) Spectra when Shear Wall Modelled with 1.0 second period.

It can be seen from Figure 13 that the mid-storey wall response peaks at the fundamental period of the wall and that the response increases with storey elevation as would be expected.

Table 9 shows a comparison between the storey elevation amplification factors, A , as predicted by the computer modelling and the proposed formula (Eqn 16). The computer modelling results were extracted from Table 8 and the ratio of the seismic resistance with and without shear wall flexibility expressed as a Storey Elevation Amplification Factor.

The EQ scaling factor that had to be applied to the NZS4203 motion to cause wall collapse was also calculated using the spectra in Figure 13 and Eqn 16. For the rigid shear wall case the spectra used were the smoothed NZS4203 spectra shown in Figure 13. For the flexible wall predictions given in column (5) in the table, the response spectra for the motion at mid-storey of the adjacent shear wall were used for the calculations.

Table 9: Comparison between Storey Elevation Amplification Factor A , Predicted by Computer Model and Equation(Eqn 16) for the NZS4203 EQ motion

Shear Wall Period & Storey	NZS4203 EQ Scaling Factor, $I_{collapse}$ Corresponding to Collapse Predicted by:					
	Computer Model			Equation(Eqn 16)		
	Rigid Wall $I_{collapse}$	Flexible Wall $I_{collapse}$	Amplification Factor A	Rigid Wall $I_{collapse}$	Flexible Wall $I_{collapse}$	Amplification Factor A
	(1)	(2)	(3) = (1)/(2)	(4)	(5)	(6) = (4)/(5)
0.5 sec Shear Wall						
3rd Storey	1.74	0.80	2.17	1.69	0.72	2.34
2nd Storey	2.55	1.20	2.12	1.52	1.29	1.18
1st Storey	2.82	2.70	1.04	1.60	1.76	0.91
1.0 sec Shear Wall						
3rd Storey	as	1.12	1.55	as above	1.32	1.28
2nd Storey	above	1.90	1.34		2.18	0.70
1st Storey		2.48	1.13		1.99	0.80
col (1)	Predicted by single storey computer model with top fixity modelled for 1st of 2nd storeys.					
col (2)	Shear wall modelled with Foundation rotation only.					
col (5)	Predicted using response spectra calculated for earthquake response at the shear wall at mid-storey elevation – For 3rd Storey and 0.5 sec shear wall, the early peak in the displacement response spectrum with a smoothed value to 250mm was used in the calculations.					

A number of observations can be made regarding the data in Table 9:

- When the collapse earthquake intensities, as predicted by the computer model and proposed formula, are compared for the rigid shear wall conditions (columns (1) & (4)), it can be seen that the resistance predicted by the formula is too conservative at the 2nd and 1st storey levels.
- When the comparable values for the flexible wall condition are compared (columns (2) and (5)), it can be seen that the proposed formula is marginally unconservative at the 2nd storey level and at the 3rd storey level when the shear wall is modelled with a period of 1.0 seconds.
- The computer model and the proposed formula both predict lower amplification factors when the shear wall is modelled with greater flexibility (i.e. 1.0 second period).

The reason for the lower amplification factors when the shear wall is modelled with a 1.0 second period rather than a 0.5 second period, can be explained by comparing the 2 sets of response spectra shown in Figure 13. The cracked masonry walls at all 3 storey levels respond, at 60% of the collapse displacement, with a period of about 1.0 second. Therefore, comparing the displacement response spectra it can be seen that higher amplification factors would be anticipated when the shear wall is modelled with a 1.0 second period.

However, when the 2 acceleration response spectra are compared it can be seen that at short structural periods a lower response can be expected when the shear wall is modelled with a 1.0-second period. This implies that a greater earthquake intensity would be required to open the cracks in the wall.

The proposed formula, Eqn 16, uses both the displacement response spectra and acceleration response spectra to predict the collapse earthquake intensity. For the 225mm thick wall used in the 3 storey model, the weighting given to the acceleration spectra (first crack opening) dominates the spectral displacement component and hence a greater collapse EQ intensity is predicted when the shear wall is modelled with a 1.0 second period. Hence, lower amplification factors are predicted in this case.

To examine whether this would still be the case if the masonry wall was thicker or thinner than the 225 mm wall modelled, the calculations were repeated for masonry walls that were twice or half as thick. In this case the response spectra at mid-height of the adjacent shear wall used in the calculations (Figure 13) were assumed to be unaffected by the thickness of the masonry wall.

The amplification factors predicted using the proposed formula given in Table 9 are repeated in Table 10 and can be compared with those predicted if the wall thickness is doubled or halved. It can be seen that the predicted amplification factor is less in all cases when the shear wall is modelled with a 1.0 second period and that the predicted amplification factor generally increases with increasing wall thickness.

Table 10: Effect of Wall Thickness on Storey Elevation Amplification Factor as Predicted by Proposed Formula using Mid-Storey Shear Wall Response.

Shear Wall Period & Storey	Storey Elevation Amplification Factor, A, for Wall Thickness		
	2 x 225 mm	1 x 225 mm*	0.5 x 225 mm
0.5 sec Shear Wall			
3rd Storey	2.50	2.34	1.94
2nd Storey	1.33	1.18	1.03
1st Storey	0.85	0.91	0.96
1.0 sec Shear Wall			
3rd Storey	1.32	1.28	1.10
2nd Storey	0.75	0.70	0.60
1st Storey	0.65	0.80	0.75
* as given by col (6) of Table 8			

5.4 Proposed Storey Elevation Amplification Factors for NZS4203 EQ Motion

The NZNSEE Guidelines make use of the NZ Loading Standard provisions for “parts” of buildings to provide a storey elevation amplification factor. The NZ loading standard provisions are relatively complex to apply and are unrealistically dependent on the proportion of the building mass located at roof level. The Uniform Building Code (UBC, 1997) has a much simpler storey elevation amplification factor given by:

$$A_{UBC} = \left(1 + 3 \frac{h_i}{h_r}\right) \quad \text{Eqn 17}$$

where: h_i is the elevation of the part under consideration (i.e. mid-storey height for face loaded walls) and:
 h_r is the elevation of the building roof.

The UBC provisions are meant to apply in almost all conditions and the UBC amplification factors appear to be too high when compared with those obtained from the analysis of face-loaded URM walls reported in this study. It is therefore proposed that the amplification factor for face-loaded URM walls be taken as 70% of the UBC value when the building period is less than 0.5 seconds. Also, the UBC provisions do not make any allowance for reduced building response for longer period structures. Where the building period, after allowing for stiffness degradation, exceeds 1.0 seconds it is proposed that the coefficient of 3 for the rate at which the amplification factor is incremented with height in Eqn 17 be reduced to 2. Linear interpolation could then be used for building periods between 0.5 and

1.0 seconds. The proposed amplification factors are intended to make allowance for any additional effect of diaphragm flexibility as discussed in the next section of the report.

In some URM buildings the shear walls may be long and squat and these walls may respond with very little elastic or inelastic shear deformations or ground deformation. In these cases the shear walls may be considered as rigid and an amplification factor of 1.4 is proposed for the upper storeys of the building to allow for diaphragm flexibility only. For the 1st storey it is proposed to reduce this amplification factor to 1.2 to allow for the fact that amplified ground motions will only be applied to the top of the first storey wall segment.

The resulting amplification factors calculated for the 3-storey computer model are shown in Table 11. Values calculated using the NZNSEE Guidelines are also given to allow a comparison to be made. Note that no amplification factor is given for the rigid shear wall/flexible diaphragm case when using the NZNSEE procedure for the reasons given in section 4.4.

Table 11: Comparison between Storey Elevation Amplification Factors Derived using NZNSEE Guidelines (i.e. NZS4203) and Proposed Modified Uniform Building Code Formula for use with NZS4203 EQ Motion

Shear Wall Period & Storey	Storey Elevation Amplification Factor A, derived using:	
	NZNSEE Guidelines	Modified UBC Formulae
Rigid Shear Walls (with flexible Diaphragms)		
1 st Storey	NA	1.2
other storeys	NA	1.4
0.5 sec Shear Wall		$\left[= .7 \left(1 + 3 \frac{h_i}{h_r} \right) \right]$
3 rd Storey	3.42	2.60
2 nd Storey	2.66	1.99
1 st Storey	1.60	1.16
1.0 sec Shear Wall		$\left[= .7 \left(1 + 2 \frac{h_i}{h_r} \right) \right]$
3rd Storey	2.25	1.96
2nd Storey	1.81	1.55
1st Storey	1.26	1.00

5.5 Effect of Diaphragm Flexibility on the Stability of Face-Loaded URM Walls

The effect of diaphragm flexibility on predicted collapse earthquake intensity for the NZS4203 EQ motion was examined by including diaphragm flexibility in the 3 storey computer model as described in section 5.1.3. Results of the analyses for diaphragm periods of 0.5 and 1.0 seconds and for the range of shear wall periods considered are summarised in Table 12. Results previously given in Table 8, for the case of a rigid diaphragm (i.e. diaphragm period 0.0-sec's) and with the shear wall modelled only with foundation rotation, are included in the table. These are provided to enable comparisons to be made with the results obtained when diaphragm flexibility was introduced into the model.

As the earthquake-scaling factor had to be incremented gradually to determine the lowest collapse intensity, the time history analysis was repeated on average 50 times for each set of parameters. Therefore, Table 8 summarises the results obtained from over 1000 analyses of the 3-storey computer model.

As described in section 5.2 the resistance of adjacent wall segments were enhanced to force collapse into the storey under investigation. In some cases a lower collapse intensity earthquake was obtained when the adjacent storey did not have seismic resistance enhancement. For example, for the second row of data in column (2) of the table, the 2nd storey wall collapsed when the earthquake-scaling factor was 1.18 when the 3rd storey resistance was not enhanced. When 3rd storey resistance was enhanced the EQ scaling factor required for collapse was the higher value of 1.43. In cases such as this, the lower EQ scaling factor is shown bracketed in columns (1) to (3) of the table.

The earthquake scaling factors corresponding to collapse, as predicted by the proposed formulae and by the NZNSEE Guidelines are also given in the table. For these predictions, the storey elevation amplification factors given in Table 11 were included in the calculations. The predicted values can be compared with the EQ scaling factors at collapse obtained using the 3-storey computer model. However, for the first row of data in the table that is applicable when the shear wall and diaphragms are rigid, the storey elevation amplification factor is not applicable. In this case, the results can be compared with the separate line of predicted values given that exclude the amplification factors.

It can be seen that the proposed formulae (i.e. Eqn 16 and the proposed storey level amplification factors) result in predicted EQ collapse intensities that are generally conservative when compared with those obtained from the computer model analyses. The correlation between the results is also much better than that obtained using the NZNSEE Guidelines.

Table 12: Effect of Diaphragm Flexibility on Predicted Collapse EQ intensity for NZS4203 EQ Motion. Also Maximum Diaphragm Forces Prior to Collapse

Wall & Diaphragm Properties + Prediction Method	EQ Scaling Factor @ Collapse for Storey Level			Max Diaphragm Force for Floor Level – kN (normalised bracketed value – given in G's)		
	3 rd	2 nd	1 st	3 rd	2 nd	1 st
	(1)	(2)	(3)	(4)	(5)	(6)
COMPUTER MODEL: • Shear wall period 0.0 sec (i.e. rigid shear wall) - diaphragm Period 0.0 - diaphragm Period 0.5 - diaphragm Period 1.0	2.34 *	2.74 *	2.92 *	-	-	-
	1.23	1.2 (1.18)	2.4	1.46 (.39)	5.6 (.56)	12.9 (.59)
	1.18	.93	2.93 (1.9)	1.10 (.3)	3.7 (.57)	10.6 (.4)
PROPOSED FORMULA: - diaphragm period 0.0 - flexible diaphragms NZNSEE Guidelines:	1.69 1.2 4.49	1.52 1.1 1.55	1.6 1.4 1.09	- - -	- - -	- - -
COMPUTER MODEL: • Shear wall period 0.5 sec - diaphragm Period 0.0 - diaphragm Period 0.5 - diaphragm Period 1.0	.78 .73 .75	1.2 1.2 1.0	2.5 2.5 (1.7) 2.7 (1.8)	- 1.5 (.64) 1.2 (.52)	- 7.3 (.9) 4.2 (.73)	- 12.8 (.56) 9.7 (.4)
PROPOSED FORMULA: NZNSEE Guidelines:	.76 1.38	.76 .55	1.37 .68	- -	- -	- -
COMPUTER MODEL: • Shear wall period 1.0 sec - diaphragm Period 0.0 - diaphragm Period 0.5 - diaphragm Period 1.0	1.12 1.0 0.9	1.9 1.6 (1.3) 1.2	2.5 2.2 2.6 (2.1)	- 1.1 (.36) 1.2 (.42)	- 5.4 (.68) 4.7 (.54)	- 6.9 (.34) 8.2 (.34)
PROPOSED FORMULA: NZNSEE Guidelines:	.86 2.1	.98 .86	1.6 .85	- -	- -	- -
<p>Notes: Cols (1) to (3) - The bracketed value indicates that collapse at this storey level occurred at a lower EQ scaling factor when an upper level storey was being modelled (i.e. governs).</p> <p>Cols (4) to (6):- 1st value is maximum diaphragm force occurring prior to collapse of the storey below the diaphragm (in kN for the modelled 490 mm length of wall). 2nd figure is diaphragm force expressed in terms of a seismic coefficient and normalised for 1.0 x the NZS4203 EQ intensity.</p> <p>* These are scaling factors obtained when storey wall segments were modelled using the 3 storey computer model. The comparable figures when the storey wall segments were modelled using the single storey computer model were 1.74, 2.55 & 2.82 for the 3rd, 2nd & 1st storeys respectively.</p>						

The maximum diaphragm forces that occur for EQ scaling factors up to the collapse intensity are also given in the table (columns (4) to (6)) for the 3 floor levels of the 3 storey computer model. Two values are given. The first is the peak diaphragm force in kN. The second (bracketed) value is the same force normalised. Normalisation was carried out by dividing the peak diaphragm force by the tributary weight of the adjacent masonry wall and by the EQ scale factor at collapse. The resulting normalised value is the seismic coefficient that the diaphragm would need to be designed for if the diaphragm was to remain elastic for an earthquake intensity of $1.0 \times$ the NZS4203 motion (although this would only be strictly true if the system was linear).

It can be seen from the table that the normalised diaphragm forces are relatively high, particularly where the diaphragm and shear wall are stiff. No results are included for the rigid diaphragm cases as diaphragm forces obtained from the computer analyses may be inaccurate under these conditions due to unrealistically high impact forces being generated in the diaphragms when the masonry wall cracks close.

The relatively high diaphragm strengths required for the diaphragms to remain elastic indicates that yielding of diaphragms may occur in many real structures.

5.6 Effect of Diaphragm Yielding on the Stability of Face-Loaded URM Walls

The tributary weight of the masonry wall associated with each of the floor diaphragms of the 3-storey computer model is given in first row of Table 13. These weights may be compared with the peak force that would occur in the diaphragms if the seismic load were applied as a static UDL load and the masonry wall cracks were just starting to open at all storey levels simultaneously. The diaphragm forces for a storey are shown diagrammatically in Figure 1 and are given in Appendix C for a range of wall thickness'. These were calculated using Eqn 3, Eqn 6 & Eqn 7. The total diaphragm forces for the 3-storey model are given in row 2 of the table.

The third row of the table gives the seismic coefficient that the diaphragms would need to be designed for if yield of the diaphragms was to be avoided under the conditions of a statically applied seismic load. In this case opening of the cracks acts as a fuse and sets an upper limit on the diaphragm forces under static conditions.

Previous research, (Blaikie Spurr, 1992) using a single (top) storey computer model, indicated that under dynamic conditions the maximum diaphragm force prior to collapse is not likely to exceed about 130% of the initial crack opening diaphragm force calculated under static conditions when the diaphragm period exceeds 1.0 seconds. However, the research indicated that this ratio might increase up to 300% if the diaphragm period is reduced to 0.5 seconds.

Table 13: Seismic Coefficient Corresponding to First Crack Opening and Diaphragm Yielding

Diaphragm Parameter	Diaphragm Floor Level		
	3 rd	2 nd	1 st
(1) Tributary weight of adjacent Masonry Wall (kN)	2.3	6.4	9.13
(2) Force in diaphragm @ first crack opening (UDL seismic load) (kN)	1.03	3.69	6.75
(3) Ratio of row (2)/(1)	0.45	0.57	0.73
(4) Seismic coefficient corresponding to diaphragm yield (= 50% of row (3))	0.23 G	0.29 G	0.37 G
(5) Elastic deflection diaphragm at yield (mm)			
- when diaphragm period = 0.5 seconds	12	17	23
- when diaphragm period = 1.0 seconds	47	68	92
Note: row (1) ½ adjacent masonry wall weight above and below diaphragm (for the 490 mm length of wall modelled)			
row (2) Force in diaphragm when cracks first open in masonry wall above and below diaphragm – walls moving in-phase – calculated using Eqn 3, Eqn 6 & Eqn 7			

It is interesting to compare the static forces expected in the diaphragms at first crack opening as given in Table 13 with the peak diaphragm forces that occur during seismic loading of the 3 storey model as given in Table 12. In general the results are similar to those found previously using the single storey model. However, the maximum ratio does not exceed 200% when the diaphragms are modelled with a 0.5 second period and when the diaphragms are modelled with a 1.0 second period the ratio is also dependent on the period used for the shear wall model. When the shear wall is more flexible (1.0 second period) the maximum ratio is only 120% but this ratio increases to 160% when the shear wall is modelled with a 0.5 second period.

To investigate the effects of diaphragm yielding on the stability of face-loaded walls the 3-storey model was modified so that elasto-plastic yielding would occur at half the static force level corresponding to 1st crack opening. The resulting seismic coefficients, corresponding to yield in the diaphragms are shown in row (4) of Table 13.

The elastic displacements of the diaphragms at the onset of yield are also given in row (5) of the table. These were used to compute displacement ductility demand factors for the yielding diaphragms.

Table 14: Predicted Collapse EQ intensity for NZS4203 EQ Motion for Diaphragms Yielding at half the Wall Cracking Opening Force. Also Maximum Diaphragm Extensions Prior to Collapse

Wall & Diaphragm Properties + Prediction Method	EQ Scaling Factor @ Collapse for Storey Level			Max Diaphragm Extension @ Floor Level – mm (bracketed value = corresponding displacement ductility factor, μ)		
	3 rd	2 nd	1 st	3 rd	2 nd	1 st
	(1)	(2)	(3)	(4)	(5)	(6)
COMPUTER MODEL: • Shear wall period 0.0 sec (i.e. rigid shear wall)						
- diaphragm Period 0.5	1.58	1.68	2.25	257 (21)	240 (14)	245 (11)
- diaphragm Period 1.0	1.25	1.5	2.25 (1.95**)	198 (4.2)	155 (2.2)	178 (1.9)
PROPOSED FORMULA:	1.2	1.1	1.4	-	-	-
NZNSEE Guidelines:	4.49	1.55	1.09	-	-	-
COMPUTER MODEL: • Shear wall period 0.5 sec						
- diaphragm Period 0.5	1.15	1.18**	2.73* (1.9)	595 (50)	190 (11)	314 (14)
- diaphragm Period 1.0	0.88	1.23	2.25* (1.77)	718 (15)	163 (2.4)	190 (2.1)
PROPOSED FORMULA:	0.76	0.76	1.37	-	-	-
NZNSEE Guidelines:	1.38	0.55	0.68	-	-	-
COMPUTER MODEL: • Shear wall period 1.0 sec						
- diaphragm Period 0.5	1.05	1.38	3.2	143 (12)	139 (8.2)	327 (14)
- diaphragm Period 1.0	0.68	0.95**	2.07* (1.95)	338 (7.2)	180 (2.6)	225 (2.4)
PROPOSED FORMULA:	0.86	0.98	1.6	-	-	-
NZNSEE Guidelines:	2.1	0.86	0.85	-	-	-
Notes: Cols (3) - The bracketed value indicates that collapse at this storey level occurred at this lower EQ scaling factor when 3 rd or 2 nd storey was being modelled (i.e. governs). Cols (4) to (6):- 1st value is maximum diaphragm extension occurring prior to collapse of the storey below the diaphragm. ** In these cases the diaphragm extension at 3 rd floor level exceeded 1000 mm at an EQ scaling factor \leq the collapse intensity but this did not appear to significantly effect the EQ collapse intensity at the 1 st or 2 nd storey levels. * In these cases the 3 rd floor level diaphragm was made elastic and the yield capacity at the 2 nd floor level was doubled as excessive diaphragm extensions (>1000 mm) at these higher levels were significantly effecting the predicted collapse capacity of the 1 st storey face loaded wall.						

Table 14 shows the results obtained from the 3-storey computer model when the diaphragms were able to yield. Layout of the table is similar to that used previously for table 12 which presented the results obtained when the diaphragms were modelled to remain elastic. However, maximum diaphragm extensions (and corresponding displacement ductility factors) have replaced maximum diaphragm forces on the right hand side of Table 14 and comparable results for the rigid diaphragm case are not included.

The diaphragm extensions given are the maximum occurring up to the increment in EQ scaling factor proceeding that corresponding to collapse. The collapse intensities predicted using the proposed formulae and the NZNSEE Guidelines, given in Table 14 are unchanged from those given in Table 12.

It can be seen from Table 14 that, when the diaphragms are modelled with a 0.5 second period the displacement demands on the diaphragms are relatively large. When these displacements are converted to displacement ductility factors using the elastic displacement at yield (given in Table 13) it can be seen that the displacement demand is unlikely to be sustainable in a real structure. If the diaphragms had been modelled with greater stiffness (period approaching 0.0) but with the same yield strength, similar extension demand would be expected in the diaphragms, as the initial elastic displacements are relatively small. The corresponding displacement ductility factors would be higher and hence would be even less sustainable.

When the floor diaphragms are modelled with a 1.0-second period, the displacements and corresponding ductility factors can be seen in general to be moderate and more likely to be sustainable. The exceptions occur at the 3rd floor level for the 2 cases where the buildings shear wall was modelled with flexibility.

Table 15 compares the maximum diaphragm extensions with and without yielding of the diaphragms. When the diaphragms are modelled with a 0.5-second period, it can be seen that yielding significantly increases the displacement demand in the diaphragms. When the diaphragms are modelled with more flexibility (1.0-second period) the displacement demand in the diaphragms, with and without yielding, is comparable except at the 3rd floor level diaphragm where excessive yielding occurred.

Table 15: Comparison of Predicted Maximum Diaphragm Extensions prior to Collapse for Diaphragms either Responding Elastically or Yielding at Half the Wall Cracking Opening Force (NZS4203 EQ Motion)

Wall & Diaphragm Properties + Prediction Method	Maximum Diaphragm Extension Prior to Collapse (mm)					
	Diaphragms Elastic			Diaphragms Yielding		
	3 rd	2 nd	1 st	3 rd	2 nd	1 st
	(1)	(2)	(3)	(4)	(5)	(6)
COMPUTER MODEL: • Shear wall period 0.0 sec (i.e. rigid shear wall) - diaphragm Period 0.5 - diaphragm Period 1.0	44 106	72 220	82 222	257 198	240 155	245 178
COMPUTER MODEL: • Shear wall period 0.5 sec - diaphragm Period 0.5 - diaphragm Period 1.0	55 128	66 190	95 220	595 718	190 163	314 190
COMPUTER MODEL: • Shear wall period 1.0 sec - diaphragm Period 0.5 - diaphragm Period 1.0	27 82	43 137	60 178	143 338	139 180	327 225
<p>Notes: Cols (1) to (3):- Diaphragm extensions corresponding to the diaphragm forces in Table 12 scaled to correspond to the same EQ collapse intensity predicted when the diaphragms modelled with yielding.</p> <p>Cols (4) to (6):- Values repeated from Table 13.</p>						

The EQ scaling factor corresponding to collapse, with and without yielding, as given in Table 14 and Table 12 respectively, are compared in Figure 14. It can be seen that diaphragm yielding tends to increase the predicted capacity of face-loaded URM walls. Most of the exceptions relate to the case where the buildings shear wall and the diaphragms are both modelled with 1.0-second periods.

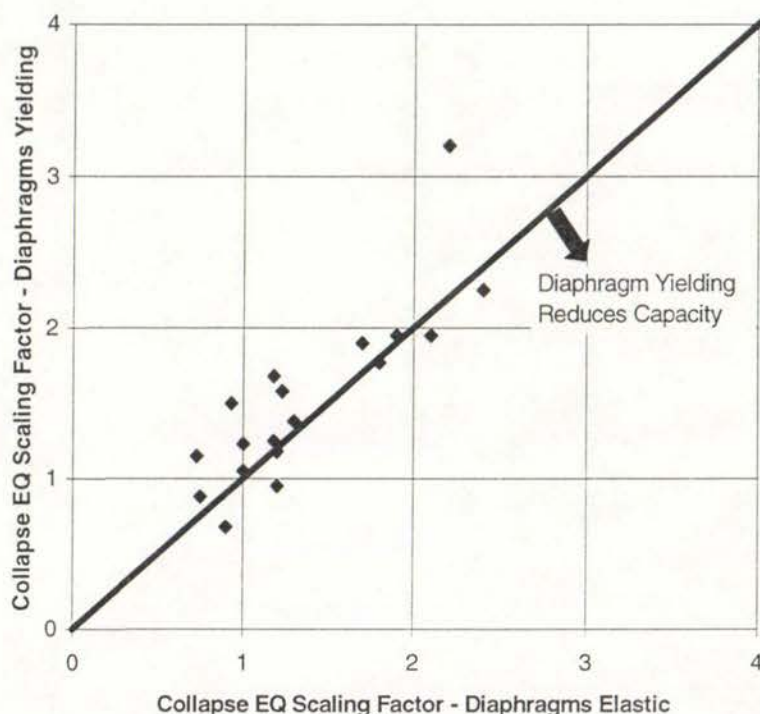


Figure 14: Effect of Diaphragm yielding on EQ Collapse Intensity for NZS4203 EQ Motion as Predicted by Computer Model

Table 14 indicates that the proposed formulae still conservatively predict the capacity of face-loaded URM walls in most of the cases examined with diaphragm yielding included in the model.

The two exceptions relate to the cases where the buildings shear wall and the diaphragms are both modelled with 1.0-second periods. Under these conditions the formulae predict that the 3rd storey wall will collapse at 86% of the NZS4203 EQ intensity while the computer model predicts that the wall can only withstand 68% of this EQ intensity. However, in this case, excessive yielding is occurring in the 3rd floor diaphragm. If the yield capacity of this diaphragm is increased by 50%, the displacement ductility factor predicted by the computer model for the 3rd floor diaphragm decreases from 7.2 to a more reasonable value of 2.6. Also, the predicted capacity of the 3rd storey face loaded wall increases from 68% to 80% of the NZS4203 EQ intensity which is closer to the 86% collapse intensity predicted by the proposed formulae.

It can be seen that the NZNSEE Guidelines are a poor predictor of the face-loaded wall capacities that were indicated by the computer modelling, and that the trend of increasing capacity with storey level, suggested by the Guidelines, is in the wrong direction.

Diaphragm yielding and diaphragm flexibility generally can be expected to give rise to differential displacements at the top and bottom of a face-loaded wall in a storey. These differential displacements would be expected to help destabilise a face-loaded wall but their significance would depend on the magnitude of the differential displacement relative to the wall thickness. They would, therefore, be less significant for thicker walls.

Flexible or yielding diaphragms may absorb more displacement demand than they generate (due to greater flexibility in the system) and any yielding would increase the effective damping in the structural system.

Relatively stiff diaphragms (period less than 0.5 seconds) that have more modest levels of yielding displacement demand than those modelled in this study, may have a more beneficial effect on the stability of face-loaded walls.

Therefore it may be postulated that more modest diaphragm yielding of stiff diaphragms, or diaphragm yielding in conjunction with thicker walls, may be beneficial to the stability of face-loaded URM walls. However, at this stage no allowance for enhanced face-loaded wall capacity due to diaphragm yielding is included in the proposed assessment procedure for the NZS4203 EQ motion given in Appendix B.

6 Response of Face Loaded URM Walls to Near Fault EQ Motions

6.1 Characteristic of Near Fault EQ Motions

Ground motions recorded in the near-fault zone during recent earthquakes (Loma Prieta 1989, Northridge 1994, Kobe 1995, Taiwan 1999 and Turkey 1999) have established that the ground motion characteristics in the near-fault zone can be quite different from those recorded at more remote sites. When the fault rupture propagates towards a site at a velocity close to the shear wave velocity, long duration acceleration pulses can develop in the ground motion. Although the peak acceleration of these pulses may not be particularly high the long duration of the pulses means they generate high peak ground velocity pulses which also have a long duration. These long duration velocity pulses can generate large displacements in structures.

Modelling of fault ruptures (Aagard *et al.*, 2000) has established that the near-fault ground motion is sensitive to the ground material properties and fault depth, moderately sensitive to the hypocentre location, rupture speed and maximum slip rate but is relatively insensitive to the distribution of slip on the fault. The distribution and characteristics of the ground motion is also dependant on the type of faulting (e.g. strike-slip or blind-thrust).

When the response of structures to near-fault ground motions is examined (Alavi, Krawinkler, 2000) the period of the main velocity pulse and peak velocity are found to be the important parameters. The period of the main pulse seems to depend mainly on the magnitude of the earthquake (with a large amount of scatter) and the peak velocity of the pulse depends on both the earthquake magnitude and shortest distance from the fault to the site where the motion is recorded.

Code design spectra and seismic design procedures have largely been developed by examining the behaviour of modelled structures subjected to earthquake motions recorded outside the near-fault zone. Until the recent Northridge and Kobe earthquakes there were only a small number of near-fault records available and there was a lack of confidence in some these (e.g. Pacoima Dam 1971, Tabas 1978). It has been estimated (Krawinkler, verbal presentation, 12WCEE) that ground motion recordings during the 1999 Taiwan and Turkey earthquakes will double the number of near-fault records available.

Design procedures developed before the availability of a large number of near fault records are likely to require considerable modification to allow for the earthquake characteristics expected in the near-fault region. For example, damping is not as effective in reducing seismic response of structures to pulse like motions as the response lacks the resonance characteristics when damping is most effective (Malhotra, 2000). Also, scaling of existing design spectra using near fault factors, as used in the 1997 version of the UBC building code, does not result in consistent ductility demand in multi-storey structures (Alavi, Krawinkler, 2000).

6.2 Kobe Earthquake Near-Fault Ground Motion

Figure 15 shows a near-fault EQ ground motion recorded during the 1995 Kobe (Great Hanshin) earthquake in the zone of greatest damage. The ground motion plotted is the Tokatori record between 1 and 16 seconds for the direction of maximum ground velocity. Both ground acceleration and ground velocity are plotted.

This earthquake motion was selected to examine the effects of near-fault ground motions on face-loaded URM walls because it originates from a primarily strike-slip earthquake which is the EQ mechanism that dominates for much of central New Zealand. Also, the magnitude of the Kobe earthquake (M_w & M_s 6.9) is approaching the expected magnitude that has been predicted for the next movement on the Wellington fault (M_s 7.5). However, an increase in magnitude from 6.9 to 7.5 could correspond to a 260% increase in peak velocities if the log relationship given by Alavi and Krawinkler proves correct (the calculated increase was evaluated assuming the Tokatori recording site was 4.3 km to the closest point on the fault as given by Alavi and Krawinkler).

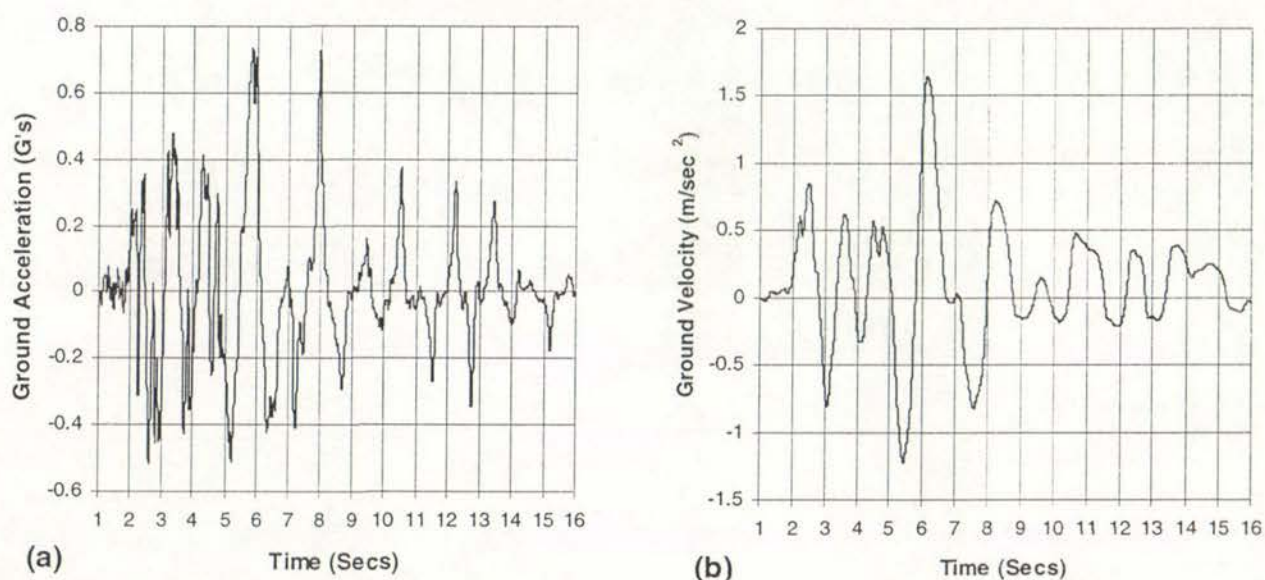


Figure 15: Near Fault EQ Ground Motion Recorded for 1995 Kobe EQ – Tokatori Record (1 to 16 seconds) for the Direction of Maximum Ground Velocity: (a) Ground Acceleration and (b) Ground Velocity

The primary velocity pulse in the EQ record can be seen to occur between 5 and 7 seconds in the record and the period of the pulse can be seen to approach 2 seconds. Scaling of the earthquake record was carried out by simple scaling of the ground accelerations used as input for the inelastic dynamic analyses. However, as observed above, the period of the primary velocity pulse is probably magnitude dependent and this period is not scaled using the simple scaling procedure.

Figure 15 shows the acceleration and displacement response spectra for the Tokatori earthquake record. The basic NZS4203 design spectra for intermediate soils are also shown

to enable a comparison with current design earthquake intensities. Except for relatively stiff structures the current design spectra can be seen to be inadequate for near-fault type motions.

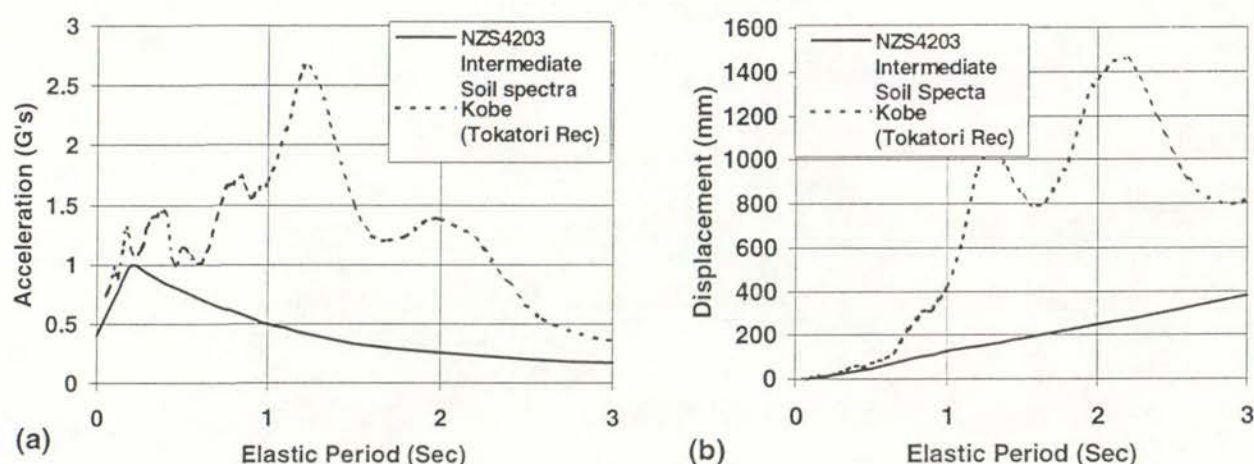


Figure 16: Response Spectra for 1995 Kobe EQ – Tokatori Record (1 to 16 seconds only) for Direction of Maximum Ground Velocity (5% damping): (a) Absolute Acceleration and (b) Relative Displacement

6.3 Effect of Boundary Conditions on Face-Loaded Wall Stability – Near-Fault EQ

Table 16 indicates the effect of top fixity on the stability of the first and second storey wall segments of the 3-storey face-loaded wall model. The results were obtained using the Kobe near-fault motion and may be compared with those obtained using the NZS4203 earthquake motion given in Table 7.

Column (1) of the table shows the collapse earthquake intensity scaling factors predicted for the 1st storey wall using a single storey computer model with and without top fixity. The collapse scaling factor predicted when the first storey segment of the wall is modelled as part of a 3 storey computer model is also given. The resulting increases in face-loaded wall capacity are given in column (2) of the table and these increases can be compared with those predicted using Eqn 13 given in column (3). Agreement can be seen to be good and is better than that obtained using the NZS4203 earthquake motion.

Similar results are given in columns (4) to (6) of the table for the 2nd storey wall segment.

Table 16: Effect of Top Fixity on Kobe Near Fault EQ Motion Collapse Intensity as Predicted by Computer Models and Proposed Formula – Rigid Shear Wall and Rigid Diaphragms.

Method of Modelling Single Storey Wall Segment	First Storey			Second Storey		
	Collapse EQ Scaling Factor	Top Fixity Increase		Collapse EQ Scaling Factor	Top Fixity Increase	
		Computer Model	F _{top} (Eqn 13)		Computer Model	F _{top} (Eqn 13)
	(1)	(2)	(3)	(4)	(5)	(6)
Without Top Fixity- as Single Wall	0.90	NA	NA	0.78	NA	NA
With Top Fixity - as Single Wall	1.10	1.22	1.22	0.90	1.15	1.17
As Part of 3 Storey Wall	1.13	1.25	1.22	0.93	1.19	1.17

6.4 Storey Elevation Amplification Factors for Near-Fault Earthquake Motions

Table 17 shows, in column (3), the storey elevation amplification factors that were predicted by the 3-storey computer model when building flexibility is included in the model. The comparable amplification factors calculated using the NZNSEE procedures are also shown (column (4)). These were calculated using the New Zealand code procedures but substituting a smoothed version of the Tokatori response spectrum for the NZS4203 basic spectra as detailed in the notes to the table.

Amplification factors calculated using modified versions of the UBC formula (Eqn 17) are also shown. Amplification factors given in Table 11, as proposed for use with NZS4203 type earthquake motions, are restated in column (5) and those proposed for use with near-fault type motions are given in column (6). The proposed amplification factors for the two types of EQ motion are identical when the shear wall has a period of 0.5 seconds. However, when the building period increases to 1.0 seconds the UBC formula has been used in an unmodified form to calculate the amplification factors proposed for use with the near-fault type motion.

When the amplification factors predicted by the computer model for the near-fault earthquake motion (column (3)) are compared with the values predicted using the NZS4203 type earthquake motion (Table 9), it can be seen that the trend of decreasing amplification factor with increasing building period has been reversed. This trend is correctly predicted using the NZNSEE Guideline procedure. It is a direct consequence of the relative shapes of the response spectrum for the two types of earthquake motion shown in Figure 16(a). Between the response periods of 0.5 and 1.0 seconds it can be seen that the response increases for the near-fault earthquake motion and decreases for the NZS4203 type motion.

When the amplification factors in columns (3) and (4) are compared it can be seen that the NZNSEE values are very conservative compared with those predicted by the computer model. The proposed near-fault amplification factors, based on the UBC formula, are also conservative as they are intended to also allow for moderate floor diaphragm flexibility and/or yielding.

Table 17: Storey Elevation Amplification Factor A, Predicted by Computer Model and Formulae for Kobe Near Fault EQ motion – Rigid Diaphragms

Shear Wall Period & Storey	Computer Model			Formulae		
	Rigid Shear Wall $I_{collapse}$	Flexible Shear Wall $I_{collapse}$	Amplification Factor A	Amplification Factor, A using:		
				NZNSEE Guidelines	Modified UBC	
					Proposed for NZS4203 (Table 11)	Proposed for Near Fault EQ
	(1)	(2)	(3) = (1)/(2)	(4)	(5)	(6)
0.5 sec Shear Wall						
3rd Storey	0.78	0.50	1.56	3.54	2.60	2.60
2nd Storey	0.93	0.70	1.33	2.74	1.99	1.99
1st Storey	1.13	1.08	1.04	1.62	1.16	1.16
1.0 sec Shear Wall						
3rd Storey	as	0.30	2.60	5.05	1.96	3.71
2nd Storey	above	0.48	1.93	3.80	1.55	2.84
1st Storey		0.85	1.32	2.00	1.00	1.65
<p>col (1) Predicted by 3 storey computer model with walls and diaphragms modelled as rigid.</p> <p>col (2) Shear wall modelled with Foundation rotation only.</p> <p>col (4) Calculated using Tokatori response spectra (Figure 16) in place of NZS4203 spectra taking effective peak ground acceleration as 0.625G and the building response as 1.25 and 1.7 G when the shear wall periods are 0.5 and 1.0 seconds respectively.</p> <p>col (6) For the case of rigid shear walls, amplification factors of 1.5 and 2.0 are proposed for 1st and other storeys respectively to allow for diaphragm flexibility only.</p>						

6.5 Effect of Diaphragm Flexibility on Storey Elevation Amplification Factors - Near-Fault Earthquake Motions

The collapse earthquake intensities and maximum diaphragm forces predicted using the 3-storey computer model, incorporating diaphragm flexibility and using the Kobe near-fault earthquake motion, are presented in Table 18. The table is similar to that described earlier

in this report where the results of similar analyses using the NZS4203 EQ motion were presented (Table 12).

The first 10 rows of Table 18 present the results obtained when the shear wall was modelled as rigid. For the case where the floor diaphragms are also modelled as rigid (diaphragm period 0.0), the earthquake collapse intensity calculated using the proposed formula can be seen to predict quite well the collapse intensity obtained using the computer model. *This result is encouraging as it illustrates that the proposed basic formula (Eqn 16) can be used for a wide range of different types of earthquake motions as the Kobe near-fault motion has a quite different frequency content and spectral shape from that used in previous analyses.* (However, previous calculations did use floor response spectra and there are interesting similarities between the floor response spectra (Figure 13) the near-fault spectra given in Figure 16)

When diaphragm and/or shear wall flexibility is introduced into the computer model it can be seen from the table that the predicted collapse capacities of the face-loaded walls decline. This trend is far more pronounced and consistent than was obtained using the NZS4203 EQ motion (Table 12).

The predicted collapse intensities using the proposed formulae for the cases where the computer model had diaphragm and/or shear wall flexibility are also given in Table 18. These were obtained by dividing the value obtained using Eqn 16 for the rigid diaphragms and a rigid shear wall condition by the amplification factor given in column (6) of Table 17. It can be seen that the proposed formulae conservatively predict the results obtained using the computer model when the diaphragm period is less than 0.5 seconds. However, when the proposed formulae are used to predict the collapse capacity when the diaphragms with 1.0 second diaphragms, a 50% increase in the amplification factors would be required to obtain reasonable agreement (i.e. proposed formulae value would then be 2/3 that shown in table).

The maximum forces that occurred in the diaphragms for EQ scaling factors up to (but excluding) the collapse intensity are also given in the table. When these values are compared with those given in Table 12 for the NZS4203 EQ motion, it can be seen that the peak diaphragm forces are similar. This indicates that the peak diaphragm forces are not sensitive to the type of earthquake motion used in the analysis. The additional sets of results for the 2 rigid diaphragm and flexible shear wall cases given in Table 18 should be treated with caution. Exaggerated impact forces associated with crack closing in the model that may not be present in a real structure may effect these 2 sets of results.

Table 18: Effect of Diaphragm Flexibility on Predicted Collapse EQ intensity for Kobe Near Fault EQ Motion. Also Maximum Diaphragm Forces Prior to Collapse

Wall & Diaphragm Properties + Prediction Method	EQ Scaling Factor @ Collapse for Storey Level			Max Diaphragm Force for Floor Level – kN		
	3 rd	2 nd	1 st	3 rd	2 nd	1 st
	(1)	(2)	(3)	(4)	(5)	(6)
COMPUTER MODEL: • Shear wall period 0.0 sec (i.e. rigid shear wall)						
- diaphragm Period 0.0	0.78	0.93	1.13	-	-	-
- diaphragm Period 0.5	0.55	0.75	1.00	1.3	5.0	8.9
- diaphragm Period 1.0	0.33	0.33	0.75	1.2	3.5	8.4
PROPOSED FORMULAE:						
- diaphragm period 0.0	0.98	0.89	0.97	-	-	-
- flexible diaphragms (A=2 or 1.5)	0.49	0.45	0.64	-	-	-
NZNSEE Guidelines:	2.87	1.00	0.70	-	-	-
COMPUTER MODEL: • Shear wall period 0.5 sec						
- diaphragm Period 0.0	0.50	0.70	1.08	8.1	6.2	10.4
- diaphragm Period 0.5	0.43	0.53	0.93	1.1	4.7	8.7
- diaphragm Period 1.0	0.23	0.30	0.63	1.0	3.8	8.1
PROPOSED FORMULAE:	0.38	0.44	0.83	-	-	-
NZNSEE Guidelines:	0.81	0.36	0.42	-	-	-
COMPUTER MODEL: • Shear wall period 1.0 sec						
- diaphragm Period 0.0	0.30	0.48	0.85 (0.78)	2.85	4.9	10.5
- diaphragm Period 0.5	0.23	0.35	0.73	0.93	4.42	9.5
- diaphragm Period 1.0	0.13	0.18	0.33	1.0	3.8	4.7
PROPOSED FORMULAE:	0.26	0.31	0.59	-	-	-
NZNSEE Guidelines:	0.57	0.26	0.35	-	-	-
Notes: Cols (1) to (3) - The bracketed value indicates that collapse at this storey level occurred at a lower EQ scaling factor when an upper level storey was being modelled (i.e. governs). Cols (4) to (6):- maximum diaphragm force occurring prior to collapse of the storey below the diaphragm (in kN for the modelled 490 mm length of wall.						

6.6 Effect of Diaphragm Yielding on Storey Elevation Amplification Factors - Near-Fault Earthquake Motions

The collapse earthquake intensities and maximum diaphragm extensions predicted using the 3-storey computer model, incorporating diaphragm yielding and using the Kobe near-fault earthquake motion, are presented in Table 19. The table is similar to that described earlier in this report (Table 14) where the results of similar analyses using the NZS4203 EQ motion were presented.

The EQ scaling factor corresponding to collapse with and without yielding, as given in Table 19 and Table 18 respectively, are compared in Figure 17. It can be seen that, on average, the diaphragm yielding tends to reduce the capacity of face-loaded URM walls. This is the opposite trend to that observed for the NZS4203 motion. The trend reflects the adverse effects of additional system flexibility, which could have been anticipated from the shape of the near-fault response spectra.

No comparable yielding diaphragm results are presented in Table 19 (or Figure 17) for the 3 cases where the diaphragms are modelled as rigid. As the elastic displacements for the 3 cases where the diaphragms were modelled with a 0.5 second period are small relative to the total displacement demand (displacement ductility factors, $\mu = 8.8$ to 32), similar collapse intensities would be expected if the diaphragms had been modelled as rigid prior to yield. When the rigid diaphragm results in Table 18 are compared with the 0.5-second diaphragm results in Table 19, it can be seen that a consistent reduction in seismic capacity of face-loaded walls is to be expected when yielding is permitted in rigid diaphragms. This reduction in seismic capacity due to rigid diaphragm yielding is more consistent than it was for the NZS4203 EQ motion (compare table 12 and 14 in a similar manner).

Comparing Table 18 and Table 19 indicates that introducing yielding into the diaphragms does not significantly degrade the correlation between the predicted collapse intensities obtained using the computer model and proposed formulae. However, there is one exception that occurs at the 1st floor level when both the shear wall and diaphragm are modelled with 0.5-second periods. However, if the diaphragm yield strengths are increased 50% in this case, the displacement ductility factor for the diaphragm reduces from 11 to a more sustainable 3.1 and the collapse intensity increases from 55% to 73% which is closer to the 83% value predicted by the proposed formulae.

Once again a 50% increase in the unmodified UBC storey elevation amplification factors would improve the correlation between the predicted collapse intensities using the computer model and proposed formulae for the 3 cases where the diaphragms were modelled with a 1.0 second period.

Table 19: Predicted Collapse EQ intensity for Kobe Near Fault EQ Motion for Diaphragms Yielding at half the Wall Cracking Opening Force. Also Maximum Diaphragm Extensions Prior to Collapse

Wall & Diaphragm Properties + Prediction Method	EQ Scaling Factor @ Collapse for Storey Level			Max Diaphragm Extension @ Floor Level – mm (bracketed value = corresponding displacement ductility factor, μ)		
	3 rd	2 nd	1 st	3 rd	2 nd	1 st
	(1)	(2)	(3)	(4)	(5)	(6)
COMPUTER MODEL: Shear wall period 0.0 sec (i.e. rigid shear wall)						
- diaphragm Period 0.5	0.48	0.68	0.75	105 (8.8)	212 (12)	162 (7)
- diaphragm Period 1.0	0.30	0.33	0.48	320 (6.8)	155 (2.3)	193 (2.1)
PROPOSED FORMULA:	0.49	0.45	0.64	-	-	-
NZNSEE Guidelines:	2.87	1.00	0.70	-	-	-
COMPUTER MODEL: Shear wall period 0.5 sec						
- diaphragm Period 0.5	0.45	0.60	0.58 (0.55)	105 (8.8)	411 (24)	250 (11)
- diaphragm Period 1.0	0.35	0.25	0.55	500 (11)	138 (2.0)	290 (3.1)
PROPOSED FORMULA:	0.38	0.44	0.83	-	-	-
NZNSEE Guidelines:	0.81	0.36	0.42	-	-	-
COMPUTER MODEL: Shear wall period 1.0 sec						
- diaphragm Period 0.5	0.28	0.28	0.58	382 (32)	150 (8.8)	382 (17)
- diaphragm Period 1.0	0.13	0.15	0.35	254 (5.4)	103 (1.5)	314 (3.4)
PROPOSED FORMULA:	0.26	0.31	0.59	-	-	-
NZNSEE Guidelines:	0.57	0.26	0.35	-	-	-
Notes: Cols (3) - The bracketed value indicates that collapse at this storey level occurred at this lower EQ scaling factor when 3 rd or 2 nd storey was being modelled (i.e. governs). Cols (4) to (6):- 1st value is maximum diaphragm extension occurring prior to collapse of the storey below the diaphragm for all EQ scaling factors up to 1 increment prior to collapse.						

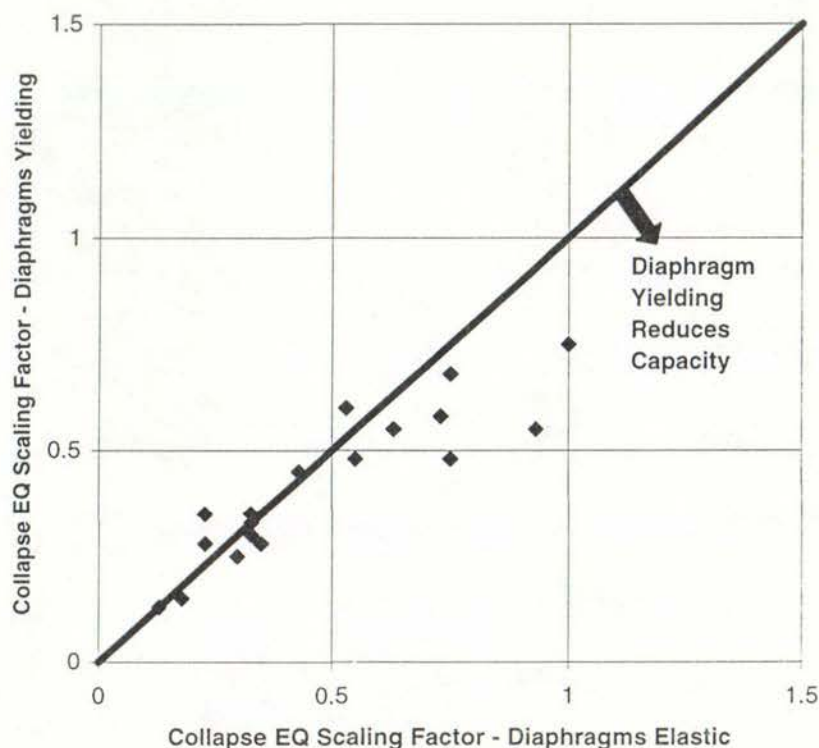


Figure 17: Effect of Diaphragm yielding on EQ Collapse Intensity for Kobe Near Fault EQ Motion as Predicted by Computer Model (flexible diaphragms only)

6.7 Capacity of Face-Loaded URM Walls Predicted by Proposed Formula – Kobe Near Fault EQ Motion

Figure 18 shows the predicted EQ scaling factors that would need to be applied to the Kobe near-fault earthquake motion to cause collapse of face-loaded URM walls. The predictions were made using the proposed formulae and are presented for a range of storey wall height to nominal wall thickness ratios and for a range of nominal wall thickness.

Assumptions made for the calculations are the same as those made in the preparation of similar plots for the NZS4203 earthquake motion detailed in Appendix B. The predicted collapse capacities shown do not allow for any increase due to top fixity (Eqn 13) or for the reduction in capacity due to building or diaphragm amplification of the EQ motion similar to those given in Table 17.

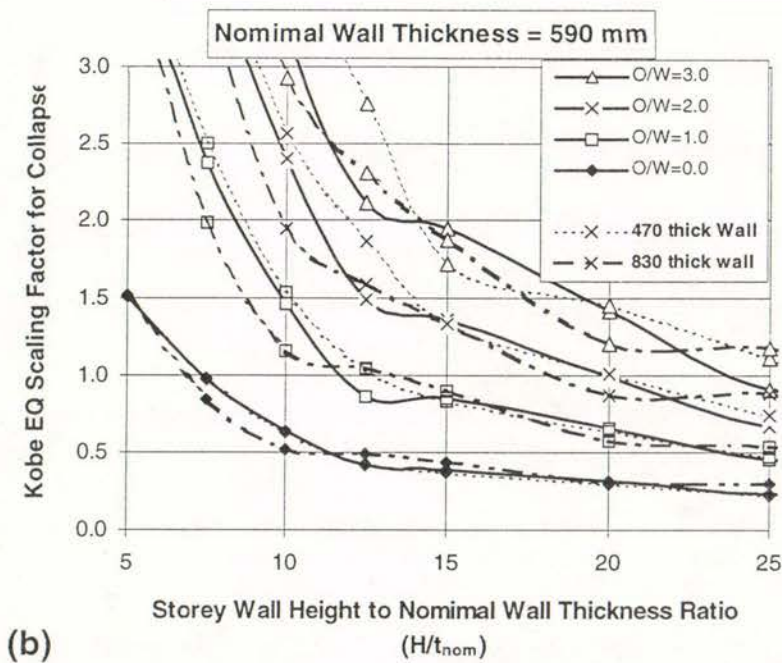
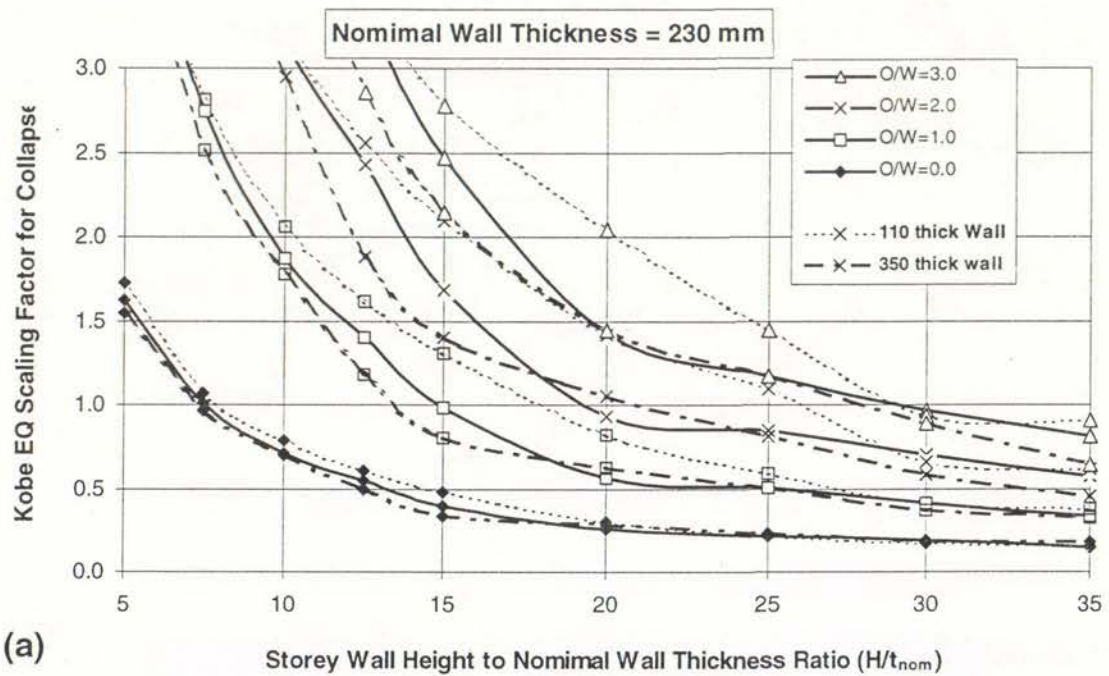


Figure 18: Face-Loaded Seismic Capacity of URM Walls Subjected to Kobe Near Fault EQ (first 1 to 16 seconds of Tokatori Record in Direction of Max Ground Velocity) (a) Principal Wall Thickness 230 mm and (b) Principal Wall Thickness 590 mm

(Note: Comparative capacities for wall thickness' one brick module less than or greater than the principal wall thickness are also shown plotted dotted and dashed respectively.)

Figure 18(b) has been truncated at a height to thickness ratio of 25. Above this ratio the elastic displacements of thicker face-loaded walls at first crack opening may become significant (they increase in proportion to t_{nom}^2 for a given H/t ratio and seismic coefficient). In an extreme case (830 mm wall and $O/W = 3$, $H/t_{nom} > 25$, $E = 1\text{GPa}$) the elastic deflection of wall exceeds $1/3$ the collapse displacement. A basic assumption of the formulation of the proposed formulae is that the elastic displacements of the wall at crack opening are not significant. Also, for these more flexible walls, the seismic coefficient corresponding to crack openings starts to become sensitive to the modulus of elasticity assumed for the face-loaded wall. This sensitivity is due to the shape of the near-fault acceleration response spectrum.

One of the interesting features of Figure 18 is that, for near-fault earthquake motions and a given storey height to nominal wall thickness ratio, the predicted collapse EQ intensity is relatively insensitive to the nominal wall thickness. This may be contrasted with the trend evident in similar plots in appendix B for the NZS4203 type motion. For more slender walls with a given H/t_{nom} ratio, these plots indicate that increasing wall thickness is associated with increased seismic collapse capacity. The same trend was evident in the data presented in Table 6 for less slender walls and two other earthquake motions.

The failure of this trend to appear for the Kobe near-fault EQ motion is a consequence of the relative contributions that the first crack opening and the spectral displacement components make to the EQ collapse intensity predicted by Eqn 16. The spectral displacement component is dependent on the period of the cracked wall when the peak displacement at the centre of the wall is $0.6 Y_{max}$ and this period increases with wall thickness. The displacement spectrum for the near-fault EQ motion (Figure 16(b)) implies that a rapid increase in displacement demand is associated with this increasing period. Although an increased wall thickness increases the collapse displacement capacity of the wall, this does not always compensate for the increased displacement demand.

The first crack opening component of the face-loaded collapse capacity in Eqn 16 is primarily dependant on the seismic coefficient required to open the cracks under static conditions, (i.e. C_d from Eqn 8). For a given H/t ratio this coefficient is independent of wall thickness. Therefore the crack opening component of the predicted capacity is insensitive to wall thickness.

When the response spectra for the NZS4203 and Kobe near-fault EQ motions are compared in Figure 16 it can be seen that the increase in spectral acceleration in the low period zone (on which the crack opening component depends) is modest. This can be contrasted with the large increase in spectral displacements in the longer period zone (on which the spectral component depends). Hence for the near-fault earthquake motion, the displacement spectra component (which is wall thickness dependent) makes up only a relatively small part of the total collapse capacity predicted using Eqn 16.

For a given H/t ratio and the near-fault EQ motion, the 3 factors given in the 3 preceding paragraphs explain the relative insensitivity of the predicted collapse capacity of face-loaded walls to a variation in wall thickness.

For the case of a 4 storey URM masonry wall with uniform wall thickness and storey height, the predictions given in Figure 18 for O/W ratios 3.0 to 0.0 may be thought of as applying to the 1st to 4th storey wall segments respectively.

However, when the EQ scaling factors given in Figure 18 are modified for top fixity (Eqn 13) and for storey level elevation amplification (using values similar that given in column (6) of Table 17) the predicted collapse capacities will be significantly reduced. For example, for the top storey (O/W=0.0) with an assumed amplification factor of 3.0, Figure 18 indicates that even a very squat wall segment with a H/t_{nom} ratio of 5 could only withstand about 50% of the Kobe near-fault EQ motion without collapse. For the storey second from the top (O/W = 1.0), the wall storey segment would require a H/t_{nom} ratio generally less than 10 to survive the near-fault EQ motion. However, as this increased seismic resistance is due to the greater overburden load, O, it would be dependent on the top storey wall segment remaining intact throughout the EQ motion.

The general conclusion that can be drawn from Figure 18 is that very few masonry buildings, of the type modelled for this study, could be expected to survive a near-fault EQ motion of the intensity recorded at the Tokatori station during the Kobe EQ.

The magnitude of the earthquake expected from a movement of the Wellington fault ($M_s=7.5$) is significantly stronger than the Kobe earthquake ($M_s=6.9$). Therefore, even stronger near-fault type motions could be expected in some parts of the Wellington region during the next Wellington fault movement.

Design earthquakes used to design new buildings for the Ultimate Limit usually have probability of exceedance of about 10% in 50 years which is, approximately, the probability of a Wellington fault movement in the next 50 years. Whether an event of this frequency should be considered for the assessment an/or strengthening of existing masonry buildings for the Collapse Limit State is essentially a political decision.

7 Comparison of Predicted Capacities Using NZSEE Guidelines and Proposed Formulae

Figure 19(a) shows the earthquake scaling factors required to cause a range of face-loaded walls to collapse as predicted by computer modelling and as predicted by the proposed formulae.

Figure 19(b) shows a similar comparison of the collapse intensities predicted by computer modelling and by the NZNSEE Guidelines.

The data used for the "No building &/or diaphragm flexibility" plots includes that given in Table 2 for the range of earthquake records used in previous research. It also includes NZS4203 EQ motion data contained in the various tables of this report.

The data used for the "flexible building &/or diaphragm" plots excludes the results obtained when yielding diaphragms were included in the computer model. Where the diaphragms were modelled with a 1.0-second period the storey level amplification factors given in Table 17 were increased by 50% to improve the correlation for the Kobe near-fault EQ motion.

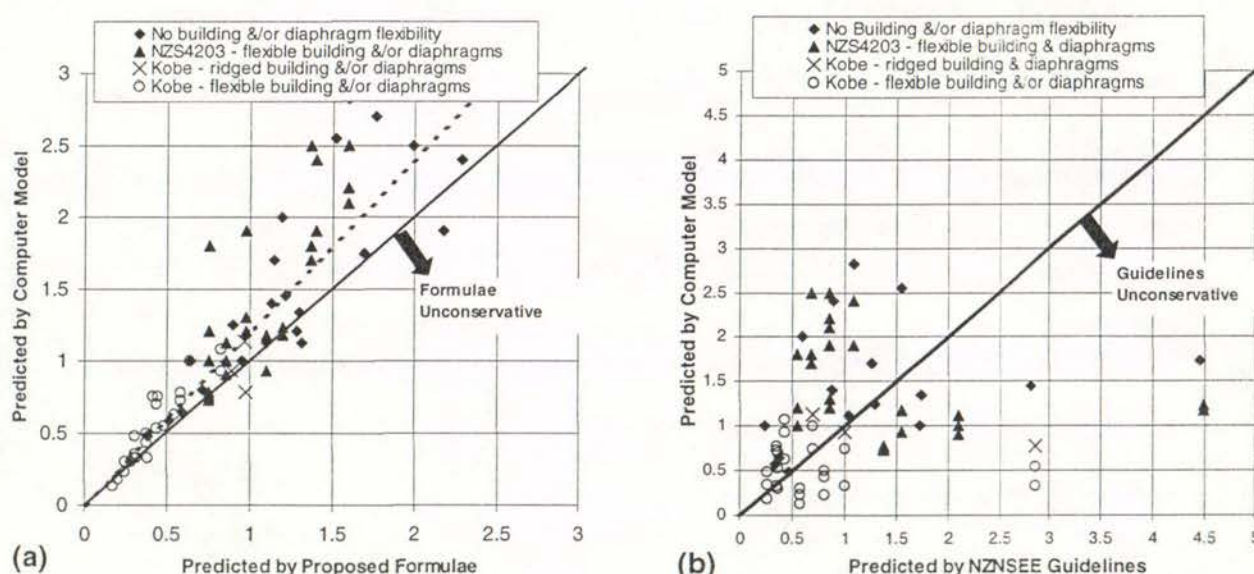


Figure 19: Earthquake Scaling Factors Required to Cause Collapse of Face-Loaded Walls – Comparison of the Values Predicted using the Computer and those Predicted using (a) The Proposed Formulae and (b) The NZNSEE Guidelines.

Figure 19(a) indicates that the proposed formulae can be used to predict the seismic face-load capacity of URM walls with a low probability of failure. In practice the 2D

computer model results should be conservative relative to the real 3D situation, where for example, the face-loaded walls may have additional resistance due to horizontal spanning between cross walls. Therefore, when the formulae are used to predict collapse intensities with a low probability of failure, no additional safety factors should be required.

Figure 19(a) includes a straight (dotted) line plotted so that 50% of the results lie above and below the line. *This plot indicates that if a mean or expected collapse intensity is required for the seismic assessment of a face-load wall, the value predicted using the proposed formulae should be increased by 20%.*

Figure 19(b) compares the EQ collapse intensities predicted by the NZNSEE Guidelines and the computer modelling. When the results up to an EQ scaling factor of 2.5 are considered, it can be seen that the NZNSEE Guideline procedures are a poor predictor of the EQ collapse intensity indicated by the computer modelling. Outside this region of the figure, it can be seen that some Guideline predictions may be unconservative by a wide margin.

The poor correlation between the EQ collapse intensities predicted by the NZNSEE Guidelines and the computer modelling is due to:

- The NZNSEE Guideline predictions are highly dependent on the initial elastic stiffness assumed for the face-loaded wall. However, the computer analyses, in this and previous studies, indicate that the initial elastic stiffness of the wall is not a significant parameter.
- The guidelines assume that the vertical component of the earthquake motion effects the stability of a cracked face-loaded wall by reducing the effective weight of the wall on which the stability of the wall depends. However, the frequency of the vertical component of the EQ motion tends to be high compared with the frequency of a cracked wall approaching collapse. Also, during any short time interval during the response, the additional vertical accelerations associated with the high frequency vertical component of the EQ have an equal probability of increasing or decreasing the effective weight of the wall. Therefore on balance the vertical component of the earthquake has little effect on the collapse intensity predicted by the computer model.
- The Guidelines assume that a storey high segment of a multi-storey wall should be considered as being supported at the mid-thickness centreline of the wall at both the top and bottom of the storey. The computer modelling indicates that the wall can be considered as being supported near the face of the wall at these locations (i.e. the wall segment can be assumed to have top and bottom fixity). This additional restraint enhances the seismic resistance of the wall.

8 Summary and Conclusions

The following is a summary of the work undertaken in this study and the conclusions reached

8.1 Laboratory Testing

Two face-loaded URM wall test specimens were displaced at mid-height to open pre-formed cracks then allowed to respond under free vibration conditions. The test specimen response was modelled using an inelastic dynamic computer model. The tests and computer modelling established that:

- The computer model can be used to model the dynamic displacement response, and hence the seismic stability, of a URM face-loaded wall.
- Over a wide range of mid-height displacements that varied between 90% and 5% of the effective wall thickness, a relatively constant proportion of the energy that was stored in the wall immediately prior to the cracks closing was lost each time the cracks closed. This feature of the dynamic wall response was used to adjust the computer model damping when parameters such as the wall height or thickness were varied from that tested.
- When the mortar in the opening joints of the test specimen was replaced with weak mortar, crushing of the mortar resulted in a smaller effective wall thickness. However, when the computer model was used to determine the seismic resistance of the face-loaded wall, it was found that the additional damping due to the movements and spalling at the opening joints might be sufficient to compensate for the smaller effective wall thickness.
- Relatively large peak reactions were measured at the top support of the test specimens. These peak reactions occur just after the impact associated with crack closing and were up to 560% of the maximum force expected when the cracks in the wall open under static loading conditions. These forces would need to be considered when evaluating diaphragm anchorage forces if the diaphragm is rigid and the anchorage load path contain brittle components.

8.2 Computer Modelling

A 2D three-storey model was developed to examine the effect of a number of parameters on the seismic stability of a cracked face-loaded URM wall. Parameters examined included interaction between the face-loaded walls segments in adjacent storeys, effect of building flexibility and effect of diaphragm flexibility and/or yielding. The analyses indicated that:

- The lower storey-high segments of a multi-storey masonry wall behave as if they have full flexural fixity at their top and bottom boundary joints. This indicates that the reactions at the opening boundary joints tend to act in the location that is most favourable to the seismic stability of each storey-high wall segment.
- The vertical component of the earthquake does not significantly effect the stability of face-loaded URM walls. The frequency of the vertical component of the EQ motion tends to be high compared with the frequency of a cracked wall approaching collapse. Also, during any short time interval during the response, the additional vertical forces associated with the high frequency vertical component of the EQ has an equal probability of either increasing or decreasing the stability of the wall. Therefore, on balance, inclusion of the vertical component of the EQ motion in the computer analysis has little effect on the predicted collapse intensity.

8.3 Assessment Methodology

An assessment methodology that can be used to predict the seismic stability of a face-loaded URM wall was developed. The methodology makes use of both the acceleration and displacement response spectra for an earthquake motion. The acceleration spectrum is used to predict the earthquake intensity that will just open the joint cracks in the wall. The displacement spectrum is used to predict the earthquake intensity that will generate mid-storey wall displacements equal to the displacement at which the wall becomes unstable. Modification factors are applied to allow for the effect of "top fixity" and to allow for amplification of the earthquake motion due to the building response and diaphragm flexibility. It was established that:

- A relatively simple formula can be used to calculate the period of the motion of a cracked face-loaded URM wall when the peak mid-storey displacement is 60% of the displacement at which the wall becomes unstable. The formula is not dependant on the wall slenderness, overburden load, wall thickness or presense of top fixity. The period calculated using the formula can be used in conjunction with a displacement spectra as part of the methodology used to predict the stability of face-loaded URM walls.
- The earthquake intensity required to collapse a face-loaded wall, as indicated by the computer modelling, is conservatively predicted by the proposed methodology.
- If the mean or expected collapse intensity is required for the seismic assessment of a face-load wall, the value predicted using the proposed methodology should be increased by 20%.

- When the earthquake intensity required to collapse a face-loaded wall, as predicted by the computer modelling and the NZNSEE Guidelines are compared, the current New Zealand Guidelines are shown to be a poor indicator of the wall's seismic resistance. In some cases the Guidelines overestimate the seismic capacity of the wall by more than 300%.
- For face-loaded walls with a given storey-height to wall thickness ratio, the seismic stability tends to increase with increasing wall thickness. However, this trend is dependent on the shape of the earthquake response spectra used to study the trend.

8.4 Effect of Near Fault Earthquake Motion

The response of the 3-storey wall model was evaluated using an earthquake motion recorded in the near-fault zone during the Kobe earthquake. The near-fault motion had a quite different frequency content and spectral shape from that used as the basis of traditional code design spectra. The analyses indicated that:

- The formula proposed for calculating the seismic resistance of face-loaded URM walls, when the building and diaphragms are rigid, can be used for a wide range of different earthquake motions.
- For the near-fault earthquake motion, the seismic stability of face-loaded walls is reduced when the structural system flexibility is increased. Hence amplification factors, included in the assessment methodology to allow for building and diaphragm flexibility, must increase with increasing building and/or diaphragm flexibility. This trend is a consequence of the shape of the near-fault earthquake response spectra. For earthquake motions that have response spectra shapes similar to those traditionally used in design codes, the opposite trend is to be expected.
- Very few masonry buildings, of the type modelled for this study, could be expected to survive a near-fault EQ motion of the intensity recorded at the Tokatori station during the Kobe EQ.

8.5 Design Charts

Design charts are provided to enable rapid assessment of a face-loaded wall in terms of the NZS4203 Loading Standard design EQ spectra. Similar design charts could be prepared for other earthquake records or code design spectral intensities using the proposed methodology.

9 References

- ABK Joint Venture (1982): "Methodology for Mitigation of Seismic Hazards in Existing Unreinforced Masonry Buildings – Report ABK-TR-08 Interpretation of Wall Tests: Out-of-plane" El Segundo, CA Agbabian Associates
- Alavi B, Krawinkler H (2000): "Consideration of Near-Fault Ground Motion Effects in Seismic Design" Proceedings 12th World Conference on Earthquake Engineering, Auckland New Zealand (Paper 2665)
- Aagaard BT, Hall JF, Heaton TH (2000): "Sensitivity Study of Near Source Ground Motion" Proceedings 12th World Conference on Earthquake Engineering, Auckland New Zealand (Paper 0722)
- Blaikie E L and Spurr D D (1992): "Earthquake Vulnerability of Existing Unreinforced Masonry Buildings". Research report sponsored by the New Zealand Earthquake and War Damage Commission, Works Consultancy Services, December 1992.
- Blaikie E L and Davey R A (2000): "Seismic Behaviour of Face Loaded Unreinforced Masonry Walls". 12th World Conference on Earthquake Engineering, Auckland New Zealand.
- Doherty KT, Rodolico B, Lam TK, Wilson JL, Griffith C (2000): "The Modelling of Earthquake Induced Collapse of Unreinforced Masonry Walls Combining Force and Displacement Principles" ". 12th World Conference on Earthquake Engineering, Auckland New Zealand.
- Lam N, Wilson J L, Hutchinson G L (1995): "The Seismic Resistance of Unreinforced Masonry Cantilever walls in Low Seismicity Areas" Bulletin of the NZNSEE Vol. 28 (3) pp.179-195.
- Malhotra PK (1999): "Response of Buildings to Near-Field Pulse Like Ground Motions" Earthquake Engineering & Structural Dynamics, Vol 28, p1390-1326
- NZNSEE (1995): "Draft Guidelines for Assessing And Strengthening Earthquake Risk Buildings" New Zealand National Society for Earthquake Engineering, 10 February 1995.
- Priestley J N (1985): "Seismic Behaviour of Unreinforced Masonry Walls" Bulletin of the NZNSEE, Vol. 18 (2) and Discussion Vol. 19 (1), 1986.
- Yim C , Chopra K and Penzien J (1980): "Rocking Response of Rigid Blocks to Earthquakes". Earthquake Engineering and Structural Dynamics, Vol 8.

Appendix A – Drain2dx Input File for Modelling Test Specimen 1

```

!UNITS L m F kn      [Inserted by RAM XLinea]
*STARTXX              ! Test 1 / t=230/H=3M/E=1
  Brick9              0 0 1 1              URM wall - mid hight crack
*NODECOORDS
C      36      0.0091      3.087
C      18      0.0085      2.933
C      17      0.0082      2.755
C      16      0.0080      2.577
C      15      0.0074      2.399
C      14      0.0090      2.221
C      13      0.0069      2.043
C      12      0.0069      1.865
C      11      0.0084      1.687
C      10      0.0091      1.554
C      9       0.0073      1.465
C      8       0.0066      1.332
C      7       0.0063      1.155
C      6       0.0059      0.978
C      5       0.0045      0.801
C      4       0.0056      0.624
C      3       0.0041      0.447
C      2       0.0042      0.270
C      1       0.0013      0.093
!
C      22      0.008      1.440
C      23     -1.113      0.010
C      24     -0.113      0.008
C      25     -0.113      0.010
C      26      0.0      0.010
C      27      0.113      0.008
C      28      0.113      0.010
C      29      1.113      0.010
!
C      30     -0.108      1.513
C      31     -0.108      1.515
C      32      0.007      1.514
C      33      0.007      1.514
C      34      0.122      1.513
C      35      0.122      1.515
C      37     -0.440      3.087
C      38     -0.002      1.487
*RESTRAINTS
S 111      23      29      6      ! floor supports
S 111      37      ! top support
S 011      24      27      3
*SLAVING
S 100      25      24
S 100      28      27
S 100      32      33
*MASSES
S 110      0.420      18      9.806      .60
S 110      0.427      17
S 110      0.426      16
S 110      0.424      15
S 110      0.417      14
S 110      0.422      13
S 110      0.424      12
S 110      0.421      11
S 110      0.224      10
S 110      0.188      9
S 110      0.393      8
S 110      0.394      7
S 110      0.396      6
S 110      0.396      5

```


Assessment of Face-Loaded URM Walls

```

S 110      0.389      4
S 110      0.392      3
S 110      0.390      2
S 110      0.374      1
!
S 001      0.0030     18
S 001      0.0030     17
S 001      0.0030     16
S 001      0.0030     15
S 001      0.0029     14
S 001      0.0030     13
S 001      0.0030     12
S 001      0.0030     11
S 001      0.0011     10
S 001      0.0009      9
S 001      0.0027      8
S 001      0.0028      7
S 001      0.0028      6
S 001      0.0028      5
S 001      0.0027      4
S 001      0.0027      3
S 001      0.0027      2
S 001      0.0026      1
*ELEMENTGROUP
  2      0      1      0.0040
  1      0      1
  1      2.0E6      0.01      .114      .00051      4      4      2      0.1
  1      1      1000.0      1000.0
  1      26      1      1      1
  2      1      2      1      1
  8      7      8      1      1
  9      8      22      1      1
  10     22      9      1      1
  11     9      32      1      1
  12     33      10     1      1
  13     10     11      1      1
  20     17     18      1      1
  21     18     36      1      1
*ELEMENTGROUP
  9      1      0      0.0
  1
  1      -2      0.8      0.9      0.25E6      0.25E6      0.25E6      0.1
  0.1
  1      24      25      1      1
  2      27      28      1      1
  3      30      31      1      1
  4      34      35      1      1
  !      5      34      35      1      2
*ELEMENTGROUP
  2      0      0      0.0040
  1      0      1
  1      1.0E6      0.01      10.0      3.00      4      4      2      0.1
  1      1      10000.0      10000.0
  1      25      26      1      1
  2      26      28      1      1
  3      30      32      1      1
  4      32      34      1      1
  5      31      33      1      1
  6      33      35      1      1
  7      32      38      1      1
*ELEMENTGROUP
  9      1      0      0.0
  1
  1      -1      0.8      0.9      10.0E6      10.0E6      10.0E6      0.1
  1      23      25      1      1
  2      28      29      1      1
*ELEMENTGROUP
  1      0      0      0.0040
  5 ** TOP SUPPORT

```

Assessment of Face-Loaded URM Walls

```

1
1 200.0E6 0.01 33.35E-6 1.0e7 1.0e7 0 0.001
1 37 36 1

*RESULTS
NSD 10 ! all nodes for Post Processor
NSV 10 ! ditto nodal velocities
NSA 10 ! ditto nodal accelerations
NSD 11 38 ! nodes also for .out file
E 10 ! all elements for Post Processor

*NODALOAD
D+S DEAD LOADS + NO SURCHARGE
S 0.0 -0.420 18
S 0.0 -0.427 17
S 0.0 -0.426 16
S 0.0 -0.424 15
S 0.0 -0.417 14
S 0.0 -0.422 13
S 0.0 -0.424 12
S 0.0 -0.421 11
S 0.0 -0.224 10
S 0.0 -0.188 9
S 0.0 -0.393 8
S 0.0 -0.394 7
S 0.0 -0.396 6
S 0.0 -0.396 5
S 0.0 -0.389 4
S 0.0 -0.392 3
S 0.0 -0.390 2
S 0.0 -0.374 1

*NODALOAD
PULL STATIC LOAD ON WALL
S 3.385 0.000 22

*ACCNREC
PULS PULSE2.DAT (10f8.0)1 G PULSE
1001 10 0 2 9.806 0.02 0.0

!*ACCNREC
! NZ42 NZS4023I (4(f10.6, f8.3))NZS4203i from ELCENTRO N-S 1940
! 1001 4 2 2 9.806

*PARAMETERS
VS 0.30 0.15 !Damping scaling
C 1.0 1.0 !Colapse Y Displ
F 1.0 !Overshoot scaling
OD 0 3 0.02 3 0.02 9999
DC 1 10 !Event Calc/Max substeps
DT 0.01 0.01 !Initial/Max Var Time step
DA 0.5 !Force Tolerances For Var time Step
*GRAV
N D+S 1.0 Gravity Load

!*STAT ! load control total load
!N PULL 1.0
!L 1.0 1.0

!*STAT
!N PULL 1.0
!D 38 23 1 0.00010 0.006 ! Disp control -1st 10mm

!*STAT
!N 1.0
!D 38 23 1 0.010 0.141 ! Displ control to max displ

*ACCN
5.0 99999 2 !Anal Time/Steps + Step Type
1 PULS 0.514

*STOP

```


Appendix B – Methodology for The Assessment of Face Loaded Walls

B1 Description of Assessment Methodology

This appendix sets out a methodology that can be used to assess the seismic stability of a face-loaded URM wall using the procedures developed in the body of the report.

Design charts are provided for use where the assessment is being carried out in terms of the NZS4203 Loading Standard design EQ spectral intensity for one of the 3 types of site soil conditions covered by the Standard.

The design charts give the EQ scaling factor $I_{collapse}$ that must be applied to the basic NZS4203 spectral intensity earthquake to cause collapse of a face-loaded wall in a rigid structure with rigid diaphragms. (Note that the methodology can be adapted for other earthquake records or code design spectral intensities by using equation Eqn 16 to calculate $I_{collapse}$).

The charts were derived using Eqn 16 and the NZS4203 basic design spectra similar to those shown in Figure 11 for each of the 3 soil types (see body of the report). The effective thickness of the wall, t , was assumed to be given by: $t = t_{nom}(0.975 - 0.025 \frac{O}{W})$ where t_{nom} is the nominal thickness of the wall. This assumes that increased damping will compensate for the reduced effective wall thickness that can be expected when weak mortar has been used in the wall. Other assumptions regarding the elastic modulus and density of the masonry were the same as given in section 4.2 of the report.

A modification factor is applied to the basic $I_{collapse}$ obtained from the charts to allow for the effect of top fixity (if present at the top of a storey wall segment being assessed). A second modification factor is then applied to allow for amplification of the earthquake motion due to the building response and diaphragm flexibility or yielding.

The resulting NZS4203 EQ scaling factor, $I_{capacity}$ represents the seismic collapse capacity of the face-loaded wall for the storey being assessed.

$I_{capacity}$ can then be compared with the scaling factor for the NZS4203 spectral intensity, I_{demand} , which must be exceeded to meet the assessment criteria.

B2 Formulation of Assessment Methodology

This formulation applies to assessments of face-loaded URM walls carried out in terms of the NZS4203 Loading Standard design EQ spectral intensity for one of the 3 types of site soil conditions covered by the Standard. The NZS4203 EQ scaling factor representing the seismic collapse capacity of a storey high segment of a face loaded wall with a low probability of exceedance is given by:

$$I_{\text{capacity}} = \frac{F_{\text{top}}}{A} I_{\text{collapse}} \quad (\text{Eqn B1})$$

Where: I_{collapse} = the EQ scaling factor that must be applied to the basic NZS4203 spectral intensity earthquake to cause collapse of a face-loaded wall in a rigid structure with rigid diaphragms and without top flexural fixity. Read from design charts (or calculated using Eqn 16)

F_{top} = top fixity modifier, 1.0 for one storey walls and the top storey of multi-storey walls.

Otherwise:

$$F_{\text{top}} = \left[\frac{1 + 2.0 \frac{O}{W}}{1 + 1.5 \frac{O}{W}} \right] \quad (\text{Eqn B2})$$

Where: O = the overburden weight acting on the wall at the top of the storey under consideration

W = the weight of the wall in the storey under consideration

A = the storey elevation amplification factor which includes the effects of diaphragm flexibility. For buildings where the shear walls (and their foundations) can be considered rigid but the diaphragms are flexible, $A = 1.2$ for first storey and 1.4 for other storeys.

Otherwise:

$$A = 0.7 \left(1 + 3 \frac{h_i}{h_r} \right) \text{ when the building period is expected to be } < 0.5 \text{ seconds}^*$$

or

$$A = 0.7 \left(1 + 2 \frac{h_i}{h_r} \right) \text{ when the building period is expected to be } > 1.0 \text{ seconds}^*$$

Where: h_i is the mid-storey height of the face loaded wall in storey being assessed and:

h_r is the elevation of the building roof.

(* period should allow for inelastic deformations and ignore diaphragm flexibility – linear interpolation is proposed for building periods between 0.5 and 1.0 seconds)

The assessed face-loaded wall in a storey is satisfactory if:

$$I_{\text{capacity}} > I_{\text{demand}} \quad (\text{Eqn B3})$$

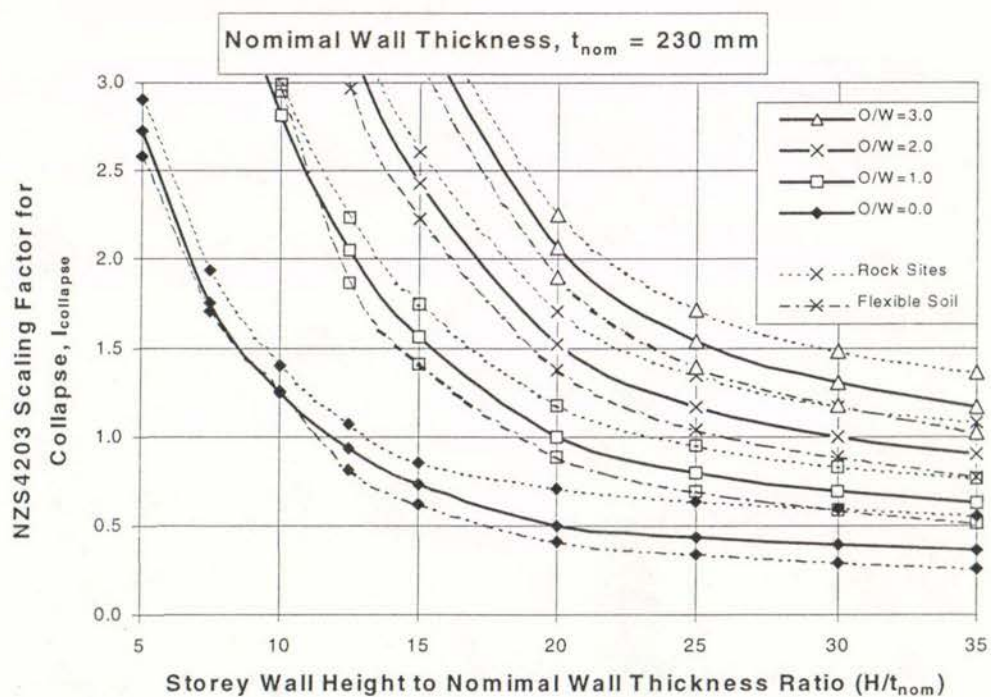
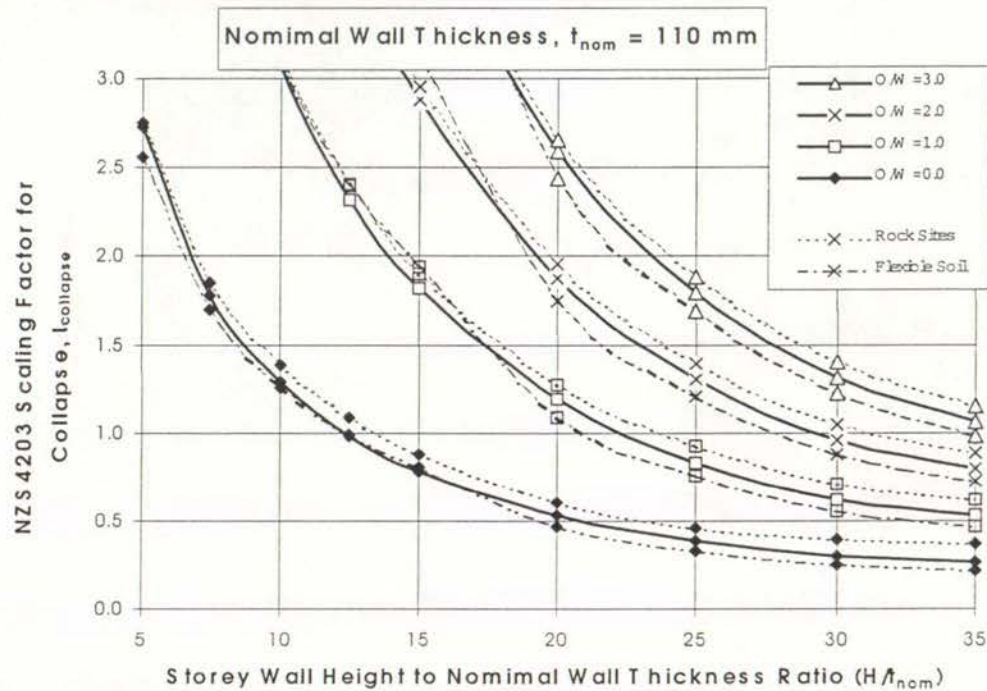
Where: $I_{\text{demand}} = S_p R Z$ when the assessment is being made to meet the criteria given in the current draft NZNSEE Guidelines.

(Note: S_p is the structural performance factor; R is the risk factor and Z is the Zone factor as given in the Guidelines. However, the Guidelines recommend $S_p = 0.6$ for the ultimate limit state and a value of $S_p = 1.0$ is probably more appropriate for the collapse limit state being addressed here.)

I_{collapse} is the assessed seismic collapse capacity with a low probability of exceedance. If a collapse capacity with a 50% probability of exceedance is required, a value of $1.2 \times I_{\text{collapse}}$ is recommended for the assessment.

EQ Scaling Factor, $I_{collapse}$, to be Applied to NZS4203 Spectral EQ Intensity to Cause Collapse of Face Loaded Walls - Rigid Building & Diaphragms

(Solid Line Plots are for Intermediate Soil sites - Comparative Capacities for Rock and Flexible Soil Sites Shown dotted and dashed respectively)



Note: W = weight (per m) of the wall within the storey under consideration
 O = Load (per m) imposed on the wall at the top of the storey under consideration

EQ Scaling Factor, $I_{collapse}$, to be Applied to NZS4203 Spectral EQ Intensity to Cause Collapse of Face Loaded Walls - Rigid Building & Diaphragms

Nominal URM Wall Thickness, $t_{nom} = 110$ mm

$\frac{O}{W}$	NZS4203 Soil Spectrum	Storey Wall Height to Nominal Wall Thickness Ratio (H / t_{nom})								
		5	7.5	10	12.5	15	20	25	30	35
0.00	Rock	2.75	1.85	1.38	1.09	0.87	0.61	0.46	0.40	0.37
	Intermed	2.73	1.77	1.28	0.98	0.78	0.53	0.39	0.30	0.27
	Soft	2.56	1.69	1.26	0.99	0.81	0.46	0.33	0.25	0.22
1.00	Rock	6.47	4.26	3.12	2.41	1.90	1.27	0.93	0.71	0.62
	Intermed	6.62	4.28	3.06	2.32	1.81	1.19	0.83	0.62	0.53
	Soft	6.38	4.19	3.08	2.40	1.94	1.09	0.75	0.55	0.47
2.00	Rock	10.20	6.67	4.86	3.74	2.95	1.96	1.39	1.05	0.88
	Intermed	10.52	6.79	4.86	3.68	2.88	1.88	1.30	0.96	0.80
	Soft	10.21	6.71	4.93	3.85	3.11	1.75	1.20	0.88	0.72
3.00	Rock	13.94	9.11	6.63	5.10	4.01	2.65	1.88	1.40	1.15
	Intermed	14.42	9.31	6.68	5.05	3.96	2.59	1.79	1.31	1.06
	Soft	14.03	9.23	6.80	5.30	4.30	2.44	1.69	1.22	0.98

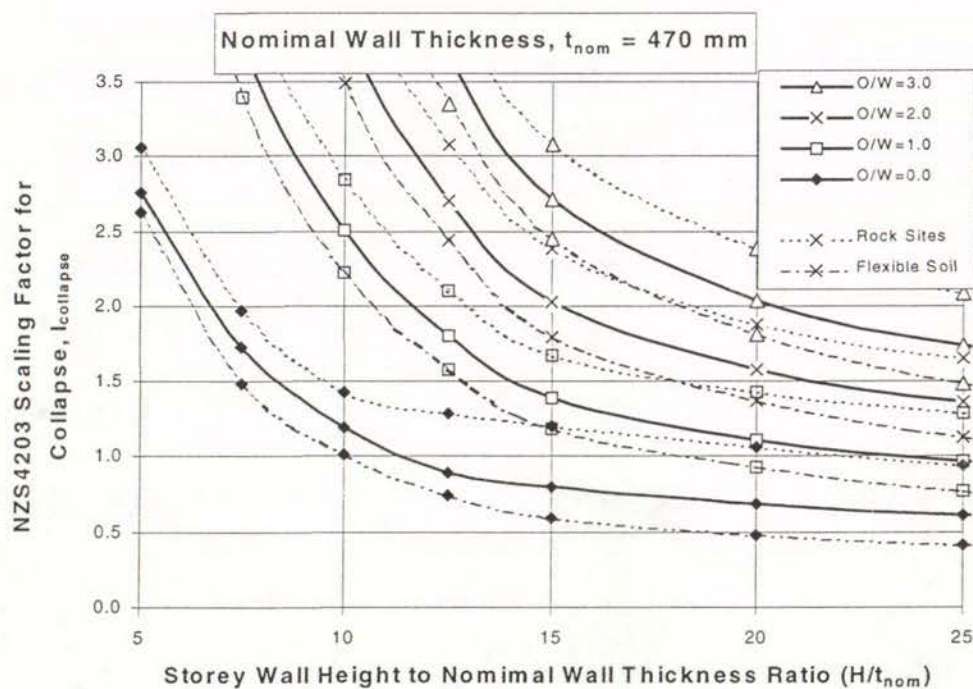
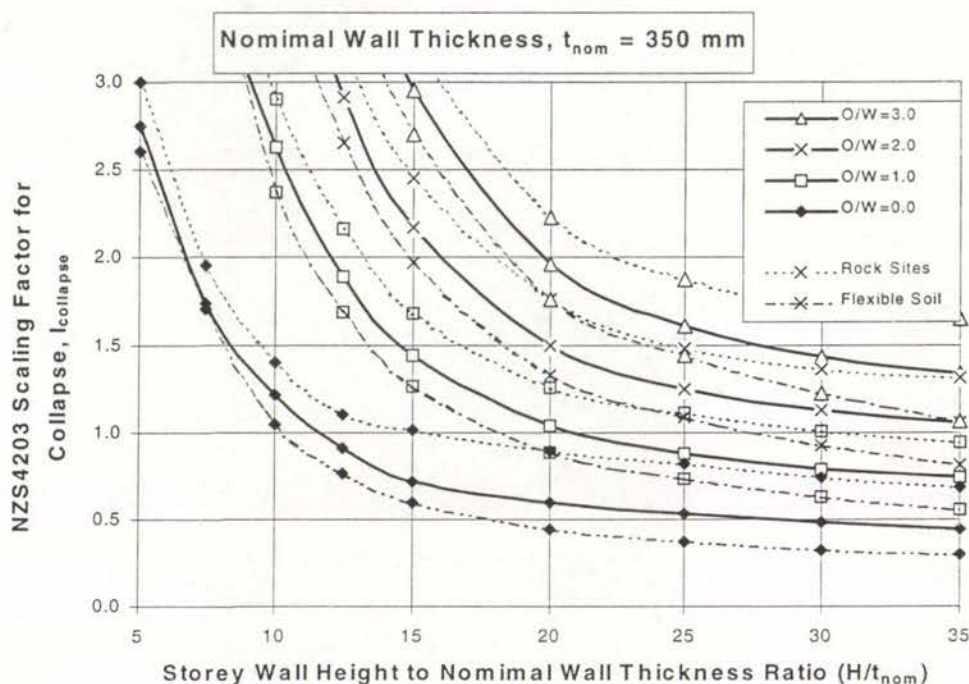
Nominal URM Wall Thickness, $t_{nom} = 230$ mm

$\frac{O}{W}$	NZS4203 Soil Spectrum	Storey Wall Height to Nominal Wall Thickness Ratio (H / t_{nom})								
		5	7.5	10	12.5	15	20	25	30	35
0.00	Rock	2.90	1.93	1.40	1.07	0.86	0.71	0.64	0.59	0.56
	Intermed	2.73	1.75	1.25	0.94	0.73	0.50	0.43	0.39	0.37
	Soft	2.58	1.70	1.25	0.81	0.62	0.41	0.34	0.29	0.26
1.00	Rock	6.54	4.23	2.99	2.24	1.75	1.17	0.95	0.83	0.76
	Intermed	6.51	4.07	2.81	2.05	1.56	1.00	0.80	0.69	0.63
	Soft	6.30	4.08	2.95	1.86	1.41	0.88	0.69	0.59	0.52
2.00	Rock	10.17	6.55	4.60	3.39	2.61	1.70	1.34	1.17	1.08
	Intermed	10.30	6.43	4.43	3.23	2.43	1.52	1.16	0.99	0.90
	Soft	10.10	6.53	4.70	2.97	2.23	1.38	1.04	0.88	0.77
3.00	Rock	13.84	8.85	6.23	4.58	3.50	2.25	1.71	1.48	1.36
	Intermed	14.11	8.82	6.08	4.43	3.34	2.07	1.54	1.30	1.17
	Soft	13.88	9.01	6.49	4.13	3.09	1.90	1.39	1.17	1.02

Note: W = weight (per m) of the wall within the storey under consideration
O = Load (per m) imposed on the wall at the top of the storey under consideration

EQ Scaling Factor, $I_{collapse}$, to be Applied to NZS4203 Spectral EQ Intensity to Cause Collapse of Face Loaded Walls - Rigid Building & Diaphragms

(Solid Line Plots are for Intermediate Soil sites - Comparative Capacities for Rock and Flexible Soil Sites Shown dotted and dashed respectively)



Note: W = weight (per m) of the wall within the storey under consideration
O = Load (per m) imposed on the wall at the top of the storey under consideration

Nominal URM Wall Thickness, $t_{nom} = 350$ mm

$\frac{O}{W}$	NZS4203 Soil Spectrum	Storey Wall Height to Nominal Wall Thickness Ratio (H / t_{nom})								
		5	7.5	10	12.5	15	20	25	30	35
0.00	Rock	3.00	1.95	1.40	1.10	1.01	0.90	0.82	0.74	0.68
	Intermed	2.75	1.74	1.22	0.91	0.71	0.60	0.53	0.48	0.44
	Soft	2.61	1.71	1.04	0.77	0.59	0.44	0.37	0.32	0.30
1.00	Rock	6.57	4.17	2.90	2.16	1.68	1.25	1.11	1.01	0.94
	Intermed	6.38	3.89	2.63	1.89	1.44	1.04	0.87	0.79	0.74
	Soft	6.23	4.00	2.38	1.69	1.27	0.89	0.73	0.63	0.56
2.00	Rock	10.16	6.38	4.36	3.18	2.45	1.76	1.48	1.36	1.31
	Intermed	10.08	6.12	4.11	2.91	2.17	1.50	1.25	1.12	1.05
	Soft	9.97	6.35	3.76	2.65	1.97	1.32	1.09	0.93	0.81
3.00	Rock	13.73	8.63	5.86	4.23	3.22	2.23	1.87	1.72	1.65
	Intermed	13.80	8.39	5.62	3.98	2.95	1.96	1.61	1.43	1.34
	Soft	13.74	8.77	5.20	3.66	2.71	1.76	1.44	1.22	1.06

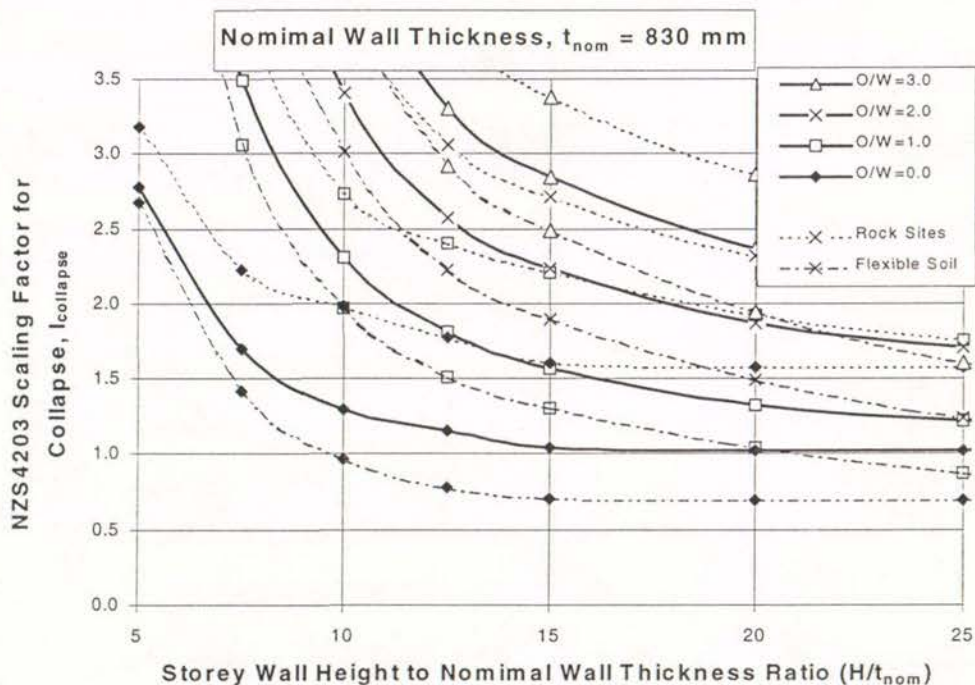
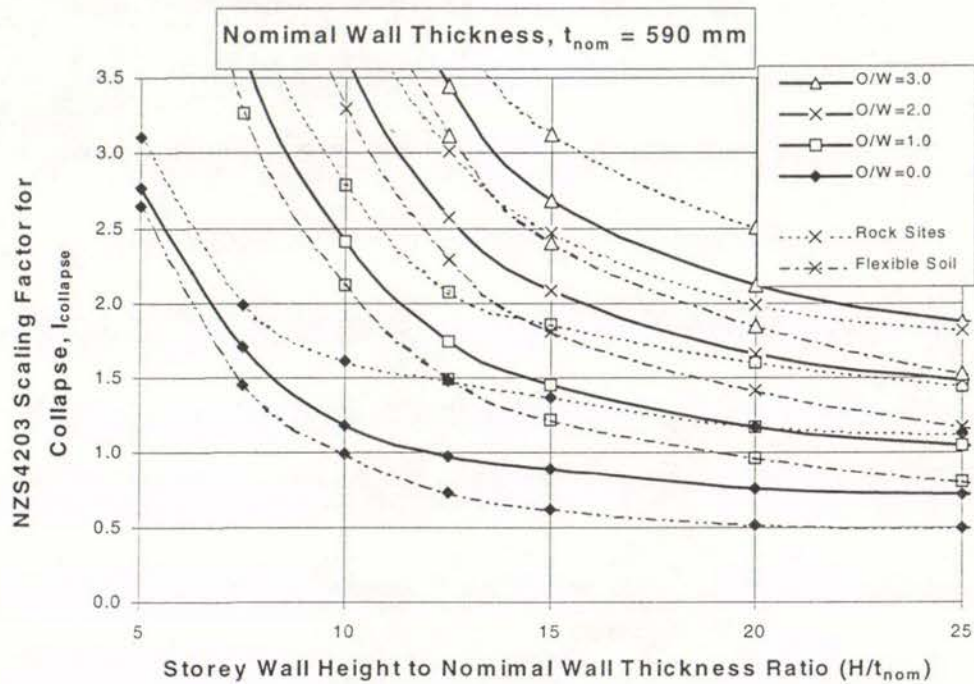
Nominal URM Wall Thickness, $t_{nom} = 470$ mm

$\frac{O}{W}$	NZS4203 Soil Spectrum	Storey Wall Height to Nominal Wall Thickness Ratio (H / t_{nom})						
		5	7.5	10	12.5	15	20	25
0.00	Rock	3.06	1.97	1.43	1.29	1.20	1.06	0.94
	Intermed	2.76	1.73	1.20	0.89	0.80	0.69	0.61
	Soft	2.63	1.48	1.01	0.74	0.59	0.47	0.41
1.00	Rock	6.60	4.12	2.84	2.10	1.67	1.43	1.28
	Intermed	6.27	3.75	2.50	1.80	1.38	1.11	0.96
	Soft	6.19	3.39	2.23	1.58	1.18	0.93	0.77
2.00	Rock	10.12	6.20	4.20	3.08	2.38	1.87	1.65
	Intermed	9.86	5.86	3.84	2.70	2.03	1.58	1.37
	Soft	9.84	6.22	3.49	2.44	1.80	1.37	1.13
3.00	Rock	13.65	8.33	5.58	4.03	3.07	2.38	2.08
	Intermed	13.49	8.00	5.25	3.66	2.71	2.03	1.74
	Soft	13.56	8.54	4.81	3.35	2.45	1.81	1.48

Note: W = weight (per m) of the wall within the storey under consideration
O = Load (per m) imposed on the wall at the top of the storey under consideration

EQ Scaling Factor, $I_{collapse}$, to be Applied to NZS4203 Spectral EQ Intensity to Cause Collapse of Face Loaded Walls - Rigid Building & Diaphragms

(Solid Line Plots are for Intermediate Soil sites - Comparative Capacities for Rock and Flexible Soil Sites Shown dotted and dashed respectively)



Note: W = weight (per m) of the wall within the storey under consideration
 O = Load (per m) imposed on the wall at the top of the storey under consideration

EQ Scaling Factor, $I_{collapse}$, to be Applied to NZS4203 Spectral EQ Intensity to Cause Collapse of Face Loaded Walls - Rigid Building & Diaphragms

Nominal URM Wall Thickness, $t_{nom} = 590$ mm

$\frac{O}{W}$	NZS4203 Soil Spectrum	Storey Wall Height to Nominal Wall Thickness Ratio (H / t_{nom})						
		5	7.5	10	12.5	15	20	25
0.00	Rock	3.11	1.99	1.61	1.48	1.37	1.18	1.12
	Intermed	2.77	1.71	1.18	0.98	0.89	0.76	0.73
	Soft	2.64	1.46	0.99	0.73	0.62	0.52	0.49
1.00	Rock	6.63	4.08	2.79	2.07	1.85	1.61	1.44
	Intermed	6.16	3.64	2.41	1.75	1.45	1.18	1.05
	Soft	6.16	3.26	2.12	1.50	1.22	0.97	0.81
2.00	Rock	10.07	6.06	4.10	3.01	2.47	1.99	1.82
	Intermed	9.66	5.63	3.64	2.57	2.08	1.66	1.48
	Soft	9.74	5.13	3.29	2.29	1.81	1.41	1.17
3.00	Rock	13.56	8.09	5.39	3.90	3.13	2.51	2.29
	Intermed	13.20	7.68	4.95	3.44	2.69	2.12	1.88
	Soft	13.40	7.06	4.51	3.11	2.40	1.85	1.53

Nominal URM Wall Thickness, $t_{nom} = 830$ mm

$\frac{O}{W}$	NZS4203 Soil Spectrum	Storey Wall Height to Nominal Wall Thickness Ratio (H / t_{nom})						
		5	7.5	10	12.5	15	20	25
0.00	Rock	3.18	2.22	1.98	1.77	1.61	1.58	1.58
	Intermed	2.77	1.69	1.30	1.15	1.04	1.02	1.02
	Soft	2.68	1.42	0.97	0.78	0.71	0.70	0.70
1.00	Rock	6.63	3.98	2.73	2.40	2.20	1.92	1.75
	Intermed	5.99	3.49	2.31	1.81	1.57	1.33	1.22
	Soft	6.11	3.06	1.97	1.51	1.30	1.04	0.87
2.00	Rock	9.92	5.88	3.98	3.06	2.71	2.32	2.21
	Intermed	9.30	5.26	3.40	2.58	2.23	1.87	1.71
	Soft	9.59	4.75	3.01	2.22	1.90	1.49	1.24
3.00	Rock	13.27	7.73	5.16	3.90	3.38	2.86	2.74
	Intermed	12.67	7.14	4.52	3.31	2.85	2.36	2.15
	Soft	13.12	6.50	4.09	2.92	2.49	1.94	1.60

Note: W = weight (per m) of the wall within the storey under consideration
O = Load (per m) imposed on the wall at the top of the storey under consideration

Appendix C – Diaphragm Reactions at First Crack opening for Face Loaded URM Walls - UDL Seismic Load

Diaphragm Reactions (kN/m) at first Crack opening for Face Loaded URM wall
- UDL Seismic Load

$\frac{O}{W}$	Diaphragm Location	Nominal URM Wall Thickness					
		t_{nom} (mm)					
		110	230	350	470	590	830
0.00	Top of Storey	0.4	1.5	3.6	6.5	10	20
	Bott of Storey	0.6	2.6	6.0	11	17	34
1.00	Top of Storey	1.3	5.5	13	23	36	72
	Bott of Storey	1.5	6.5	15	27	43	85
2.00	Top of Storey	2.1	9.3	22	39	61	121
	Bott of Storey	2.4	10	24	43	68	134
3.00	Top of Storey	2.9	13	30	54	85	167
	Bott of Storey	3.2	14	32	58	91	180

Notes:

1. W = weight (per m) of the wall within the storey under consideration.
2. O = load (per m) imposed on the wall at the top of the storey under consideration.
3. Top fixity assumed at top of storey under consideration. This does not effect the reactions when $O/W = 0.0$.
4. Reactions are independent of storey height.
5. Calculations ignored elastic displacement of the wall and hence will be conservative if elastic deflection is significant compared with thickness of wall (i.e. thick slender walls).
6. In the equation (Eqn 6) used to calculate the differential reactions at the top and bottom of the wall storey segment the term $[O+W]$ becomes just $[W]$ when the wall has top fixity.

